Table of Contents

Lipid Coated Nanobubbles as Theragnostic Agents: from Theory to Application

D.V.B. Batchelor, R.H. Abou-Saleh, P.L. Coletta, AF Markham, S.A. Peyman, J.R. McLaughlan, and S.D. Evans

School of Physics and Astronomy, University of Leeds, United Kingdom

Abstract:
The fate of bubbles in water is to either to rise to the surface and burst or to dissolve in the aqueous phase. As the bubbles become smaller there is a concomitant increase in the Laplace pressure driving the rate of dissolution ever faster. As such nanobubbles (NBs) are expected to exhibit vanishingly short lifetimes before their dissolution. Coupled with their decreasing size the pressure within such nanoscale bubbles increases and the temperature at which encapsulated gases vaporise is increased.[1]
In this presentation, we consider the predicted behaviour of a number of perfluorocarbon gases that have been used as ultrasound contrast agents in microbubbles as the bubble size is reduced to the nanoscale. Further, we look at the production and characterisation of lipid coated nanobubbles.[2] Finally, we consider the potential of "nested nanobubbles" in which lipid coated NBs are encapsulated within 300 nm liposomes for ultrasound triggered release of therapeutic agents.

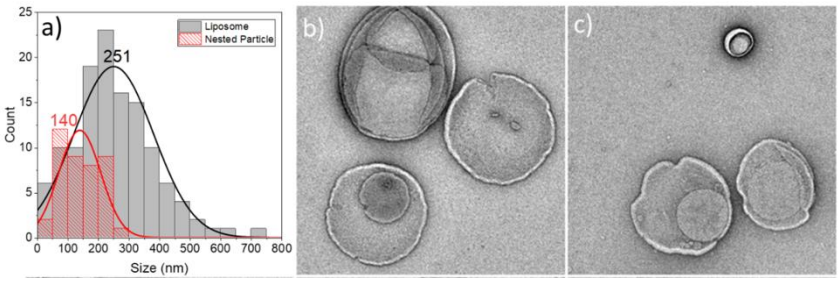

1. Evans DR, Parsons DF, Craig VS. Physical properties of phase-change emulsions. Langmuir. 2006;22(23):9538-45.
2. Peyman SA, McLaughlan JR, Abou-Saleh RH, Marston G, Johnson BRG, Freear S, … Evans SD On-chip preparation of nanoscale contrast agents towards high-resolution ultrasound imaging. Lab on a Chip. 2016;16(4):679-87.

Nanobubble production

The Controllable Formation of Nanobubbles and Nanodroplets on Nanopatterned Structures

Limin Zhou[1], Shuo Wang[2], Jun Hu[1,2], and Lijuan Zhang[1,2]*

1 *Shanghai Synchrotron Radiation Facility, Shanghai Advanced Research Institute, Chinese Academy of Sciences, Shanghai 201204, China*
2 *Shanghai Institute of Applied Physics, Chinese Academy of Sciences, Shanghai 201800, China*

E-Mail corresponding authors: zhanglijuan@zjlab.org.cn

Abstract

The nucleation and stability of nanoscale gas bubbles/nanodroplets located at a solid/liquid interface are attracting significant research interest. It is known that the physical and chemical properties of the solid surface are crucial for the formation and properties of the surface nanobubbles/nanodroplets. Herein, we will report the formation of nanobubbles/nanodroplets on nanostructured substrates [1]. Two kinds of nanopatterned surfaces, namely, nanotrenches and nanopores, were fabricated using an electron beam lithography technique and used as substrates for the formation of nanobubbles. Atomic force microscopy images showed that all nanobubbles were selectively located on the hydrophobic domains but not on the hydrophilic domains. The sizes and contact angles of the nanobubbles became smaller with a decrease in the size of the hydrophobic domains. The results indicated that the formation and stability of the nanobubbles could be controlled by regulating the sizes and periods of confinement of the hydrophobic nanopatterns. The formation of nanodroplets has a similar rule as that of nanobubbles. The experimental results were also supported by molecular dynamics simulations. The present study will be very helpful for understanding the effects of surface features on the nucleation and stability of nanobubbles/nanodroplets at a solid/liquid interface.

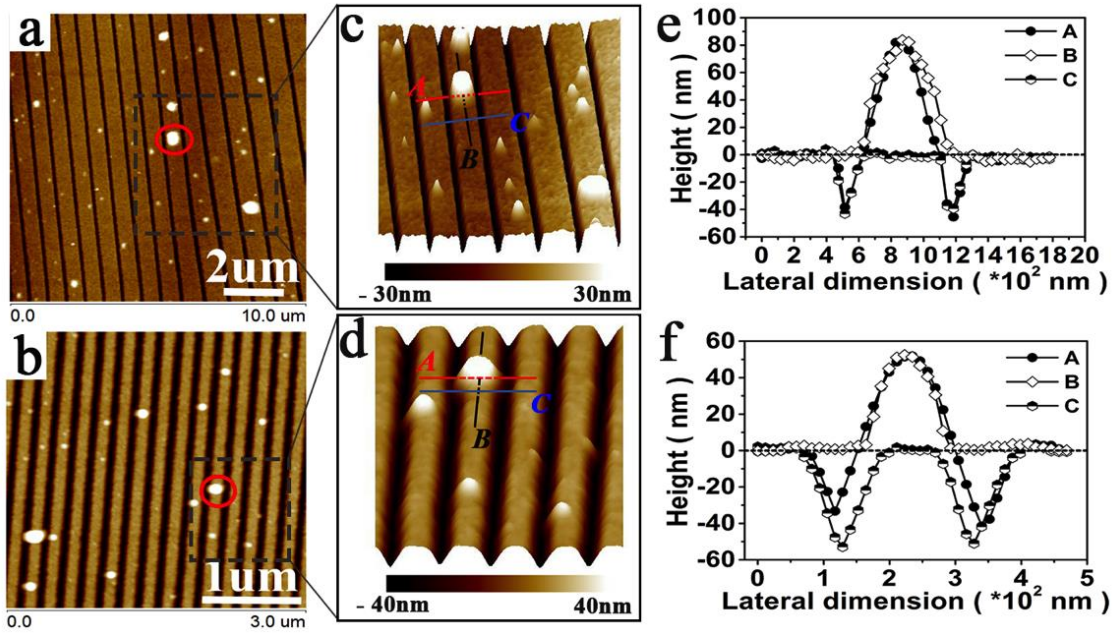

Figure 1. Figure 3 AFM imaging of nanobubbles formed on flat and nanotrench surfaces. (a) Nanobubbles on ZEP coated silicon surface (period/stripes: 500 nm/400 nm). (b) Nanobubbles on PMMA coated silicon surface (period/stripes: 200 nm/100 nm). (c, d) the typical 3D images for the zoom in of (a, b). (e, f) the section profiles of the nanobubbles marked in (a) and (b).

Acknowledgements

The authors thank the staffs at beamline 08U1A in Shanghai Synchrotron Radiation Facilities (SSRF). This work was supported by the National Natural Science Foundation of China (Nos. 11874379, 11575281, 11290165, 11305252, U1532260, 51474254), the Knowledge Innovation Program of the Chinese Academy of Sciences (No. KJZD-EW-M03) and the Key Research Program of Frontier Sciences， CAS (No. QYZDJ-SSW-SLH019).

References

[1] L. Wang, X. Wang, L. Wang, J. Hu, Ch. Wang, B. Zhao, X. Zhang, R. Tai, M. He, L. Chen, and L. Zhang, Formation of Surface Nanobubbles on Nanostructured Substrates. Nanoscale 2017, 9, 1078–1086.

Extrusion: A new method for rapid formulation of high-yield, monodisperse nanobubbles

Claire Counil[1]*, Eric Abenojar[1], Reshani Perera[1], and Agata A. Exner[1]

1 *Department of Radiology, Case Western Reserve University, 10900 Euclid Avenue, Cleveland, Ohio 44106-7207, USA*

E-Mail corresponding authors: claire.counil@case.edu

Background: The use of nanobubbles (NB) has rapidly accelerated in the past decade, with applications ranging from agriculture, to the food industry to medical imaging. In biomedical applications, NBs are used as ultrasound contrast agents for molecular imaging and for targeted drug and gene delivery. Efficient formulation of uniformly sized nanobubbles remains challenging. Current techniques are cumbersome, time consuming and/or require specialized instrumentation, such as microfluidics. In this work, we demonstrate for the first time, the use of simple extrusion, typically utilized for liposome formulation, as a method to generate high-yield, monodisperse lipid shelled nanobubbles. Extrusion represents a quick, low cost alternative to microfluidic formulation that could be easily adapted and scaled up to industrial production of NBs.

Methods: For extruder NBs (e-NB) the standard mini-extrusion setup available from Avanti Polar Lipids was used (Figure 1. A.) [1]. Lipids dissolved in propylene glycol (composition as in [2]) and C_3F_8 gas were placed in gas-tight syringes and the solution was passed 30 times through a 0.8 µm extruder membrane. The resulting solution was centrifuged to isolate the foam and then passed through a polyethersulfone (PES) 0.45 µm filter to ensure complete microbubble removal. For *in-vivo* application, after the extrusion, the resulting NB solution was passed through a 0.8 µm MCE filter and centrifugation was omitted. As a comparison, control NBs (v-NB) were formulated using self-assembly via mechanical agitation using the Vialmix device, as previously described [2]. NBs were characterized by resonant mass measurement (RMM). The acoustic response of the NBs was assessed in a "T"shaped agarose phantom, using a clinical ultrasound system with a 12 MHz center frequency linear array transducer in contrast harmonic imaging mode (MI: 0.2, 1 fps, 65 dB dynamic range, 70 dB gain). The formulations were normalized to the same theoretical gas volume. *In vivo* NB imaging was carried out in mice with the same US probe, and the same parameters (at 0.2 frame/s).

Results: The extrusion process resulted in NBs that are smaller and more monodisperse than those made by mechanical agitation (160 ± 50 nm vs 320 ± 100 nm) (Figure 1.B.). The concentration obtained was lower using the extruder compared to the Vialmix ($6.2 \pm 1.8 \times 10^{10}$ vs $3.2 \pm 0.7 \times 10^{11}$), but the total volume of e-NB was 2.5-3 mL vs 0.5 mL for v-NB. On US imaging, v-NBs had a higher initial acoustic response, in the three regions of interest, Z1, Z2 and Z3, with 30 ± 1 dB compared to 17 ± 5 dB for eNBs for focal region (Z2) (Figure 1.C. and D.). For e-NBs, signal was primarily apparent in Z2 compared to v-NBs where significant activity was also seen in Z1 and Z3. This result suggests a strong pressure dependent acoustic response, which, as predicted, becomes more apparent with a more monodisperse bubble population. After 8 min of US exposure, minimal signal decay was observed for v-NBs. For e-NBs a 50% decay of the initial signal was observed from 17 ± 5 dB to 8 ± 5 dB (Figure 1.D.). Despite the faster signal decay under ultrasound exposure, the acoustic response of e-NBs is considerably more localized. *In vivo*, the acoustic signal was recorded for 30 min in the kidney and liver of the mice. Similar to *in vitro* results, a lower acoustic response and faster signal decay was observed with e-NBs compared to v-NBs (Figure 1.E. and F.). Also, the e-NBs had a lower initial peak response than v-NBs for both liver (9 ± 2 dB vs 13 ± 8 dB) and kidney (13 ± 2 dB vs 17 ± 4 dB) (Figure 1F). This faster decay of *in*

vivo e-NBs may be a result of the improved monodispersity because of the sensitive dependence of acoustic response to NB diameter. In v-NBs, the bubbles likely decay at different rates due to their variable response. [3]

Conclusions: We present proof of concept data for directly producing monodisperse, lipid-shelled C_3F_8 nanobubbles for biomedical applications via a simple extrusion process, which was previously utilized only for liposome and other lipid nanoparticle production. Compared to mechanical agitation, the extrusion process requires no initial MB formulation or differential centrifugation and results in high NB concentration. e-NB stability and acoustic properties can be tuned by optimizing process parameters, which will be the subject of future work.

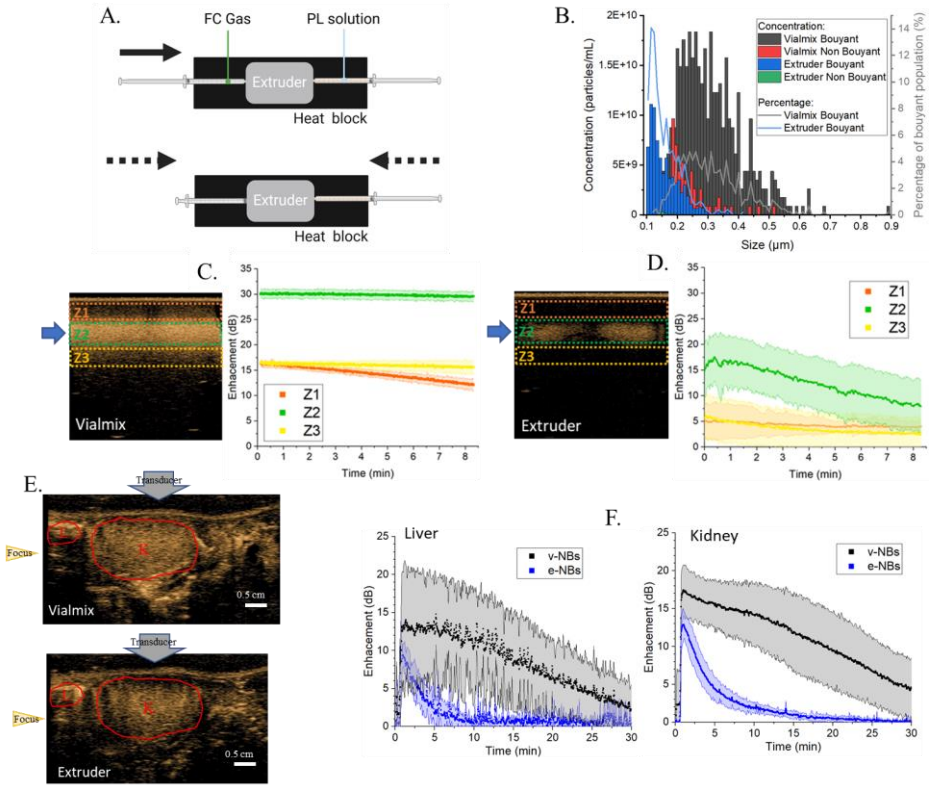

***Figure 1**.(A) Schematic of the extruder process, initial statement (up), pass through the membrane present in the extruder. (B) Physical characterization of buoyant and non-buoyant particles using resonant mass measurement; Contrast harmonic images (12MHz, MI:0.22) at t=0 (left) and representation of the enhancement over 8 min (right) of v-NBs (C) and e-NBs (D). Contrast harmonic images of in vivo e-NBs and v-NBs at t=1min (E).Representation of enhancement of liver (L) and of kidney (K) for v-NB and in vivo e-NBs over 30 min with a NB injection at 30 s (12 MHz, MI:0.2) (F)*

Acknowledgements

We would like to acknowledge funding from the Case-Coulter Translational Research Partnership from CWRU, the National Institutes of Health (Award No. R01EB028144). We thank Dr. Michael Kolios and Dr. Amin Sojahrood from Ryerson University for spirited discussions about NB formulation.

References

[1] Biondi, A. C.; Disalvo, E. A., Biochimica et Biophysica Acta (BBA) - Biomembranes 1990, 1028 (1), 43-48.

[2] A. De Leon, R. Perera, C Hernandez, M. Cooley, O. Jung, S. Jeganathan, E. Abenojar, G. Fishbein, A. J. Sojahrood, C. C. Emerson, P. L. Stewart, M. C. Kolios, A. A. Exner, Contrast enhanced ultrasound imaging by nature-inspired ultrastable echogenic nanobubbles, Nanoscale, 2019 11, 33, 15647-15658

[3] Sojahrood, A. J.; Falou, O.; Earl, R.; Karshafian, R.; Kolios, M. C., Nonlinear Dynamics 2015, 80 (1-2), 889-904. DOI 10.1007/s11071-015-1914-7.

Interaction of drops and bubbles with nano- and microstructured surfaces

Hans-Jürgen Butt

Max Planck Institute for Polymer Research, Ackermannweg 10, 55128 Mainz, Germany

Wetting phenomena surround us every day and are relevant for technological applications such as printing, painting, coating, heat transfer, flotation, bringing out herbicides and insecticides. Making surfaces with defined wetting properties is one of the big engineering challenges, in particular fabricating liquid repellent surfaces. Liquid repellency includes two aspects: High receding contact angles and low friction of drops. In the first case, sessile drops show a low adhesion in normal direction; they can easily be taken off vertically. Super liquid-repellent surface fall in this category. In the second case, drops have low lateral adhesion and slide off surfaces, which are only slightly tilted. Some polymer brushes, lubricant-infused polymer brushes and lubricant-infused porous surfaces belong to this category. Different types of liquid repellent surfaces will be discussed. Effects leading to friction are described and methods to characterise surface are highlighted.

Generation of bulk nanobubbles in pure alcohol

Harsh Sharma[1] and Neelkanth Nirmalkar[1]*

1 *Department of Chemical Engineering, Indian Institute of Technology Ropar, Rupnagar140001, Punjab, India*

E-Mail corresponding authors: n.nirmalkar@iitrpr.ac.in

Abstract

Nanobubbles (NB's) are extremely small gas pockets with diameters in the nanometer range. The applications of nanobubbles in process industries has been grown rapidly over the last decade due to their extraordinary properties, for instance, long-term stability in aqueous solutions, ROS generation capability, high gas transfer efficiency in bulk liquids, and enhanced rate of mass transfer coefficient. The extralongevity of the nanobubbles in water plausibly may be due to the dangling OH bonds and the surface charge on the bubbles, however, the exact mechanism is still not clear. Most of the recent literature dedicated to the formation of bulk nanobubbles in water and their usage in diverse engineering and medical applications, the scant experimental studies have been reported the nanobubbles in organic solvents but there is no strong scientific evidence were provided. In this work, we successfully generated bulk nanobubbles in pure alcohols and provided a scientific evidence based on the refractive index measurement of individual nanobubbles. The acoustic cavitation method is utilized to generate nanobubbles in ethanol and isopropyl alcohol (IPA). A probe-type ultrasonic processor have been used, to generate nanobubbles in pure alcohol. The ultrasonication amplitude varied ranging from 25 to 98 percent with 5 mins of sonication time. Nanobubbles were characterized using NTA (Nanoparticles tracking analysis) and DLS (Dynamic light scattering). The population, diameter, refractive index, and zeta potential of NBs in alcohols were demonstrated, and shown in **Fig. 1**. The formation of nanobubbles was observed to be higher in IPA than in ethanol, with a maximum bubble number density of 8.56 X 10^7 bubbles per ml at 40 percent amplitude. The zeta potential values and the diameter of the generated nanobubbles are shown in Fig. 1(c) and (b), respectively; the diameter of the nanobubbles in both alcohols was in the range of 120-140 nm at every ultrasonication amplitude. The zeta potential in ethanol is negative, which enables them for long-term stability in solution, whereas in IPA, the zeta potential values are around ±5 mV. The probable reason for the zero surface in IPA could be absence of the dangling OH bond at the interface [1]. Furthermore, to distinguish the nanobubbles from the nanoparticles, we have calculated the refractive index of each nanobubble suspension using Mie scattering theory [2]. The refractive index values for all nanobubbles samples were found to be close to one (RI for air = 1), indicating that the nanoparticles produced are gas-filled nanobubbles. From application viewpoint, nanobubbles in alcohol system has the potential to significantly improve the reactions and interactions of gas-liquid in alcohols.

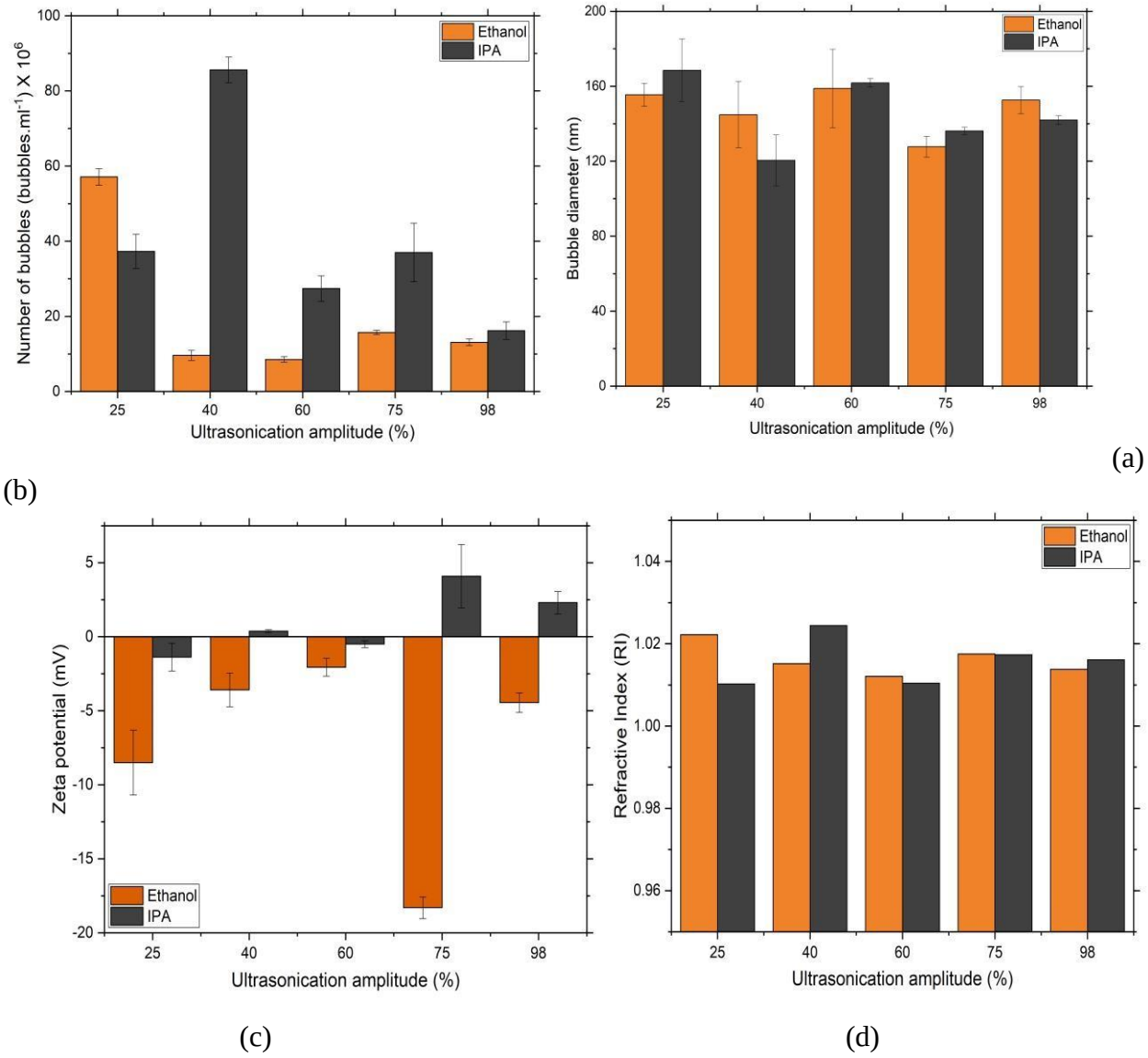

Figure 1. Bulk nanobubbles generated by ultrasonic cavitation method; (a) Bubble number density, (b) Bubble diameter, (c) Zeta potential values, (d) Refractive Index.

Acknowledgements

TIF-AWaDH (Technology Innovation Hub- Agriculture and Water Technology Development Hub), Department of Science and Technology, India, provided funding for this research.

References

[1] Ji, Yuwen, et al. "Generating bulk nanobubbles in alcohol systems." *ACS omega* 6.4 (2021): 2873-2881.
[2] Agarwal, Kalyani, Mohit Trivedi, and Neelkanth Nirmalkar. "Does salting-out effect nucleate nanobubbles in water: Spontaneous nucleation?." *Ultrasonics sonochemistry* 82 (2022): 105860.

Diameter Dependence of CO_2 Ultra Fine Bubble between Zeta Potential and Water Ions

Yoshikatsu Ueda[1]*, Seina Ozeki[1], Tetsuji Okuda[2], and Yomei Tokuda[3]

1 *Research Institute for Sustainable Humanosphere, Kyoto University*
2 *Faculty of Advanced Science and Technology, Ryukoku University*
3 *Faculty of Education, Shiga University*

E-Mail corresponding authors: yueda@rish.kyoto-u.ac.jp

Abstract

Fine Bubbles (FB) of typically smaller than 100 µm in size is defined by ISO/TC 281 (Fine bubble technology). They also defined Micro Bubbles (MB) of bigger than 1 µm and less than 100 µm and Ultra Fine Bubbles (UFB) of less than 1 µm. The study of UFB has recently attracted much attention, but it is specialized in applied research applications. On the other hand, although the fundamental properties of UFBs are gradually being elucidated, there are still many fundamental principles that are not yet understood, such as the control of particle size and the mechanism of action for applied use. In order to understand the basic principle of UFB, we generated UFB water using carbon dioxide and measured its properties. In particular, the relationship between the properties of the water (pH and conductivity) and the properties of the bubbles (particle size distribution and zeta potential) was confirmed in detail.

The zeta potential of UFB refers to the state of electrical charge. It can be measured as a characteristic of the gas-liquid interface between water and bubbles, and bubbles are generally negatively charged. Since carbon dioxide dissolves well in water, it is possible to easily change the pH and electrical conductivity of water without adding other impurities. For carbon dioxide UFB, UFB water was prepared under the same conditions by running the generator with cooling. By diluting the UFB water with pure water, the pH and electrical conductivity were changed easily, and the bubble characteristics were measured simultaneously.

As a result, we found that the particle size of carbon dioxide UFB changes due to the change in pH and electrical conductivity caused by dilution. In carbon dioxide UFB water, there are hydroxide ions and carbonate ions as water ions. The pH is around 4, the only carbonate ion presents as H_2CO^-, and there are only two types of negative ions, including hydroxide ions. According to our measurements, the hydroxide ions may gather around the bubbles and change the bubble size smaller. In the near future, the relationship between the negative ions in the water and the UFB size should be clarified by direct detection of the internal pressure of the UFB and measurement of the -dissolved gas concentration of carbon dioxide, which are currently being conducted in our study group.

Formation and stability of nanobubbles and pre-nucleation clusters during ultrasonic treatment of hard and soft water

Eavan Fitzgerald, Sruthy Poulose and J. M. D. Coey*

School of Physics, Trinity College, Dublin, Ireland

**E-Mail jcoey@tcd.ie*

Abstract

A series of eight water samples ranging in hardness from deionized Millipore water to commercial hard mineral water with 332 mg/L $CaCO_3$ were continuously sonicated for periods of 5′ - 45′ using a 100 W, 30 kHz ultrasonic generator. The resulting temperature, z-potential, conductivity and pH and of the water were analysed, together with the crystal structure of any calcium carbonate precipitate. Quasi-stable populations of bulk nanobubbles characterized by a z-potential of -45 to -30 mV were formed in Millipore and soft water, decaying with a half-life of 72 h (Figure 1), but nanobubble loading of the hard water was impeded after 10′ of sonication when the ambient temperature reached 45°C. The z-potential then jumped from -15 mV to almost +20 mV (Figure 2) and the water turned cloudy. This is attributed to the appearance of colloidal amorphous calcium carbonate (ACC) [1]. The z-potential remained positive for several days, but if subjected further heating to 100℃, crystalline calcium carbonate is precipitated and the z-potential of the suspension falls to -5 mV. If the solution is then allowed to settle and the supernatant is sonicated, there is an increase in its conductivity and pH, but no further precipitation occurs and z remains below 0 mV. The residue was dried in an oven at 80℃ and the solid material was found by X-ray diffraction and scanning electron microscopy to be mainly composed of needle-shaped aragonite crystals. Heating the hard water on a hotplate without any prior sonication also gives aragonite, but when the water is evaporated in an oven at 80℃, the precipitate is mostly calcite. Analysis of the change of conductivity of the hard water before and after sonication leads to a new estimate of the proportion of Ca^{2+} present in nanoscale prenucleation clusters (also known as DOLLOPS [2]), which exceeds 25%. It is suggested that nanobubbles created in the early stage of sonication of hard water (<10′) may be associated with the nanoscale colloidal DOLLOPS.

Acknowledgements
The authors are grateful for support from the Marie Curie Horizon 2020 International Training Network on Magnetism and Microhydrodynamics (MAMI) contract number 766007.

References

[1] Gale Raiteri P, Gale J D Water Is the Key to Nonclassical Nucleation of Amorphous Calcium Carbonate J. *Amer Chem* Soc 132 176223 (2010)
[2] Demichelis R, Raiteri P, Gale J D, Quigley D and Gebauer D, Stable prenucleation mineral clusters are liquid-like ionic polymers, *Nature Communications* 2 590 (2011)

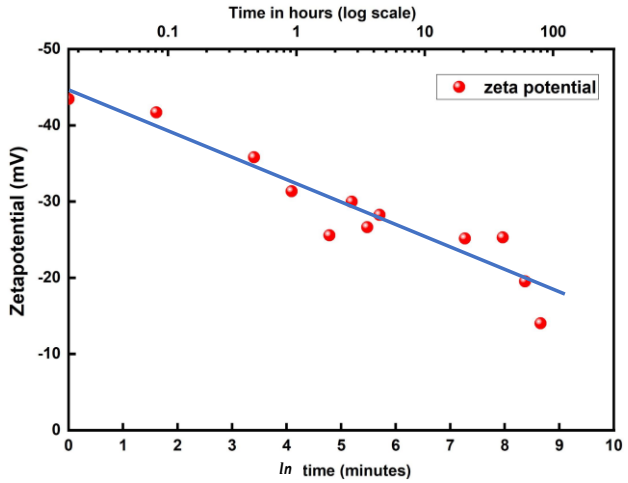

Figure 1. Decay of ζ-potential of sonicated Millipore water over four days.

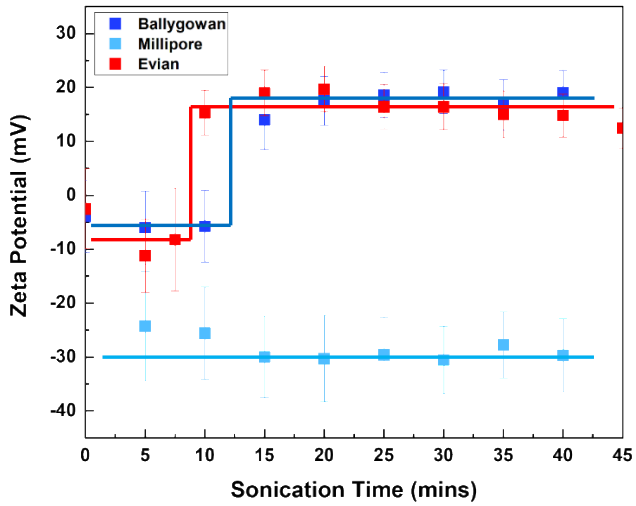

Figure 2. Evolution of the ζ-potential of Millpore, and two hard waters with sonication

Laser Induced Nanobubbles: Characterization Methods and Future Perspectives

Juan Manuel Rosselló[1,*] and Claus-Dieter Ohl[1]

1 Otto von Guericke University Magdeburg, Institute of Physics, Department of Soft Matter, Universitätsplatz 2, 39106 Magdeburg, Germany

E-Mail corresponding authors: jrossello.research@gmail.com

Abstract

In this work we present a tailored system used for producing multiple nanobubbles homogeneously distributed in a defined volume of filtered water. The bubble nucleation method consists in illuminating the liquid with a non-focused high-power laser beam, as described by Rosselló and Ohl in Ref. [1]. This novel bubble generation method has many advantages regarding the "cleanness" of the nanobubble preparation. As the laser nucleation technique do not require of moving parts, like for instance the usual mechanical agitation methods, the final sample is unlikely to get contaminated with additional oil drops or solid particles originated, for instance, by cavitation erosion [2]. An important part of our experimental method was the implementation of an acoustic bubble detection technique, which consists in passing a rarefaction wave through the volume where the bubbles were formerly "seeded" by the laser beam.

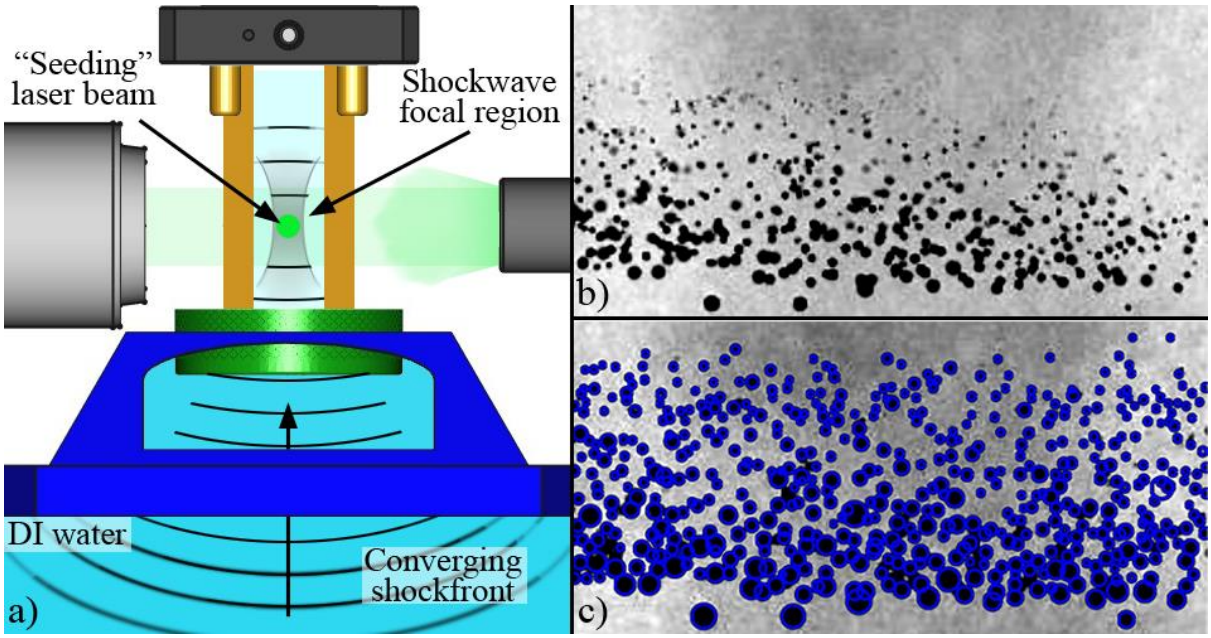

Figure 1. A reduced volume of the liquid sample contained in a tailored 3D printed cuvette is illuminated with a high-power laser pulse and bulk nanobubbles are produced. After a time Δt, a medical grade lithotripter focuses a shock/tension wave on the cuvette and the nanobubbles become visible. (a) General view of the setup. The tailored cuvette of 1.5 cm of side is held from its top from four points and partially submerged in the DI water which transmits the pressure wave generated by the lithotripter plate. The illumination in the shadowgraph images is performed with a green pulsed laser light transported with an optical fiber. (b) As the rarefaction wave advances the produced bubbles became visible from a direction perpendicular to the seeding laser beam. (c) The bubble number, size and position was characterized using a state of the art bubble recognition algorithm based on the Hough transform [3].

The expansion of the bubbles provoked by the rarefaction wave was key to observe the cavitation nuclei though standard optical microscopy, as shown in Figure 1. The seeding and expansion of the gas cavities was captured using high-speed video recordings taken at 5 Mfps and femtosecond laser illumination. The images were analyzed with a *state of the art* bubble

recognition algorithm based on the Hough transform [3]. This allowed us to characterize the number of bubbles within a region of interest for a variety of experimental scenarios. In particular, we explored the effect of having different energy in the seeding laser pulse and different amplitudes of acoustic pressure in the rarefaction wave. Finally, we estimated the rest radius of the bubble cluster by comparing the results with numerical simulations performed using the Keller-Miksis model for bubble dynamics [4] or the Epstein-Plesset theory for bubble dissolution [5].

Acknowledgements

J.M.R acknowledges support by the Alexander von Humboldt Foundation (Germany) through the Georg Forster Research Fellowship.

References

[1] J. M. Rosselló and C.-D. Ohl, "On-Demand Bulk Nanobubble Generation through Pulsed Laser Illumination", *Phys. Rev. Lett.* **2021,** 127 (4), 044502.
[2] A. J. Jadhav and M. Barigou, "Bulk Nanobubbles or Not Nanobubbles: That is the Question", *Langmuir* **2020**, 36 (7), 1699–1708.
[3] T. Atherton, D. Kerbyson, Size invariant circle detection, *Image and Vision Computing* 17 **1999**, 11, 795–803.
[4] U. Parlitz, V. Englisch, C. Scheffczyk, and W. Lauterborn, Bifurcation structure of bubble oscillators, *The Journal of the Acoustical Society of America* **1990**, 88, 1061.
[5] P. B. Duncan and D. Needham, Test of the Epstein-Plesset model for gas microparticle dissolution in aqueous media: Effect of surface tension and gas undersaturation in solution, *Langmuir* **2004**, 20, 2567.

Predicting nucleation in real fluids

F. Magaletti[1], M. Gallo[2], and C.M. Casciola[2]*

1 *Advanced Eng. Centre, School of Computing Engineering and Mathematics, Univ. of Brighton, Lewes Road, Brighton, BN2 4GJ, UK.*
2 *Dept. of Mechanical and Aerospace Eng., Sapienza University of Rome, via Eudossiana 18 Roma, Italy.*

E-Mail corresponding author: carlomassimo.casciola@uniroma1.it

Abstract

Cavitation is a ubiquitous phenomenon whose prediction proved a formidable task, particularly in the case of water. Here a self-contained model is discussed which is shown able to accurately reproduce cavitation data for bulk water over the most extended range of temperatures for which accurate experiments are available — left panel in fig. 1. The computations are based on a diffuse interface model which, as only inputs, requires a reliable equation of state for bulk free energy and interfacial tension of the water-vapor system combined with rare event techniques borrowed from statistical mechanics. By consistently including thermal fluctuations in the spirit of Fluctuating Hydrodynamics, the approach is extended to dynamic conditions in presence of solid walls of different wettability — right panel in fig. 1 — to allow coupling with fluid motion. The talk will focus on the wall wettability in compliance with the fluctuation-dissipation balance, a crucial point in the context of the fluctuating hydrodynamics theory. Depending on time availability, new, still unpublished results concerning the coupling of nucleation and fluid flow (fig. 2), the effect of micro-confinement, and time-changing thermodynamic conditions will also be addressed.

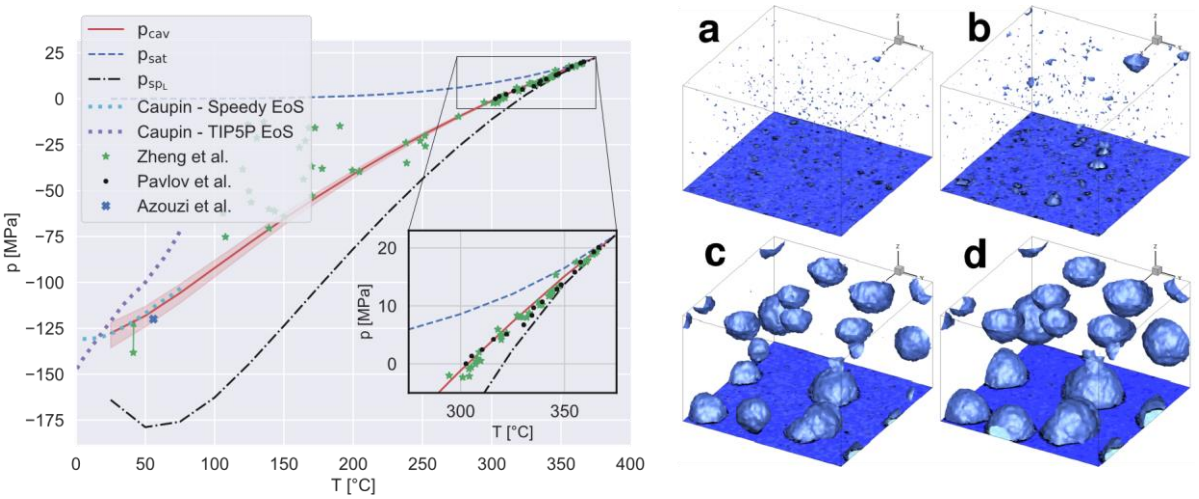

Figure 1: (left) Cavitation pressure as a function of temperature in bulk water (experiments vs simulations). (b) Dynamic bubble nucleation at a solid wall.

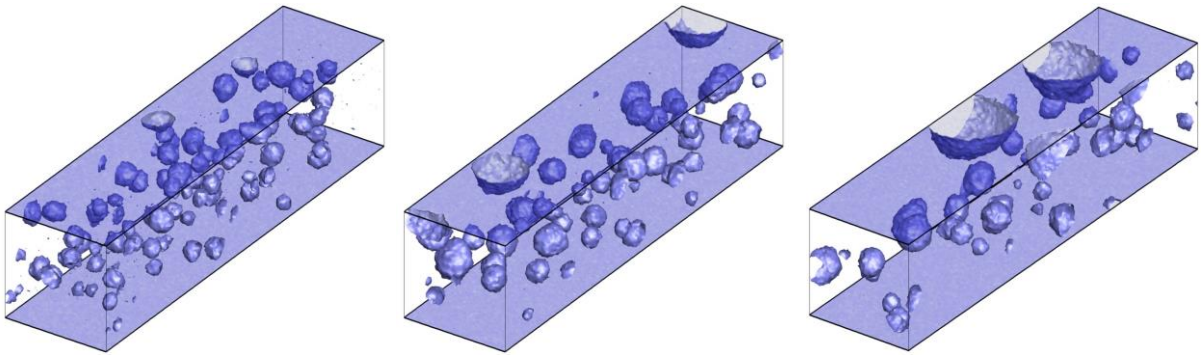

Figure 2: Bubble nucleation in a liquid flowing over solid surfaces

Acknowledgments

Generous computer resources on Marconi 100 CINECA obtained in the context of the PRACE call 20 project BIMI are kindly acknowledged.

References

[1] F. Magaletti, M. Gallo, C.M. Casciola, Water cavitation from ambient to high temperatures, Scientific Reports 2021, 11 1.
[2] M. Gallo, F. Magaletti, C.M. Casciola, Heterogeneous bubble nucleation dynamics, Journal of Fluid Mechanics 2021, 906 10.
[3] M. Gallo, F. Magaletti, D. Cocco, C.M. Casciola, Nucleation and growth dynamics of vapor bubbles, Journal of Fluid Mechanics 2020, 883. [3] M. Gallo, F. Magaletti, C.M. Casciola, Thermally activated vapor bubble nucleation: the Landau-Lifshitz/Van der Waals approach, Phys. Rev. Fluids. 2018, 3, 053604

Molecular Dynamics

Molecular dynamics analysis of interfacial tensions of surface nanobubbles: mechanical and thermodynamic approaches

Hideaki Teshima[1,2]*, Hiroki Kusudo[3], Carlos Bistafa[3], and Yasutaka Yamaguchi[3,4]

1 *Department of Aeronautics and Astronautics, Kyushu University, Nishi-Ku, Motooka 744, Fukuoka, 819-0395*
2 *International Institute for Carbon-Neutral Energy Research (WPI-I2CNER), Kyushu University, Nishi-Ku, Motooka 744, Fukuoka, 819-0395*
3 *Department of Mechanical Engineering, Osaka University, 2-1 Yamadaoka, Suita, 5650871*
4 *Water Frontier Research Center (WaTUS), Tokyo University of Science, Shinjuku-Ku, Kagurazaka 1-3, Tokyo, 162-8601*

E-Mail corresponding authors: hteshima05@aero.kyushu-u.ac.jp

Abstract

Surface/interfacial nanobubbles have been investigated since the first experimental observation in 2000 [1,2] and a number of studies have reported their unique properties [3], such as larger contact angles than those observed on a macroscale, long-lifetime that cannot be explained by classical thermodynamic theory, and superstability against the disturbance. Recently, a scanning transmission X-ray microscope experiment by Zhou et al. [4] revealed a new characteristic of surface nanobubbles: oxygen surface nanobubbles confined in an X-ray window have a density one to two orders of magnitude higher than that under ambient conditions. This ultrahigh inner density of surface nanobubbles gives us a new question of whether their interfacial tensions are changed due to more frequent interactions among atoms at interfaces. If changed, it will be a new candidate to rationalize the unique characteristics of surface nanobubbles. However, although the quantification of their interfacial tensions is highly desired, direct experimental measurement of them is extremely difficult because of the inherently involved various uncertainties. Moreover, to the best of my knowledge, quantitative values of the solid-gas and solid-liquid interfacial tensions of surface nanobubbles have not been reported so far.
In this contribution, we quantified the liquid-gas, solid-gas, and solid-liquid interfacial tensions of nitrogen nanobubbles at the interface of graphite and water (Figure 1) by molecular dynamics analysis via mechanical and thermodynamic approaches. Based on the obtained results, we discuss how far the change of interfacial tensions caused by ultrahigh inner gas density can explain the experimentally observed contact angles of surface nanobubbles (150-175°) without considering pinning effect.

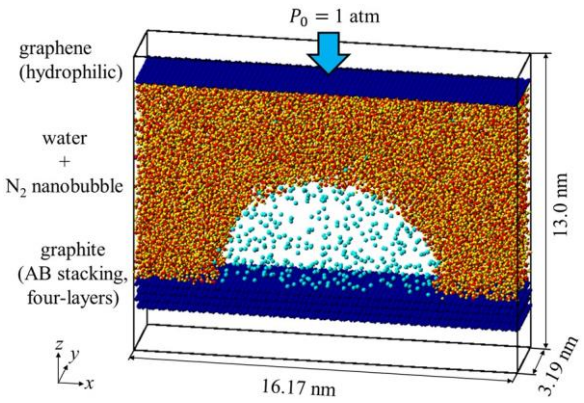

Figure 1. Simulation system of a nitrogen nanobubble in water.

The liquid-gas and solid-gas interfacial tensions were calculated by Bakker's equation, whereas the solid-liquid interfacial tension was quantified by the thermodynamic integration method. These types of calculation methods of interfacial tensions [5] are called the "mechanical route" and "thermodynamic route", respectively. The details of the methods used for the calculation of interfacial tensions are found in [6].

We found that the values, especially for the solid-gas interfacial tension, were affected by the gas density inside nanobubbles (Figure 2(a)). However, our simulations expanded to submicron-sized surface bubbles (Figure 2(b)) also revealed that the gas density effect on the contact angles becomes negligible when the footprint radius is larger than 50 nm, which is a typical range observed in experiments. In addition, even for the footprint radius smaller than 100 nm, the estimated contact angles did not reach the typical experimental values of 150-170°. Our results indicate that the van der Waals interaction-induced gas molecular adsorption cannot explain the flatness of surface nanobubbles and show the necessity of the pinning for the satisfactory explanation of the unique properties of surface nanobubbles.

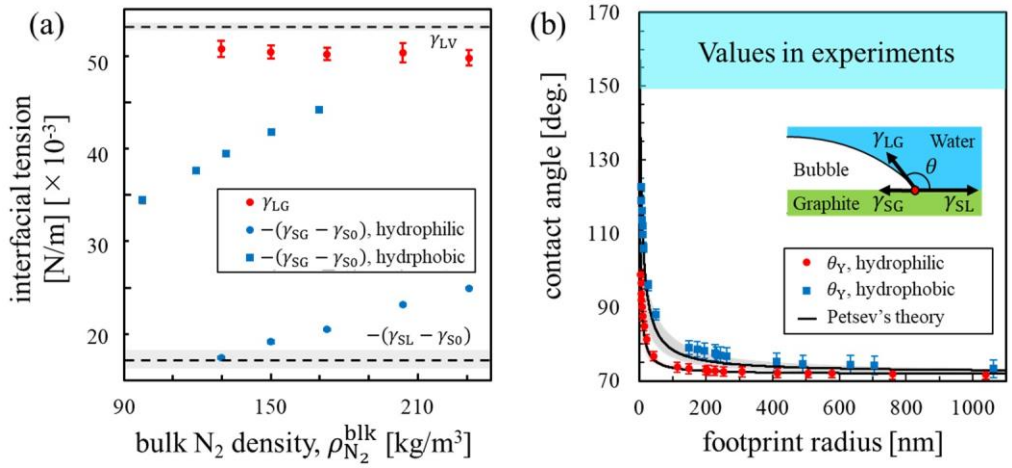

Figure 2. (a) Interfacial tensions versus the bulk nitrogen density inside nanobubbles. (b) A semispherical nanobubble's contact angle versus footprint radius.

Acknowledgements

This work was partially supported by JST CREST Grant No. JPMJCR18I1, JSPS KAKENHI Grant No. JP18K03978 and JP21K20405, and the Grant-in-Aid for **JSPS** Research Fellow No. JP20J01307 and JP20J20251.

References

[1] N. Ishida, T. Inoue, M. Miyahara, K. Higashitani, Nano bubbles on a hydrophobic surface in water observed by tapping-mode atomic force microscopy, *Langmuir*. **2000**, 16 6377–6380.

[2] S.-T. Lou, Z.-Q. Ouyang, Y. Zhang, X.-J. Li, J. Hu, M.-Q. Li, F.-J. Yang, Nanobubbles on solid surface imaged by atomic force microscopy, *J. Vac. Sci. Technol. B Microelectron. Nanom. Struct.* **2000**, 18 2573.

[3] D. Lohse, X. Zhang, Surface nanobubbles and nanodroplets, *Rev. Mod. Phys.* **2015**, 87 981–1035.

[4] L. Zhou, X. Wang, H.J. Shin, J. Wang, R. Tai, X. Zhang, H. Fang, W. Xiao, L. Wang, C. Wang, X. Gao, J. Hu, L. Zhang, Ultrahigh Density of Gas Molecules Confined in Surface Nanobubbles in Ambient Water, *J. Am. Chem. Soc.* **2020**, 142 5583–5593.

[5] Y. Yamaguchi, H. Kusudo, D. Surblys, T. Omori, G. Kikugawa, Interpretation of Young's equation for a liquid droplet on a flat and smooth solid surface: Mechanical and thermodynamic routes with a simple LennardJones liquid, *J. Chem. Phys.* **2019**, 150 044701.

[6] H. Teshima, H. Kusudo, C. Bistafa, Y. Yamaguchi, Quantifying interfacial tensions of surface nanobubbles: How far can Young's equation explain?, *Nanoscale*. **2022**, 14 2446–2455

Synergy between Surface Nanobubbles and the Interfacial Gas Enrichment Layer : A Molecular Dynamics Study

Binu Varghese[1] and Sarith P. Sathian[1]

Department of Applied Mechanics, Indian Institute of Technology Madras, Chennai 600036, India

sarith@iitm.ac.in, binuammi15@gmail.com

Abstract

Submicroscopic bubbles or nanobubbles sit on a bed of dense gas layer, which forms over the hydrophobic substrate. The interfacial gas enrichment layer acts as a gas reservoir for the nanobubble. We perform molecular dynamics simulations to study the characteristics and stability of the interfacial gas enrichment layer over graphene substrate and report the conditions for the stability of the dense gas layer. The thickness of the gas enrichment layer is 7.0 nm, and the Knudsen number is ~ 0.2, indicating an early transition regime. Simulations point out that gases show no particular liking for hydrophobic substrates, but the weak interaction between graphene and water molecules makes the adsorption of gas molecules at high density possible. However, gases prefer adsorption at walls for minimum energy irrespective of the wetting characteristics of the wall. We then extend our simulations to study surface nanobubbles sitting on top of the gas layer and evaluate the response of the nanobubble and the gas layer throughout simulation time. The nanobubble is characterized using the base radius, contact angle, and the number of gas molecules inside the bubble and find that the nanobubble could remain immune to dissolution over the whole simulation period. Continuous gas exchange between the nanobubble and the gas enrichment layer occurs, which plays an essential role in the stability of the nanobubble. The mass flux moving out of the bubble surface at the gas-liquid interface is compensated by the mass influx from the gas layer. Our study provides data to relate the response of the nanobubble-gas layer system to shear flows quantified using the rarefied gas cushion model. We expect our study to aid in the understanding of the synergy between the nanobubble and the interfacial gas enrichment layer, which can help design better fluid mechanical nanoscale devices.

Anomalous thermal effects in oscillating bulk nanobubbles

Duncan Dockar[1], Livio Gibelli[1], and Matthew K. Borg[1]

1 *School of Engineering, Institute of Multiscale Thermofluids, The University of Edinburgh, Edinburgh EH9 3FB, UK*

E-Mail corresponding authors: d.dockar@ed.ac.uk

Abstract

Bulk nanobubbles are being employed in waste-water treatment, biomedicine, and cleaning of microfluidic devices. Exploiting their cavitation dynamics for these applications requires understanding of the internal gas' thermal expansion behaviour, which can be represented by an exponent term k in the polytropic gas law: $P_g R^k = \text{const.}$, where P_g is the gas pressure, and R is the bubble radius. Classical models show how k varies between 1 and 1.4 (in air bubbles) for the limits of isothermal and adiabatic expansion, respectively, by increasing the Péclet number Pe **[1–3]**. However, these models fail to predict the apparent adiabatic behaviour of nanobubbles, observed in recent simulations **[4]**. Here we show how the non-ideal and non-equilibrium internal gas phase gives rise to adiabatic-like behaviour at much lower Péclet numbers than previously expected, and find good agreement with our Molecular Dynamics (MD) simulations. Our proposed model incorporates the van der Waals gas equation of state, and a temperature jump at the liquid-gas interface, which become important for all nanobubble with radii $R < 10^{-6}$ m. We also critically discuss how the thermal behaviour of the nonideal gas can affect our usual interpretation of the polytropic gas law, and we determine more accurate limits of k for isothermal and adiabatic expansion in nanobubbles.

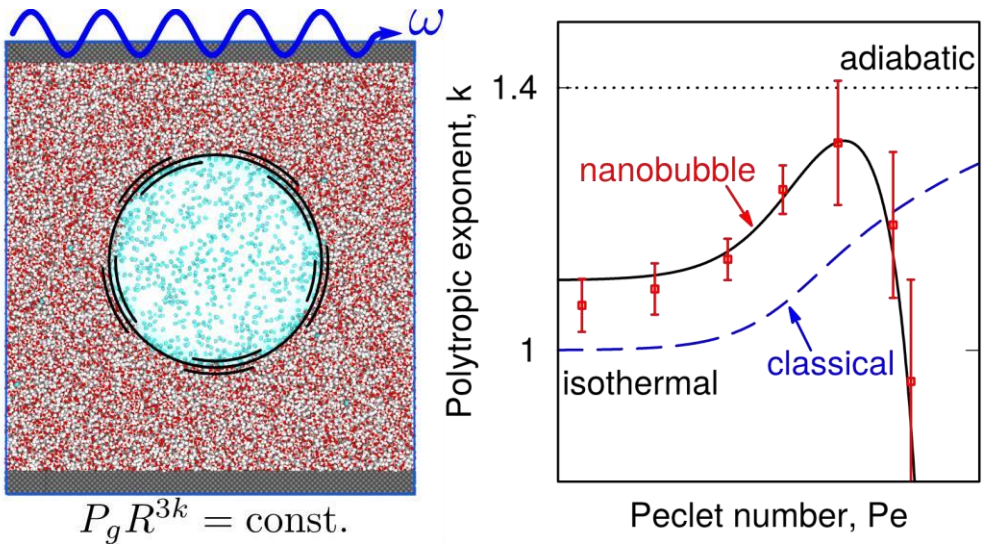

Figure 1. Left: schematic of Molecular Dynamics (MD) simulation (left). Right: variation in polytropic exponent k with Péclet number Pe, for our MD simulations (symbols), and compared with classical theory (dashed line) and our proposed "nanobubble" theory (solid line).

Acknowledgements

This work is supported in the UK by the Engineering and Physical Sciences Research Council (EPSRC) under grants EP/N016602/1, EP/R007438/1 and EP/V012002/1. All MD simulations were run on ARCHER2, the UK's national supercomputing service.

References

[1] C. Devin, Survey of Thermal, Radiation, and Viscous Damping of Pulsating Air Bubbles in Water, *J. Acoust. Soc. Am.* **1959***, 31*, 1654–1667.

[2] A. Prosperetti, L. A. Crum and K. W. Commander, Nonlinear bubble dynamics, *J. Acoust. Soc. Am.* **1988***,* 83, 502–514.

[3] A. Prosperetti, "The thermal behaviour of oscillating gas bubbles," *J. Fluid Mech.* **1991***,* 222, 587–616.

[4] D. Dockar, L. Gibelli and M. K. Borg, Forced oscillation dynamics of surface nanobubbles, *J. Chem. Phys.* **2020***,* 153, 184705.

Investigating Gas Cluster in Water without Pinning Ions Using Molecular Dynamics Simulation

Tsu-Hsu Yen*

Department of Marine Science, R.O.C. Naval Academy, No. 669, Junxiao Road, Zuoying, Kaohsiung 813, Taiwan, R.O.C.

E-Mail corresponding authors: g960403@gmail.com

Abstract

Gas clusters suspended in an aqueous solution are considered a source of interfacial and bulk nanobubbles. According to The Young-Laplace equation, the high internal gaseous pressure should drive gas molecules to resolve into the water domain within milliseconds. In addition, the perturbation in the nanobubble's radius should destroy the equilibrium causing the dissolution of the nanobubble even under ambient gas oversaturation conditions. However, the fact that bulk nanobubbles exist raises questions about the mechanism underlying their stability. Researchers [1-3] have posited a number of theories to explain the stability of bulk nanobubbles (BNBs). Some researchers have attributed stability to hydrophobic contamination adsorption at the gas-water interface. The hydrophobicity of solid segments greatly reduces interfacial tension with a corresponding effect on BNB stability. Other researchers have attributed these effects for pinning charge at the interface, where electrostatic repulsion between charges at the gas-water interface alters pressure in the region proximal to the interface, thereby leading to equilibrium.

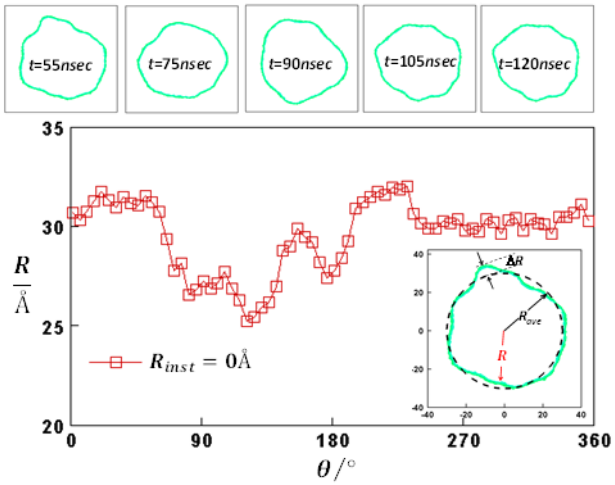

Figure 1. Instantaneous radius, R, as a function of radial direction in a deformed 2D cylindrical gas cluster. The time evolution contours of the water-gas interface are shown in the top panels. The insert shows a contour typical of a water-gas interface indicating the average radius, instantaneous radius, and difference between the two.

In the current study, we used molecular dynamics simulation to investigate cylindrical gas clusters in pure water. To analyze the gas-water interface with high precision, we adopted the spatial coarsegraining (SCG) method [4] to enable the calculation of instantaneous density. Fig. 1 presents a typical instantaneous radius profile in the angular direction. We first compared the density profiles of water and gas proximal to the interface using the SCG method. We then calculated the size and fluctuations in radius for various gas species. The interfacial properties were examined by calculating fluid densities, the molecular orientation of water, the average

number of hydrogen bonds and atomic partial charge distribution proximal to the gas-water interface.

In our simulations, proportional to density inside the cluster, the magnitude of gas concentration demonstrated the necessity of high oversaturation conditions in the ambient water region. Our spectral analysis revealed that despite changes in the size of gas a cluster, high-frequency morphological deformation can prevent it from entering a negative cycle and thereby enhance cluster stability. Pressure in the gaseous region was shown to have little influence on the structure of the interfacial water network. By contrast, increasing ambient pressure was shown to increase $\langle n_{HB} \rangle$ in the gaseous region with a corresponding decrease in the amplitude of density oscillation of oxygen atoms in the solvent region. The unique allocation of interfacial charges may be indicative of electrostatic stress. The calculated electrostatic stress was far below the magnitude of interfacial tension; however, it induce considerable reverse stress within the area proximal to the interface. In the current study, several effects were shown to work together to stabilize the gas clusters in water, including high-frequency morphologyical deformation, reduced interfacial tension, and gas oversaturation conditions. Our results suggest that gas clusters can exist in water under gas oversaturation conditions in the absence of hydrophobic contaminates or pinning ions at interfaces.

Acknowledgements

We acknowledge financial support from the Ministry of Science and Technology ROC 110-2221-E012-002

References

[1] L. Zhou, S. Wang, L. Zhang, J. Hu, Generation and Stability of Bulk Nanobubbles: A Review and Perspective, Current Opinion in Colloid & Interface Science, 2021, Vol. 53, 101439.

[2] H. Zhang, Z. Guo, X. Zhang, Surface enrichment of ions leads to the stability of bulk nanobubbles, Soft Matter, 2020, Vol. 16, pp.5470-5477.

[3] B.H. Tan, H. An, C.-D. Ohl, Stability of surface and bulk nanobubbles, Current Opinion in Colloid & Interface Science, 2021, Vol. 53, 101428.

[4] A.P. Willard, D. Chandler, Instantaneous liquid interfaces, The Journal of Physical Chemistry B, 2010, Vol. 114, pp. 1954-1958.

Cavitation in lipid bilayers poses strict negative pressure stability limit in biological liquids

Matej Kanduč,[1] Emanuel Schneck,[2] Philip Loche,[3] Steven Jansen,[4] H. Jochen Schenk,[5] and Roland R. Netz[3]

1 *Department of Theoretical Physics, Jožef Stefan Institute, 1000 Ljubljana, Slovenia*
2 *Physics Department, Technische Universität Darmstadt, 64289 Darmstadt, Germany*
3 *Fachbereich Physik, Freie Universität Berlin, 14195 Berlin, Germany*
4 *Institute of Systematic Botany and Ecology, Ulm University, 89081 Ulm, Germany*
5 *Department* of Biological Science, California State University, Fullerton, CA 92831

E-mail: matej.kanduc@ijs.si

Many biological and technological processes involve liquids under negative pressure. A prominent example is plants, which use negative pressures to suck water from the soil into their leaves. A long-debated mystery is why the maximal negative pressures are approximately -100 bar. We investigated [1] how small solutes and lipid bilayers, both constituents of all biological liquids, influence the formation of cavities under negative pressures. We quantified cavitation rates on biologically relevant length scales and timescales by combining molecular dynamics simulations with kinetic modeling. In contrast to small solutes, we find that lipid bilayers increase the rate of cavitation, which remains unproblematically low at the pressures found in most plants. Cavitation occurs only when the negative pressures approach -100 bar on biologically relevant timescales. Our findings suggest that lipid aggregates impose an upper stability limit for the magnitude of negative pressures in biological liquids [1].

[1] M Kanduč, E Schneck, P Loche, S Jansen, HJ Schenk, RR Netz, Proc. Natl. Acad. Sci. U.S.A.117 (20), 10733-10739

Formation and Location of H_2 Microbubbles from a Surface Nanodroplet Reaction

Xuehua Zhang

Chemical and Materials Engineering, University of Alberta, 116 St. and 85 Ave, Edmonton, AB T6G 2R3, Canada

Compartmentalizing chemical reactions in micro-sized droplets allows for efficient chemical conversion and simplifying procedures for biphasic processes. Reactions in small droplets have also been shown to greatly accelerate the rate of many chemical reactions. The accelerated growth rate of nanobubbles from nanodroplet reactions is demonstrated in this work. The gaseous products from the reaction at the nanodroplet surface promoted nucleation of hydrogen nanobubbles within multiple *organic* liquid nanodroplets. The nanobubbles were confined within the droplets and selectively grew and collapsed at the droplet perimeter, as visualized by microscopy with high spatial and temporal resolutions. The growth rate of the bubbles was significantly accelerated within small droplets and scaled inversely with droplet radius. The acceleration was attributed to confinement from the droplet volume and effect from the surface area on the interfacial chemical reaction for gas production. The gas transport from the droplet surface to bubbles and the collective consumption of the gas product by bubbles inside the droplet lead to the preferential location of nanobubbles inside the droplets. Our theoretical analysis predicts that the product concentration decreases from the droplet surface to the droplet center, which is in good agreement with the bubble growth rate in our experimental results. The results of this study provide further understanding for applications in droplet enhanced production of encapsulated nanobubbles.

Fundamentals and Theory of Nanobubbles

Effect of Dissolved Salt on Nanobubbles

Kalyani Agarwal[1] and Neelkanth Nirmalkar[1,*]

1 Department of Chemical Engineering (Indian Institute of Technology Ropar, Rupnagar, Punjab 140001, India)

E-Mail corresponding authors: n.nirmalkar@iitrpr.ac.in

Abstract

Nanobubbles are defined as the bubbles having a mean diameter less than 1 µm, often also termed as ultra-fine bubbles. These nanoscale bubbles are long-lasting gaseous cavities formed at the solidliquid interface as surface nanobubbles and persist in bulk solution as bulk nanobubbles, respectively [1]. The peculiar characteristics can possibly demarcated by its high Laplace pressure charged liquidgas interface followed by large specific surface area, substantially high zeta potential at the bubbles surface, and production of Reactive oxygen species [2]. Owing to these characteristics, it has sparked a flurry of fundamental research considering the environmental protection and precise medical technology. In addition, nanobubble technology spreads out in a wide range of industrial applications, waste disposal processes, pharmaceuticals and cosmetics, food production and filtration systems [3]. To apprehend the stability of nanobubbles, the boundary layer permits to unfold the mystery underlying unusual stability of these nanoscale bubbles in aqueous solution. The significant attraction of negative charge at bubble interface results in charge enrichment, and the ensuing electric field energy direct towards the thermodynamic metastability of the charged bulk nanobubbles [4].

Salts have been known to de-stabilize bubbles colloidal state by its detrimental effects on the electrostatic double layer in the boundary layer between gas and liquid system. In other words, nanobubble generation in presence of enriched charged ions may possibly hinder its formation. Therefore, in this work, generation, and characterization of nanobubbles in a saline solution have been carried out.

A systematic study of the effect of monovalent salt concentration on nanobubble at different concentration has been conducted over the range up to 1M. The addition of salt leads to a drop in bubble density as shown in Fig. 1d. Smaller nanobubbles should be effectively neutralised and destabilised, resulting in the observed decrease in bubble number density. The zeta potential of negative magnitude in Fig. 1b, depicts the decrement with the exceeding salt concentration followed by screening of electric double layer formed due to presence of co-ions. These findings support the theory that bulk nanobubbles that presence of ions in the water decreases the population of nanobubbles with respect to the pure water.

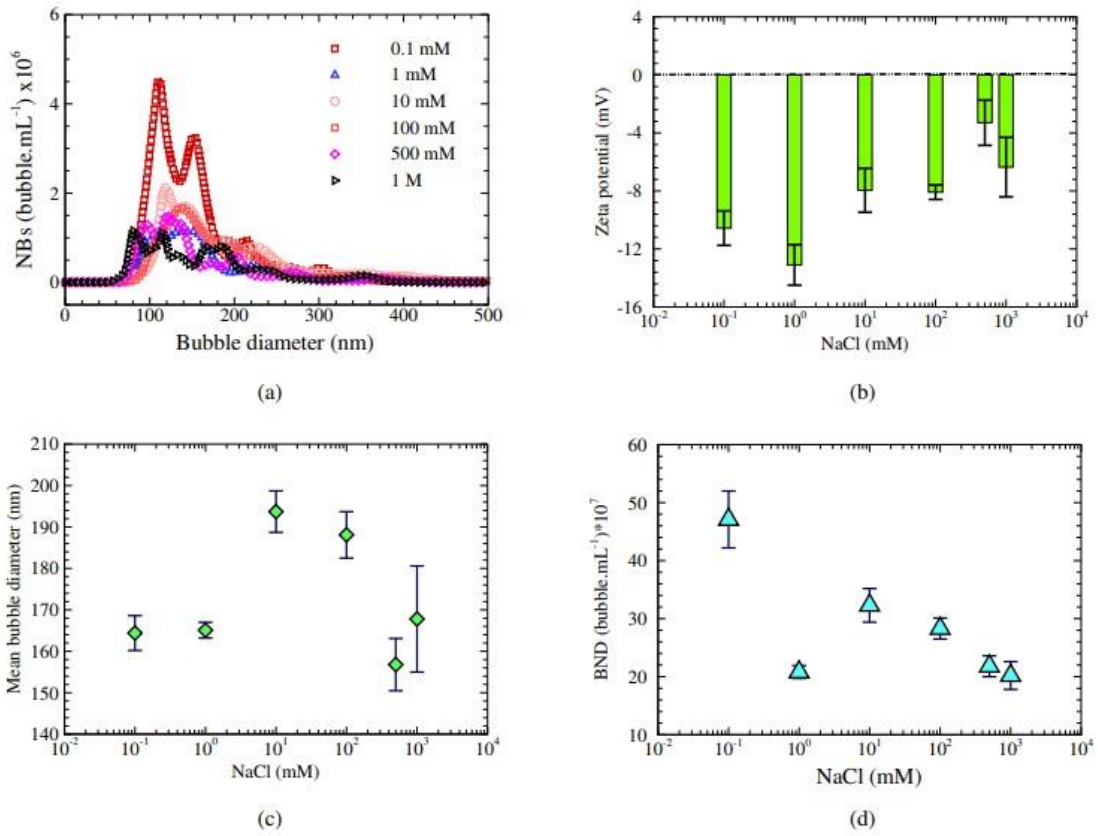

Figure 1. Nanobubbles in aqueous NaCl solution of varying concentration (a) Bubble size distribution (b) zeta potential (c) mean bubble diameter (d) bubble number density.

Acknowledgements

The authors gratefully acknowledge the DST-INSPIRE for funding and support.

References

[1] Nirmalkar N, Pacek AW, Barigou M, On the existence and stability of bulk nanobubbles. Langmuir **2018**, 34(37), 0964-73.
[2] Jadhav AJ, Barigou M, On the clustering of bulk nanobubbles and their colloidal stability, Journal of Colloid and Interface Science **2021**, 601, 816-24.
[3] Sun L, Zhang F, Guo X, Qiao Z, Zhu Y, Jin N, Cui Y, Yang W, Research progress on bulk nanobubbles, Particuology **2022**, 60,99-106.
[4] Zhou L, Wang S, Zhang L, Hu J, Generation and stability of bulk nanobubbles: A review and perspective, Current Opinion in Colloid & Interface Science **2021**, 53, 101439.

Ion adsorption stabilizes bulk nanobubbles

Mingbo Li,[1] Xiaotong Ma,[1] Patricia Pfeiffer,[2] Julian Eisener,[2] Claus-Dieter Ohl[2], and Chao Sun[1]*

1 *Center for Combustion Energy, Key laboratory for Thermal Science and Power Engineering of Ministry of Education, Department of Energy and Power Engineering, Tsinghua University, Beijing 100084, China*

2 *Otto von Guericke University Magdeburg, Institute of Experimental Physics, Universitätsplatz 2, 39016 Magdeburg, Germany*

E-Mail corresponding authors: chaosun@tsinghua.edu.cn

Abstract

The mechanism leading to the extraordinary stability of bulk nanobubbles in aqueous solutions remains an outstanding problem in soft matter, modern surface science, and physical chemistry science. In this work, the stability of bulk nanobubbles in electrolyte solutions under different pH levels and ionic strengths is studied. Nanobubbles are generated via the technique of ultrasonic cavitation, and characterized for size, number concentration and zeta potential under ambient conditions. Experimental results show that nanobubbles can survive in both acidic and basic solutions with pH values far away from the isoelectric point. We attribute the enhanced stability with increasing acidity or alkalinity of the aqueous solutions to the effective accumulation of net charges, regardless of their sign. The kinetic stability of the nanobubbles in various aqueous solutions is evaluated within the classic DLVO framework. Further, by combining a modified Poisson-Boltzmann equation with a modified Langmuir adsorption model, we describe a simple model that captures the influence of ion species and bulk concentration and reproduce the dependence of the nanobubble's surface potential on pH. We also discuss the apparent contradiction between quantitative calculation by ion stabilization model and experimental results. This essentially requires insight into the structure and dynamics of interfacial water on the atomic-scale.

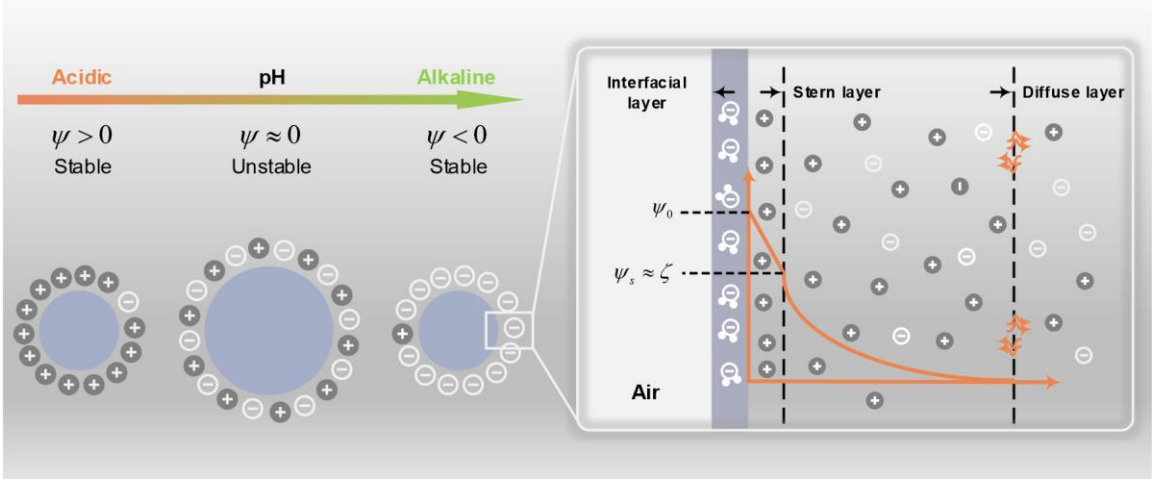

Figure 1. Schematic of the charged nanobubbles under various solution pH and diffused electrical double layer formed around a negatively charged surface.

Acknowledgements
This work was financially supported by the joint Research Pro gramme of the National Natural Science Foundation of China (NSFC, No. 11861131005), the China Postdoctoral Science Founda tion (No. 2020M680524), the Deutsche Forschungsgemeinschaft (Program No. OH 75/3-1), and the European Social Fund (No. ZS/2019/10/103050) as part of the initiative ‘‘Sachsen-Anhalt WIS SENSCHAFT Spitzenforschung/Synergien”.

References
[1] Xiaotong Ma, Mingbo Li, Patricia Pfeiffer, Julian Eisener, Claus-Dieter Ohl, Chao Sun, Ion adsorption stabilizes bulk nanobubbles, Journal of Colloid and Interface Science, 2022, 606: 1380-1394.

Reponses of surface micro- and nanobubbles to strong shear flows and acoustic waves

Zibo Ren[1], Shuhong Liu[1,*], Beng Hau Tan[2], Zhigang Zuo[1,*] and Claus-Dieter Ohl[3*]

1 *State Key Laboratory of Hydro Science and Engineering, and Department of Energy and Power Engineering, Tsinghua University, 100084 Beijing, China*
2 *Low Energy Electronic Systems, Singapore-MIT Alliance for Research and Technology, 1 Create Way, 138602 Singapore*
3 *Department Soft Matter, Institute for Physics, Otto-von-Guericke-Universität Magdeburg, Universitätsplatz 2, 39106 Magdeburg, Germany*

E-Mail corresponding authors: liushuhong@mail.tsinghua.edu.cn, zhigang200@mail.tsinghua.edu.cn, claus-dieter.ohl@ovgu.de

Abstract

Cavitation inception from immersed solid boundaries is widely attributed to the presence of entrapped gaseous bubbles in the micro- and nanostructures of surface crevices of hydrophobic materials. The crevice model of cavitation nuclei cannot explain cavitation inception from planar smooth surfaces. The discovery of long-living surface-attached micro- and nanobubbles raises hopes that they are the candidates for cavitation nuclei on smooth surfaces. Surprisingly, a large number of experiments show that these spherical cap shaped bubbles are robust and unresponsive to tensile stresses, thus excluding their possibility of serving as cavitation nuclei.

Here, we propose a unique and previously unanticipated mechanism for the generation of cavitation nuclei from surface micro- and nanobubbles. Using optical microscopy, we show that strong shortlived shear flows induced by cavitation jetting cause pinch-off of tethers from the surface micro- and nanobubbles and lead to the release of daughter bubbles into the flow that act as free nuclei.

Finally, we observe the responses of spherical cap shaped bubbles of radii from ~100 µm down to the scale of ~10 µm to ultrasonic waves propagating along surfaces with hydrophobic coatings. We show that the surface oscillation modes and cavitation inception from these bubbles are dependent on the bubble sizes and the driving frequencies and pressure amplitudes of the ultrasonic waves. The experimental results may answer why surface micro- and nanobubbles have long been believed to be unresponsive to tensile stresses in previous studies.

Acoustic and Hydrodynamic Cavitation Models using a Novel Reduced-Order Gas Pressure Law for Micro/Nanobubbles and their Applications

Can F. Delale[1], Erkan Ayder[2], Senay Pasinlioglu[3], Mehmet Kaya[2], and Ugurcan Morkoyun[2]

1 *Dept of Mechanical Engineering, MEF University, Ayazaga Cad. No.4, 34396 Sariyer, Istanbul, Turkey*
2 *Dept of Mechanical Engineering, Istanbul Technical University, Inonu Cad. No.65, 34437 Beyoglu, Istanbul, Turkey*
3 *Dept of Mathematics, Istanbul Technical University, Ayazaga Kampusu 34469 Sariyer, Istanbul, Turkey*

E-Mail corresponding author: delalec@mef.edu.tr

Abstract

The thermal behavior of a spherical gas bubble in a liquid excited by an acoustic pressure signal is investigated by constructing an iterative solution of the energy balance equations between the gas bubble and the surrounding liquid in the uniform pressure approximation. The iterative solution leads to exact hierarchy equations for the radial partial derivatives of the temperature at the bubble wall. A closure relation for the hierarchy equations is introduced based on the ansatz that approximates the rapid change of state during the collapse of the bubble from almost isothermal to almost adiabatic behavior by time averaging over a relatively short characteristic time. This, in turn, yields the desired reduced order gas pressure law [1] exhibiting power law dependence on the bubble wall temperature and on the bubble radius, with the polytropic index depending on the isentropic exponent of the gas and on a parameter which is a function of the Peclet number anda characteristic time scale. Results of the linear theory for gas bubbles are recovered. The novel gas pressure law is also validated against the near-isothermal solution of Prosperetti [2], as shown in Figure 1, and against the results of the numerical simulations of the original energy balance equations using spectral methods.

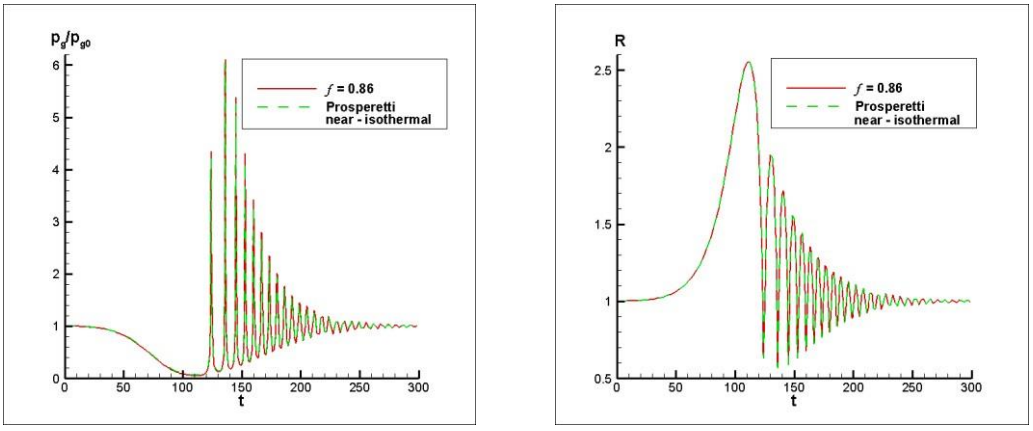

(a) (b)

Figure 1. Comparison of the temporal evolution of the normalized (a) internal bubble gas pressure and (b) bubble radius near-isothermal excitation of an acoustic cavitation bubble using the near-isothermal gas pressure law of Prosperetti [2] and the novel reduced-order gas pressure law.

An acoustic cavitation model that accounts for phase change, but neglects mass diffusion is constructed by employing the novel reduced order gas pressure law together with the Plesset-Zwick solution for the bubble wall temperature and the Keller-Miksis equation for spherical bubble dynamics. Results obtained using variable interface properties for acoustically driven cavitation bubbles in water show that the time variations of the bubble radius lie between those obtained by the isothermal and adiabatic laws depending on the value of the parameter.
A hydrodynamic cavitation model that is compatible with the results of the experiments and that can be adopted to commercial software is constructed. For this reason a hydrodynamic cavitation model that takes into account all of the damping mechanisms using the novel bubble gas pressure law is developed for quasi-one-dimensional bubbly cavitating nozzle flows. In this model the bubbly liquid is assumed to be a two-phase homogeneous mixture, the Rayleigh-Plesset equation is employed for bubble dynamics, and bubble nucleation process is neglected. The first order system of equations thus obtained for quasi-one-dimensional cavitating nozzle flows is transformed into an initial value problem for the bubble radius and the pressure coefficient. A numerical code is then written to solve this initial value problem by the adaptive step size Runge-Kutta-Fehlberg method. Results obtained at the experimental conditions were compared and interpreted with the results of experiments for cavitating nozzles. Cavitation performance of 3D radial pumps using modified models of cavitation based on the novel reduced order gas pressure law in the commercial codes is also discussed.

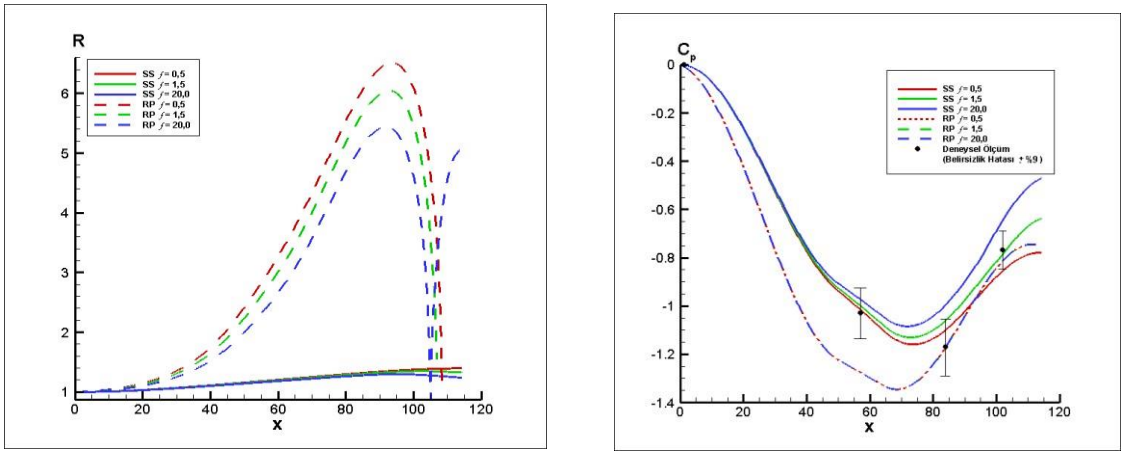

(a) (b)

Figure 2. Comparison of the distributions of (a) the normalized bubble radius and (b) pressure coefficient along the nozzle axis of a cavitating nozzle using Rayleigh-Plesset (RP) type and commercial code (SS) bubble dynamic laws together with the novel reduced-order gas pressure law against measured wall static pressures.

Acknowledgements

This work has been supported by TÜBİTAK under project no. 117M072.

References

[1] C.F. Delale, Ş. Pasinlioğlu, Acoustic cavitation model based on a novel reduced order gas pressure law, AIP Advances **11** (2021) 115309.
[2] A. Prosperetti, The thermal behavior of oscillating gas bubbles, *J. Fluid Mech.* **222** (1991) 587-615.

Viscous and capillary effects on the dynamics of sub-micron bubbles attached to walls

Mandeep Saini[1,(a)] and Daniel Fuster[1,(b)]

1 Sorbonne Universite, Univ Paris 06, CNRS, UMR 7190 Institut Jean Le Rond d'Alembert, F-75005 Paris, France

E-Mail: (a)mandeep.saini@sorbonne-universite.fr (b)daniel.fuster@sorbonne-universite.fr

Abstract

The process of heterogeneous bubble nucleation occurs when the bubble nuclei attached to wall experience a pressure lower than the critical pressure and expand by several orders of magnitude before collapsing[1,2]. In this work we investigate the influence of viscous and capillary effects on the dynamics of bubbles in contact with walls in different regimes using a compressible solver which includes both, viscous and capillary effects in liquid as well as gas phase[3]. For a pressure drop of the order of the critical pressure intrinsic to the bubble the response is shown to depend on the boundary condition at the wall. Thus the same bubble subjected to same pressure drop can be stable or unstable depending upon the boundary condition at the wall (see fig 1 for the differences between a pinned bubble and a free slip boundary condition).

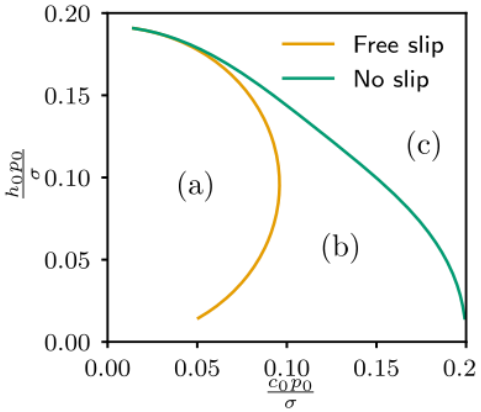

Figure 1. Stability diagram for different bubble sizes defined by length of contact at the wall (c_0) and the height of bubble (h_0) for a pressure drop equal to -10p_0 (p_0 being the ambient pressure) .Bubbles lying in region (a) are stable and unstable in region (c). In region (b) bubbles can be stable or unstable depending on the boundary condition and the motion of contact line.

For bubbles lying in region (c) we will use DNS results to examine the influence of the characteristic Ohnesorge and Capillary number on the expansion process of the bubble.

In the second part of the presentation we will present DNS results for the collapse stage typically observed when the ambient pressure is higher than the equilibrium pressure. We show that the bubble shape at the instant prior to compression, and in particular the effective contact angle observed at this instant, is critical to characterize the dynamics of the collapsing bubble and its interactions with the surroundings. For flat bubbles a re-entrant annular jet is observed (figure 2 right) that is eventually suppressed if the size of the bubble is comparable to the thickness of the viscous boundary layer. The transition from jetting to non-jetting behavior of collapsing bubbles is shown to depends on the characteristic Reynolds number Re = $(p_\infty \rho)^{1/2} R_c/\mu$). For values of the Reynolds number below a critical value of the Reynolds number around Re_c =10 no jet appears (figure 2 left).

Figure 2. Temporal evolution of the interface contours during the collapse of a spherical cap shaped bubble at two different Reynolds numbers. L*eft: Re = 10 Right: Re = 1000. The initial bubble pressure is small* $p_0 << p_\infty$.

The results of this study sheds some light on how the effects induced by the activation and later collapse change when the bubble size becomes increasingly small.

Acknowledgements

This work is supported by European Union (EU) under MSCA-ITN program called Ultrasound Cavitation in sOft Matters (UCOM).

References

[1] Borkent, Bram M., et al. "Nucleation threshold and deactivation mechanisms of nanoscopic cavitationnuclei." *Physics of fluids* 21.10 (2009): 102003.
[2] Atchley, Anthony A., and Andrea Prosperetti. "The crevice model of bubble nucleation." *The Journal of the Acoustical Society of America* 86.3 (1989): 1065-1084.
[3] Fuster, Daniel, and Stéphane Popinet. "An all-Mach method for the simulation of bubble dynamics problems in the presence of surface tension." *Journal of Computational Physics* 374 (2018): 752-768.

How surface nanobubbles survive: from experiments to theory

Beng Hau Tan[1], Hongjie An[2], and Claus-Dieter Ohl[3,*]

1 *KB Corporation, 7500A Beach Road, 199591 Singapore*
2 *Otto von Guericke University Magdeburg, Institute of Experimental Physics, Universitätsplatz 2, 39016 Magdeburg, Germany*
3 *Queensland Micro and Nanotechnology Centre, Griffith University, 170 Kessels Road, Nathan, Queensland 4111, Australia*

E-Mail corresponding authors: btan023@e.ntu.edu.sg

Abstract

Bubbles exhibit a remarkable diversity in behaviour in space and time. Some lead transient and violent lives, but others seem to live forever. A particular class of bubbles, nanobubbles, has attracted controversy since they were first proposed to exist. Not only are nanobubbles difficult to image, but their properties—they are long-lived and robust to destruction or dissolution—defy most classical expectations for how bubbles should behave.

Sustained academic scepticism over the very existence of nanobubbles stands in tension with their place at the centre of a US$40 billion industry. Although application has long steamed ahead of fundamentals, the yawning gap between the two must be bridged if nanobubbles are to be safely deployed in ambitious frontiers such as medicine.

Do nanobubbles exist? How do we prove it unambiguously? How do they survive? This talk summarizes our winding journey in surface nanobubbles, from overcoming an unexpected contamination issue affecting many early papers (including our own), to the development of a single model capable of explaining most known properties of surface nanobubbles. Finally, I discuss how our experiences with surface nanobubbles help to advance our still shaky understanding of freely standing bulk nanobubbles, also known as ultrafine bubbles.

On the role of surface charge and surface tension on stabilizing bulk nanobubbles

Xiaotong Ma[1], Xuefei Xu[1], Chao Sun[1], and Mingbo Li[1]*

1 Center for Combustion Energy, Key laboratory for Thermal Science and Power Engineering of Ministry of Education, Department of Energy and Power Engineering, Tsinghua University, Beijing 100084, China

E-Mail corresponding authors: mingboli@mail.tsinghua.edu.cn

Abstract

Bulk nanobubbles refer to nanoscopic gaseous domains present in the liquid phase environment[1]. Their special properties have brought newly emerging concepts and great potential in industrial applications, which have quickly received widespread attention. The extraordinary long-term stability of bulk nanobubbles breaks through the prediction of classical theory that spherical gas bubbles cannot achieve stable equilibrium[2]. It is worthwhile to address the outstanding and bewildering issue. In this work, the stability of bulk nanobubbles in ionic, cationic and nonionic surfactant solutions over a wide range of concentration is studied. Bulk nanobubbles featuring size distributions (<~500 nm) are generated using ultrasonic cavitation method. Generally, the presence of surfactants leads to a rise in bubble number density, either violently or gently, which means the surfactants provide more nuclei to form nanobubbles and enhance the stability as well. Based on the results of zeta potential, we consider that surface enrichment of net charges is predominantly responsible for the stability, instead of reduction of surface tension. The origin of surface charges could be ascribed to the adsorption of charge carriers, surfactants and ions, at the gas-liquid interface with limited adsorption sites. Applying the modified Poisson-Boltzmann equation incorporated effect of the adsorption layer thickness, we demonstrate the surface potential and the strong interfacial affinity of surfactants and ions in the vicinity of the air-water interface. Simultaneously, the DLVO theory is used to evaluate the colloidal stability of bulk nanobubbles suspensions with ionic surfactants. The effects of surfactants on the stability of bulk nanobubbles provide new and comprehensive insights into the underlying mechanism.

Acknowledgements

This work was financially supported by the joint Research Programme of the National Natural Science Foundation of China (NSFC, No. 11861131005), the China Postdoctoral Science Foundation (No. 2020M680524), the Deutsche Forschungsgemeinschaft (Program No. OH 75/3-1), and the European Social Fund (No. ZS/2019/10/103050) as part of the initiative “Sachsen-Anhalt WISSENSCHAFT Spitzenforschung/Synergien”.

References

[1] Tan B H, An H, Ohl C D. Stability of surface and bulk nanobubbles[J]. Current Opinion in Colloid & Interface Science, 2021, 53: 101428.

[2] Epstein P S, Plesset M S. On the stability of gas bubbles in liquid-gas solutions[J]. The Journal of Chemical Physics, 1950, 18(11): 1505-1509.

A Diffused Double Layer Model of Bulk Nanobubbles in Aqueous NaCl Solutions

Hilman Syaeful Alam[1,2]*, Priyono Sutikno[1], Tubagus Ahmad Fauzi Soelaiman[1], and Anto Tri Sugiarto[2]

1 *Department of Mechanical Engineering, Faculty of Mechanical and Aerospace Engineering, Institut Teknologi Bandung, Jl. Ganesha No.10, Bandung 40132, Indonesia.*
2 *National Research and Innovation Agency, Jl. Sangkuriang Kampus BRIN Gd. 80, Bandung 40135, Indonesia.*

**E-Mail corresponding authors: hilm003@lipi.go.id*

Abstract

Research on nanobubbles has attracted attention to their extraordinary characteristics, especially their long lifespans due to electrically charged interfaces [1]. The surface's negative charge, which inhibits bubble dissolution, might be in balance with the Laplace pressure due to the surface tension of the liquid [2]. In this study, The surface charge properties of oxygen nanobubbles formed in varying concentrations of NaCl solutions were evaluated using a diffused double layer model and the ionic repulsion model due to microbubble shrinkage [3]. Based on the previous study, the addition of NaCl to the nanobubble suspension lowered the repulsive electrostatic interactions between the nanobubbles by expanding their size and lowering their negative zeta potential [4]. The surface charge density, electrostatic repulsion force, double layer thickness, and the interaction energy between bubbles were calculated to estimate their effect on preventing bubble coalescence and dissolution. Figure 1 shows the calculated surface charge density of oxygen nanobubbles at different NaCl concentrations. The higher the concentration of NaCl, the zeta potential decreases, but the surface charge density increases. The higher NaCl concentration resulted in a thinner double-layer compared to the lower NaCl concentration. The ionic repulsion model of microbubble shrinkage confirmed the mechanical equilibrium between the Laplace pressure and the repulsion pressure owing to the electric charge on the bubble surface. These results corresponded to the experimental results of the zeta potential of microbubbles smaller than 50 µm.

Keywords: zeta potential, surface charge density, electrostatic repulsion force, double layer thickness, bulk nanobubbles

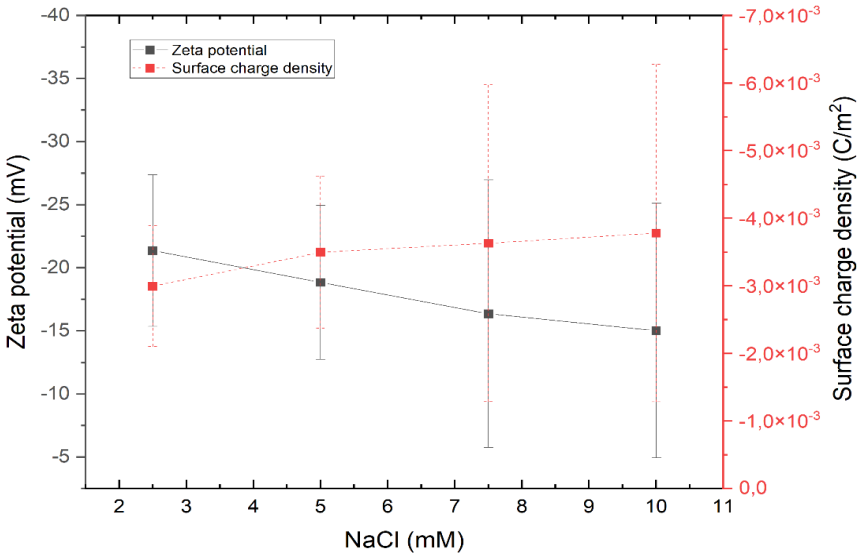

Figure 1. The calculated surface charge density of oxygen nanobubbles at different NaCl concentrations

Acknowledgments

The author would like to thank the Ph.D. by Research program provided by a decree from the Head of the Indonesian Institute of Sciences (Number: 149/H/2019).

References

[1] Hewage SA, Kewalramani J, Meegoda JN. Stability of nanobubbles in different salts solutions. *Colloids and Surfaces A: Physicochemical and Engineering Aspects* 2021; 609: 125669.
[2] Yasui K. Mechanism for Stability of Ultrafine Bubbles. *Japanese J Multiphase Flow* 2016; 30: 19–26.
[3] Satpute PA, Earthman JC. Hydroxyl ion stabilization of bulk nanobubbles resulting from microbubble shrinkage. *Journal of Colloid and Interface Science* 2021; 584: 449–455.
[4] Alam HS, Sutikno P, Soelaiman TAF, et al. Bulk Nanobubbles: generation using a two-chamber swirling flow nozzle and long-term stability in water. *J Flow Chem*. Epub ahead of print 20 October 2021. DOI: 10.1007/s41981-021-00208-8.

Dynamics of bubbles in a graphene liquid cell

Sota Hirokawa[1,2], Hideaki Teshima[1,2], Pablo Solís Fernández[3], Hiroki Ago[3], Yoko Tomo[4], Qin-Yi Li[1,2], and Koji Takahashi[1,2]

1 *Department of Aeronautics and Astronautics, Kyushu University, 744 Motooka, Nishi-ku, Fukuoka 819-0395, Japan*
2 *International Institute for Carbon-Neutral Energy Research (WPI-I2CNER), Kyushu University, 744 Motooka, Nishi-ku, Fukuoka 819-0395, Japan*
3 *Global Innovation Center, Kyushu University, 6-1 Kasuga-koen, Kasuga-city, Fukuoka 816-8580, Japan*
4 *Department of Mechanical Engineering, Kyushu University, 744 Motooka, Nishi-ku, Fukuoka 819-0395, Japan*

E-Mail corresponding authors: takahashi@aero.kyushu-u.ac.jp

Abstract

Transmission electron microscopy using graphene liquid cells, in which a liquid is sandwiched between two sheets of graphene, enables direct observation of fluid phenomena inside nanoscale space with the highest spatio-temporal resolution. This study aims to elucidate the physics of the unique behaviour exhibited by water and bubbles enclosed in nanospace using graphene liquid cells. Observations revealed the existence of directional nucleation of new bubbles, as seen in Figure 1, which is beyond the explanation of conventional diffusion theory.[1] We also observed the pinning phenomena that occur without direct contact with the bubbles.[2] These phenomena are explained by considering the strong intermolecular interactions between water molecules and solid surfaces.

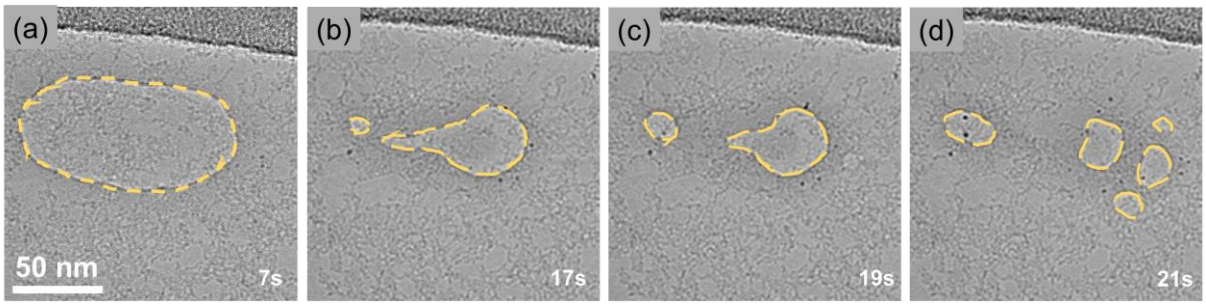

Figure 1 (a-d) Snapshots of the bubble shrinkage and nucleation inside the graphene liquid cell. Outline of bubbles are emphasized by yellow dashed lines.

Acknowledgements
This work was partially supported by the Japan Science and Technology Core Research for Evolutional Science and Technology (CREST) (grant no. JPMJCR18I1), the Japan Society for the Promotion of Science Grants-in-Aid for Scientific Research (KAKENHI) (grant nos. JP20H02089 andJP20H02090), Japan, and Grant-in-Aid for JSPS Fellows (grant no. JP21J21976). Some of the TEM observations were performed at the Ultramicroscopy Research Center at Kyushu University.

References
[1] S. Hirokawa, H. Teshima, P.S. Fernández, H. Ago, Y. Tomo, Q.Y. Li, and K. Takahashi, “Nanoscale Bubble Dynamics Induced by Damage of Graphene Liquid Cells,” ACS Omega, **2020**, 5, 11180–11185.
[2] S. Hirokawa, H. Teshima, P. Solís-Fernández, H. Ago, Q.-Y. Li, and K. Takahashi, “Pinning in a Contact and Noncontact Manner: Direct Observation of a Three-Phase Contact Line Using Graphene Liquid Cells,” Langmuir, **2021**, 37, 12271–12277.

Physicochemical hydrodynamics of a plasmonic bubble in a binary liquid: Nucleation and bouncing

Detlef Lohse

Physics of Fluids, University of Twente

The physicochemical hydrodynamics of bubbles and droplets out of equilibrium, in particular with phase transitions, display surprisingly rich and often counter-intuitive phenomena. Here I will discuss the nucleation and early evolution of plasmonic bubbles in a binary liquid consisting of water and ethanol. Remarkably, the plasmonic nanobubble is found to be periodically attracted to and repelled from the nanoparticle-decorated substrate, with frequencies of around a few kHz. The competition between solutal and thermal Marangoni forces is the origin of the periodic bouncing. The former arises due to the selective vaporization of ethanol at the substrate's side of the bubble, leading to a solutal Marangoni flow towards the substrate, which pushes the bubble away. The latter arises due to the temperature gradient across the bubble, leading to a thermal Marangoni flow away from the substrate which sucks the bubble towards it.

Reference: B. Zeng et al., PNAS 118, e2103215118 (2021)

Applications: Biology and Medicine I

Influence of oxygen and nitrogen nanobubble presence on metabolic activity of animal cell cultures

Karol Ulatowski[1]*, Kamil Wierzchowski[1], Paulina Trzaskowska[2], Julia Fiuk[1], and Paweł Sobieszuk[1]

1 *Warsaw University of Technology, Faculty of Chemical and Process Engineering, Waryńskiego 1, 00-645, Warsaw, Poland*
2 *Warsaw University of Technology, Centre for Advanced Materials and Technologies CEZAMAT, Poleczki 19, 02-822 Warsaw, Poland*

E-Mail corresponding authors: Karol.Ulatowski@pw.edu.pl

Abstract

Nanobubbles have been found useful in various branches of industry, including wastewater treatment and flotation, fuel enrichment and surface cleaning [1]. However, for us especially interesting are the interactions of nanobubbles with living matter. Presently, the most common interaction of carbon dioxide or ozone nanobubbles with microorganisms is the disinfection. Nanobubbles were used in inactivation of *E. coli* suspended in saline solution using carbon dioxide nanobubbles [2] and bubbles generated by ultrasonication in LB broth [3]. Other studies report disinfection of plant roots using ozone nanobubbles [4]. In the contrary, the positive interaction of nanobubbles with living matter is also observed. The oxygen nanobubbles are reported to promote the growth of animals (mice, rainbow trout and sweetfish) and plants (*Brassica campestris*, lettuce) [5].

In this work activity of animal cells in presence of nanobubbles was investigated. The aim of this study is to lay foundation for broad investigation of the mechanism and influence of nanobubble presence on animal cell lines, as it is still not reported in literature. Influence of two gases was studied: nitrogen and oxygen. Nitrogen, as the inert gas, was used to determine the impact of gas nanoobjects in bulk of solution on metabolic activity of investigated cells. Oxygen, as the respiratory gas, was used to check whether presence of oxygen in nanoscale bubbles has any impact. Nanobubbles of these gases were generated in pure water using porous membrane system (pore diameter 0.2 µm) where the gas (nitrogen or oxygen) was pressurised through the membrane and was cut off by the shear stress induced by flowing liquid. The dispersion was cycled for 60 minutes in closed-cycle. After generation solution was filtered using syringe filters (pore diameter 0.22 µm) in sterile conditions as the generation was carried out in non-sterile environment.

During this study we have performed cultures of cells from two cell lines: L929 (murine fibroblasts) and HL-60 (human leukemia cells) and focused on answering four questions, which will be summarised below.

1. Do the nanobubbles influence the growth and metabolic activity of animal cells in short-term cultures?

2. Do the nanobubbles have any impact on animal cells during long-term cultures?

3. Is there a different reaction to the nanobubble presence from the adherent and nonadherent cells?

4. Is there a difference between oxygen and nitrogen enclosed in nanobubbles for the growth of animal cells?

At the beginning we have performed short-term cultures with 24h contact of cells with nanobubbles, where we have checked how do the nanobubbles affect the metabolic rate of L929 cells, where the nanodispersion generated in pure water was diluting the medium. Ratios between nanodispersion and

medium (DMEM) ranged from 5:1 (most diluted DMEM) to 1:100 (least diluted DMEM). Next, the XTT assay test was carried out to assess the metabolic activity of cells.

The nitrogen nanodispersion is significantly increasing the metabolic activity of cells in broad range of concentrations. The non-cytotoxic conditions for DMEM with nitrogen nanodispersion are achieved for 1:1 ratio of nanodispersion:DMEM, i.e. the culture medium is twofold diluted. For ratios 1:5 and 1:10 the metabolic activity exceeds 120%, what indicates increased metabolic activity. For samples where the medium is least diluted (ratios 1:20, 1:50, 1:100) the results from cultures with nanodispersions are similar to results from cultures with water. The oxygen nanobubbles are mostly non-affecting metabolic activity as it is similar to reference cultures with water. In that way we have answered the first of four questions – nanobubbles

Next, we have carried out the long-term cultures which lasted for 8 days without additional supplementation. We have performed these studies on both L929 and HL-60 cells. That allowed us to check whether adherent L929 cells react differently to nanobubble presence than non-adherent HL-60 cells during 8-day cultures. Once again, we compared reactions to both oxygen and nitrogen nanobubbles, which this time were generated directly in the culture medium (DMEM for L929 cells and RPMI for HL-60 cells). We performed cell density measurement, cytotoxicity tests for both cell lines, confocal microscopy visualisation and metabolic activity tests such as lactic dehydrogenase (LDH) activity, PrestoBlue assay. Additionally, the glucose (substrate) consumption rate was assessed.

L929 cells cultured with nitrogen nanobubble addition to media had a much higher proliferation rate in the first days of culture than reference cultures, higher glucose consumption without loss in viability, or increased LDH leakage to the medium. Oxygen nanobubbles added to L929 culture also increased the proliferation rate, albeit not as high as nitrogen nanobubbles, higher metabolic activity, and comparable viability to the reference cultures. However, different effects were visible for the HL-60 cells, where the addition of nanobubbles has decreased the mentioned parameters of the culture – lower cell density, lower substrate consumption, and lower metabolic activity. These parameters are better for nanodispersions than reference only in the last two days of culture, but it is linked to a very low glucose concentration in reference cultures, which is the direct consequence of higher consumption in previous days. The described effect may be linked to the flotation by the nanobubbles what causes non-adherent HL-60 cells to rise to the surface of the medium or surround the cells by the nanobubbles, which hinders the mass transfer of both substrates and metabolites.

Acknowledgements
This work was supported by the National Science Centre, Poland (grant number 2018/29/B/ST8/00365).

References

1] S. Khuntia, S. K. Majumder, P. Ghosh, Microbubble-aided water and wastewater purification: A review, *Reviews in Chemical Engineering* **2012**, 28, 191–221
[2] F. Kobayashi, Y. Hayata, H. Ikeura, M. Tamaki, N. Muto, Y. Osajima, Inactivation of Esherichia coli by CO2 Microbubbles at a Lower Pressure and Near Room Temperature, Transactions of ASABE **2009**, 52, 1621–1626.
[3] T. Q. Luu, P. N. Hong Truong, K. Zitzmann, K. T. Nguyen, Effects of Ultrafine Bubbles on Gram-Negative Bacteria: Inhibition or Selection?, Langmuir **2019**, 35, 13761-13768.
[4] F. Kobayashi, H. Ikeura, S. Ohsato, T. Goto, M. Tamaki, Disinfection using ozone microbubbles to inactivate Fusarium oxysporum f. sp. melonis and Pectobacterium carotovorum subsp. carotovorum, Crop Protection **2011**, 30, 1514–1518.
[5] K. Ebina, K. Shi, M. Hirao, J. Hashimoto, Y. Kawato, S. Kaneshiro, T. Morimoto, K. Koizumi, H. Yoshikawa, Oxygen and Air Nanobubble Water Solution Promote the Growth of Plants, Fishes, and Mice, PLoS One **2013**, 8, 2–8.

Assessing tumoral vascular permeability and nanoparticle extravasation with nanobubble contrast-enhanced ultrasound imaging

Michaela B. Cooley,[1] Dana Wegierak,[1] Reshani Perera,[2] Eric Abenojar,[2] Youjoung Kim,[1] Michael C. Kolios,[3] and Agata A. Exner[2]

1 *Department of Biomedical Engineering, Case Western Reserve University, Cleveland, Ohio 44106, United States*
2 *Department of Radiology, Case Western Reserve University, Cleveland, Ohio 44106, United States*
3 *Department of Physics, Ryerson University, Toronto, Ontario M5B 2K3, Canada*

Background. The tumor microenvironment is characterized by dysfunctional endothelial cells, resulting in heightened vascular permeability. Many drug delivery systems attempt to use the enhanced permeability and retention effect as the primary strategy for drug delivery, but this has not proven to be as effective as anticipated [1]. The potential of contrast-enhanced ultrasound (CEUS) to examine tumor microenvironment characteristics noninvasively and in real time is largely unexplored. Nanobubbles (NBs) are an ideal ultrasound contrast agent for this purpose because they are capable of extravasation, unlike clinically available microbubbles [2]. This work examines whether multiparametric dynamic CEUS imaging using NBs could help predict tumor vascular permeability and retention of doxorubicin (DOX)-loaded liposomes.

Methods. Athymic nude mice were injected (hind limb) with either LS174T (colorectal adenocarcinoma, n=5; highly permeable) or U87 (glioblastoma, n=5; minimally permeable) cells. Mice were imaged with nonlinear CEUS (VisualSonics Vevo 3100, 18 MHz, 4% power, 1 frame per second) using NBs injected via tail vein weekly for 2-3 weeks, depending on tumor size. NBs (~275 nm diameter) were fabricated according to de Leon et al [3]. 1 day before euthanasia, doxorubicin-loaded liposomes were injected into the mice. DOX-loaded liposomes (~95.5 nm, reported by Avanti®) represent a model nanoparticle capable of extravasation and DOX has intrinsic fluorescence for histological analysis. Time-intensity curve (TIC) and decorrelation analysis (created with MATLAB) were performed. Decorrelation analysis began at time = 50% of peak intensity in the wash-out portion of the TIC for 200 s. This time point was chosen to represent the randomness of NB motion in the extravascular space. Tumors were frozen in optimal cutting temperature compound (OCT) and sectioned by the Tissue Resources Core facility at CWRU. A Zeiss AxioScan.Z1 slide scanner was used to image the slides and Zeiss ZEN software was used for data analysis.

Results. Parameters including peak intensity, area under the curve, area under the rising curve (AUC_R), time to peak, and decorrelation time (DT) were extracted from the TIC data. This data was compared between tumor types (LS174T vs U87) and to corresponding fluorescent DOX nanoparticle data through histology. Larger LS174T tumors showed a 4.8-fold larger AUC_R and 2.8-fold higher peak intensity than U87 tumors (Figure 1a-b). Smaller tumors did not show similar differences between tumor types. Ultrasound tumor data and corresponding histology were split into quadrants for analysis and compared (Figure 1c). Example LS174 tumor measurements are shown. The lateral aspects of the tumor (highlighted in green) had a greater DT than medial aspects (highlighted in blue) by at least 1.6x and average fluorescent intensity was greater by at least 1.4x. While not depicted here, when the average DT for the entire tumor was compared between U87 and LS174T tumors at their final time points, the DT of LS174T tumors was 2.3x greater than U87 tumors with $p<0.5$. These parameters may be correlated to nanoparticle

extravasation and retention in tumors. Further histological analysis and image processing are ongoing.

Conclusions. Substantial differences in NB-generated TIC parameters AUC_R, peak intensity, and DT were noted between LS174T and U87 tumors. Further, DT preliminarily corresponds to fluorescent intensity in each quadrant of the tumor and the DT is significantly longer in LS174T tumors than U87 tumors. This suggests that NBs may be useful in determining tumor permeability and could be used as a biomarker for patient responsiveness to nanoparticle therapies.

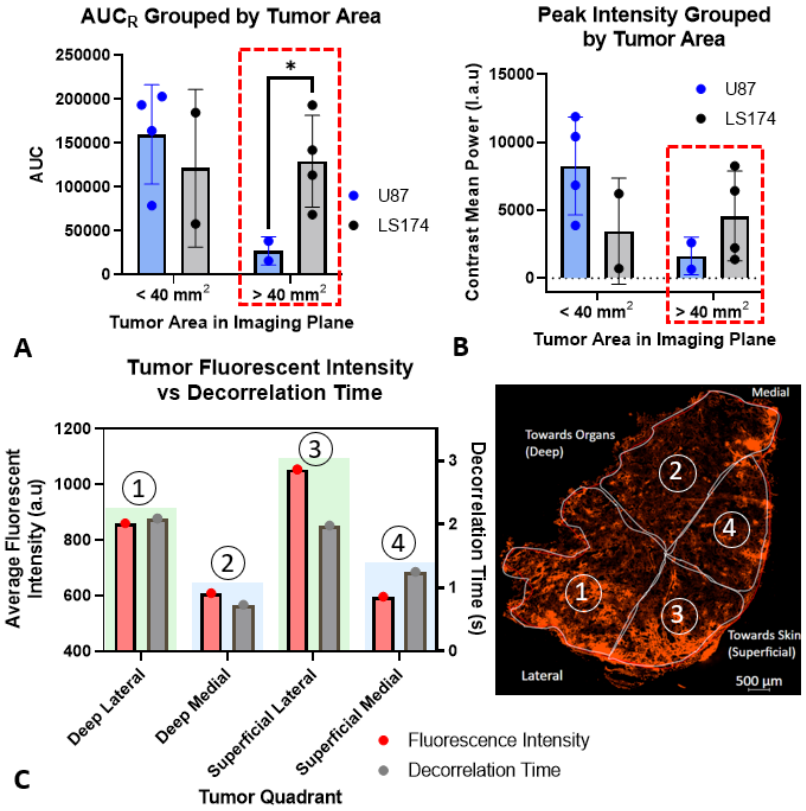

Figure 1. *Sample of Contender Parameters for Measuring Tumor Microenvironment Characteristics with Contrast-Enhanced Ultrasound Imaging.* (a) Area under the rising curve (AUC_R) comparing LS174 and U87 tumors of different sizes (* denotes $p < 0.05$). (b) Peak intensity comparing tumors of different sizes. Like the AUCR, larger tumors tend to show greater differences between tumor type than smaller tumors. (c) *Left*. Example comparison between average fluorescent intensity found through histological analysis and average decorrelation time extracted from NB contrast-enhanced ultrasound imaging using an LS174T tumor. *Right*. Corresponding fluorescent image.

Acknowledgements
The authors would like to acknowledge funding from NIBIB (R01EB025741 and R01EB028144), CWRU MSTP and NIGMS (T32GM07250), and NHLBI (F30HL160111)

References

[1] S. Wilhelm, A.J, Tavares, Q. Dai, S. Ohta, J. Audet, H.F. Dvorak, W.C.W. Chan, Analysis of nanoparticle delivery to tumours, Nature Reviews Materials **2016**, 1, 16014.
[2] H. Wu, E. A. Abenojar, R. Perera, A.C. de Leon, T. An, A.A. Exner, Time-intensity-curve Analysis and Tumor Extravasation of Nanobubble Ultrasound Contrast Agents, Ultrasound Med Biol **2019**, 45(9), 2502-2514.
[3] A. De Leon, R. Perera; X. Hernandez, M. Cooley, O. Jung, S. Jeganathan, E. Abenojar, G. Fishbein, A.J. Sojahrood, C.C. Emerson, P.L. Stewart, M.C. Kolios, A.A. Exner, Contrast enhanced ultrasound imaging by nature-inspired ultrastable echogenic NBs, Nanoscale **2019**, 11, 15647-15658.

rtPA-loaded targeted nanobubbles as a new thrombus-specific thrombolytic strategy

M. Argenziano[1], S. Capolla[2], P. Durigutto[2], M. Colucci[3], PL. Meroni[4], F. Tedesco[4], P. Macor[2], and R. Cavalli[1]

1 *Department of Drug Science and Technology, University of Turin, Via P.Giuria 9, 10125 Torino*
2 *Department of Life Sciences, University of Trieste, via Giorgeri 5, 34127 Trieste, Italy*
3 *Department of Biomedical Sciences and Human Oncology, University of Bari "Aldo Moro", Piazza G. Cesare, 11, 70124 Bari*
4 *Clinical Immunology and Rheumatology Research Department, Auxologico Institute Milan, IRCCS*

E-Mail corresponding author: monica.argenziano@unito.it

Abstract

The visualization and the safe resolution of formed thrombi remain a concrete medical need in vascular thrombosis. Intravenous thrombolytic therapy, which often employs recombinant enzymes analogue to tissue plasminogen activator (rtPA), is the treatment of choice for thrombosis. However, the thrombolytic drugs used in clinical have limitations such as a short half-life in plasma, a low targeting ability and significant incidence of haemorrhagic complications [1]. The use of a targeted nanodelivery system to selectively release the thrombolytic drugs to the thrombus site may be a viable option to overcome these drawbacks. The activated form of Beta2- glycoprotein I (Beta2-GPI) can represent an interesting target to allow selective delivery of fibrinolytic agent to thrombi since it was expressed on activated endothelial cells and platelets and detected in blood clots [2].

This work aims at developing a new biocompatible theranostic nanoplatform to visualize the thrombi in the vascular tree and to dissolve the blood clots.

Nanobubbles (NBs) with a perfluoropentane core and a chitosan shell conjugated with MBB2, a cross-reactive scFv-CH3 recombinant antibody against the activated form of Beta2-GPI were formulated. They were loaded with rtPA through covalent conjugation by carbodiimide-mediated amide bond formation. Fluorescent formulations were prepared by labelling the core with 6-coumarin. NB formulations were *in vitro* characterized evaluating their physico-chemical parameters, morphology, loading capacity, in vitro release and stability.

The capability of NBs to bind thrombi was evaluated in *in vitro* and *in vivo* studies by immunofluorescence. The thrombolytic activity of rtPA-loaded NBs was evaluated *in vitro*, using platelet-rich blood clots, and *in vivo* in different animal models of thrombosis.

Stable NBs with average diameter of about 400 nm and positive surface charge were obtained. Targeted NBs bound preferentially to platelets and leukocytes within thrombi and to endothelial cells through β2-GPI expressed on activated cells. *In vitro*, rtPA-targeted NBs (rtPA-tNBs) induced greater lysis of platelet-rich blood clots than untargeted NBs. In addition, the administration of rtPA-tNBs caused rapid dissolution of thrombi and prevented new thrombus formation in rat models of thrombosis.

In conclusion, rtPA-loaded NBs targeted to β2-GPI have shown to be effective in dissolving thrombi and prevent rethrombosis in different animal models of thrombosis.

References

[1] AM. Thiebaut; M. Gauberti; C. Ali; S. Martinez De Lizarrondo; D. Vivien; M. Yepes; BD. Roussel. The role of plasminogen activators in stroke treatment: Fibrinolysis and beyond, Lancet Neurol. **2018**, 17, 1121-1132
[2] C. Agostinis; P. Durigutto; D. Sblattero; MO. Borghi; C. Grossi, F. Guida; R. Bulla; P. Macor; F. Pregnolato; PL. Meroni; F. Tedesco. A non-complement-fixing antibody to beta2 glycoprotein I as a novel therapy for antiphospholipid syndrome, Blood. **2014**, 123, 3478-3487

On the physical mechanisms of the surprising high echogenicity of lipid coated nanobubbles in diagnostic ultrasound

A.J. Sojahrood[1,2,3]*, Agata A. Exner,[4] Michael C. Kolios [1,2], and David E. Goertz[3]

1 *Department of Physics, Ryerson University, Toronto, Ontario, M5B2K3, Canada*
2 *Institute for Biomedical Engineering and Science Technology, A Partnership between Ryerson University and St. Michael's Hospital, Toronto, Ontario M5B 1T8, Canada*
3 *Department of Physical Sciences, SunnyBrook health Science Center, Toronto, Ontario, M4N3M5, Canada*
4 *Department of Radiology and Biomedical Engineering, Case Western Reserve University, Cleveland, Ohio, 44106, USA*

E-Mail corresponding authors: amin.jafarisojahrood@ryerson.ca

Abstract

Applications of lipid coated nanobubbles (NBs) in diagnostic and therapeutic ultrasound (US) have attracted a great level of interest. Unlike microbubbles (MBs), NBs are not limited to the vasculature and can extravasate through leaky tumor vasculature. Due to their small size, their conceived linear resonance frequency is in the range of ~50MHz-200MHz. Thus, despite the experimental evidence on the strong contrast to tissue ratio in diagnostic US applications [1], the origin of this echogenicity has been the subject of strong debate and controversy. In this study, dynamics of uncoated and lipid shell NBs and MBs are studied using a novel bifurcation analysis [2] in tandem with the analysis of the frequency component of the scattered pressure. The Marmottant model [3] is used to simulate the lipid coated bubble oscillations as it effectively captures the influence of the buckling and rupture of the lipid shell. We focus on the US frequency and pressure ranges of 6-12 MHz and 0.1-1.2MPa used in contrast enhanced US [4]. Results show that, despite the increased linear resonance frequency and increased viscous damping due to the lipid shell, the buckling and rupture of the shell enhances the generation of the 2nd and 3rd harmonic resonance at pressures as low as 200kPa not observed in case of the uncoated NBs. The generation of the superharmonic (SuH) resonances are concomitant with an abrupt increase in the 2nd and 3rd harmonic frequency component of the scattered pressure (Fig. 1). The pressure threshold for the enhancement increases with decreasing NB size. For the same gas volume, the maximum non-destructive 2nd and 3rd harmonic power of NBs with 200-700nm size can be 20-60 dB higher than the 2-4µm size MBs (Fig. 2). In clinically applied amplitude modulation techniques, due to the abrupt pressure dependence of the 2nd and 3rd harmonic enhancement, the residual signal from NBs can be very strong, leading to enhanced echogenicity. In conclusion, linear viscoelastic shell models cannot capture the dynamic variation of the NB effective surface tension due to buckling and rupture. However, buckling and rupture of the lipid shell as captured by the Marmottant model, enhances the generation of the 2nd harmonic resonances at frequencies well below the NB linear resonance frequency. This is likely one of the key reasons for the acoustic echogenicity of the NBs.

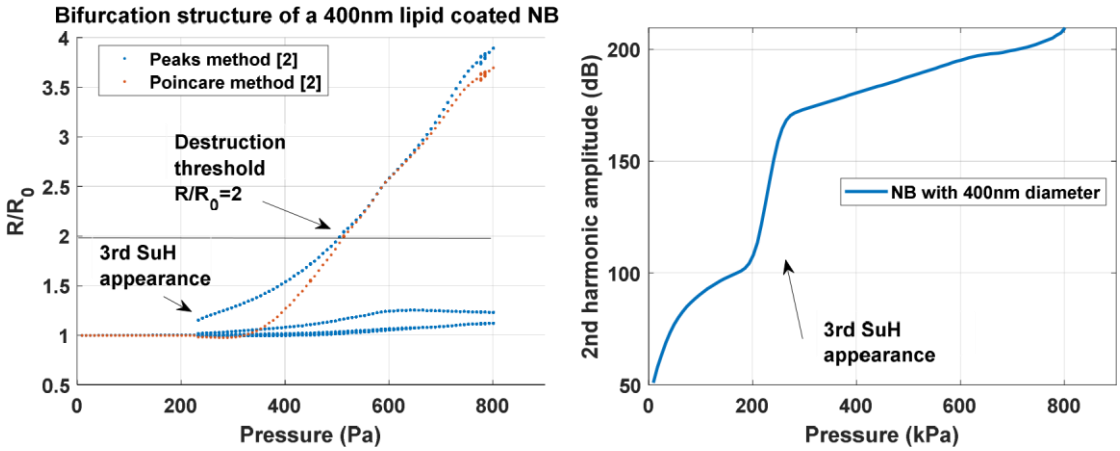

***Figure 1**: Pressure dependent dynamics of a 400nm lipid coated NB sonicated with f=8MHz a) Bifurcation structure, b) 2nd harmonic component of the scattered pressure by the NBs (gas volume of 4*10^9 µm^3/mL).*

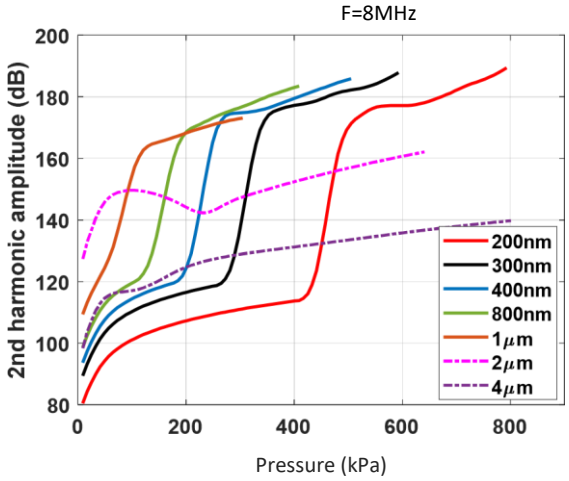

***Figure 2**: Nondestructive 2nd harmonic amplitude of the scattered pressure from lipid coated NBs and MBs as a function of peak negative applied acoustic pressure (2 cycles pulse length). Number of the MBs and NBs are determined through volume matching.*

References

[1] Exner, A.A. and Kolios, M.C., 2021. Bursting microbubbles: how nanobubble contrast agents can enable the future of medical ultrasound molecular imaging and image-guided therapy. Current Opinion in Colloid & Interface Science, 54, p.101463.

[2] Sojahrood, A.J., Wegierak, D., Haghi, H., Karshfian, R. and Kolios, M.C., 2019. A simple method to analyze the super-harmonic and ultra-harmonic behavior of the acoustically excited bubble oscillator. Ultrasonics sonochemistry, 54, pp.99-109.

[3] Marmottant, P., Van Der Meer, S., Emmer, M., Versluis, M., De Jong, N., Hilgenfeldt, S. and Lohse, D., 2005. A model for large amplitude oscillations of coated bubbles accounting for buckling and rupture. The Journal of the Acoustical Society of America, 118(6), pp.3499-3505.

[4] Jafari Sojahrood, A., de Leon, A.C., Lee, R., Cooley, M., Abenojar, E.C., Kolios, M.C. and Exner, A.A., 2021. Toward precisely controllable acoustic response of shell-stabilized nanobubbles: High yield and narrow dispersity. ACS nano, 15(3), pp.4901-4915.

Measurement of Nanobubbles Methods & Techniques

Observation of Mesoscopic Clathrate Structures in Gas-Supersaturated Water with Transmission Electron Microscopy

Ing-Shouh Hwang[1] and Wei-Hao Hsu[1]

1 Institute of Physics, Academia Sinica, Taipei 115, Taiwan.

E-Mail corresponding author: ishwang@phys.sinica.edu.tw

Abstract

Dissolution of gases in liquid water is a general and fundamental phenomenon across living and nonliving things. Conventionally it has been assumed that dissolved gas molecules are well dispersed as monomers. The concentration of gas molecules at a given time and position has been used to describe the gas condition in aqueous solutions, even when the dissolved gas concentration is near or above the saturation level. However, many mysteries about gas dissolved in water, such as the nucleation mechanism of gas bubbles in water and whether nanobubbles exist in bulk water, persist up to now. Recent experiments suggest that gas concentration alone is not sufficient to describe gas dissolved in water, thus we sought to examine whether dissolved gas forms any microstructures in water. Transmission electron microscopy (TEM) of graphene liquid cells (GLCs) can reveal structures in liquid with sub-nanometer or atomic resolution [1]. We thus encapsulated water between two laminated graphene layers spanning the holes in TEM grids; we investigated degassed water, deionized water, and water supersaturated with pure gas (N_2, O_2, Ar, Xe, CO_2, and SF6) at room temperature. While neither degassed water nor deionized water yielded specific features, two major microscopic structures were evident in gas-supersaturated water: (1) individual polycrystalline nanoparticles (typically several nanometers in diameter) in liquid water, and (2) mesoscopic clathrate structures (often ~100 nm or larger in lateral size). The latter was seen much more frequent than the former [2].

Fig. 1 shows bright-field and dark-field TEM of a clathrate state for N2-supersaturated water encapsulated in a GLC. This state features a high density of tiny cells: in a pocket containing N2-supersaturated water, these cells appear as white spots at underfocus (Fig. 1a) and as dark spots at overfocus (Fig. 1b). In focus, the cells have very low contrast and are difficult to discern [2]. Similar structures were visualized in GLCs containing water supersaturated with other gases, including O_2, Ar, Xe, SF6, and CO_2. Interestingly, selected area electron diffraction (SAED) patterns acquired on the clathrate structures contained additional diffraction spots other than those associated with graphene (Fig. 1c). These diffraction spots are not commensurate with graphene's lattices and were consistently observed in all water pockets containing this intriguing state. Dark-field TEM imaging revealed regions of honeycomb-like structures with water molecules forming a solid matrix hosting the tiny gas-containing cells (Fig. 1d).

Similar clathrate structures were also observed when ethanol-water (EW) mixtures at ~10% volume fraction ethanol, which is also gas supersaturated, were sandwiched between two laminated graphene layers. Although we are not certain whether clathrate structures are also present in bulk water, we did observe the coexistence of liquid water with the clathrate structures inside the same water pocket [2]. A study of liquid water in equilibration with high-pressure gas using infrared spectroscopy indicated the existence of structures with water hydrogen bonds strengthened to levels observed in ice and clathrates [3]. Vibrational spectroscopies based on Raman scattering and infrared absorption techniques have also demonstrated a sharp increase in strength of hydrogen bonds with increasing ethanol concentration in EW mixtures [4].

The clathrate structures reported here may be the bulk nanobubbles. Our gas-supersaturated water was prepared by pressurizing gas in water and then decompressing the water to ambient pressure, which has

been known to produce bulk nanobubbles. Many groups have reported generation of bulk nanobubbles by mixing water with ethanol. Observation of the clathrate structures is also consistent with a recent report of a density of ~0.91 g/cm3 measured for the mesoscopic structures in EW mixtures [5] and explains abnormal thermodynamic properties of gas-saturated water as well as EW mixtures [6].

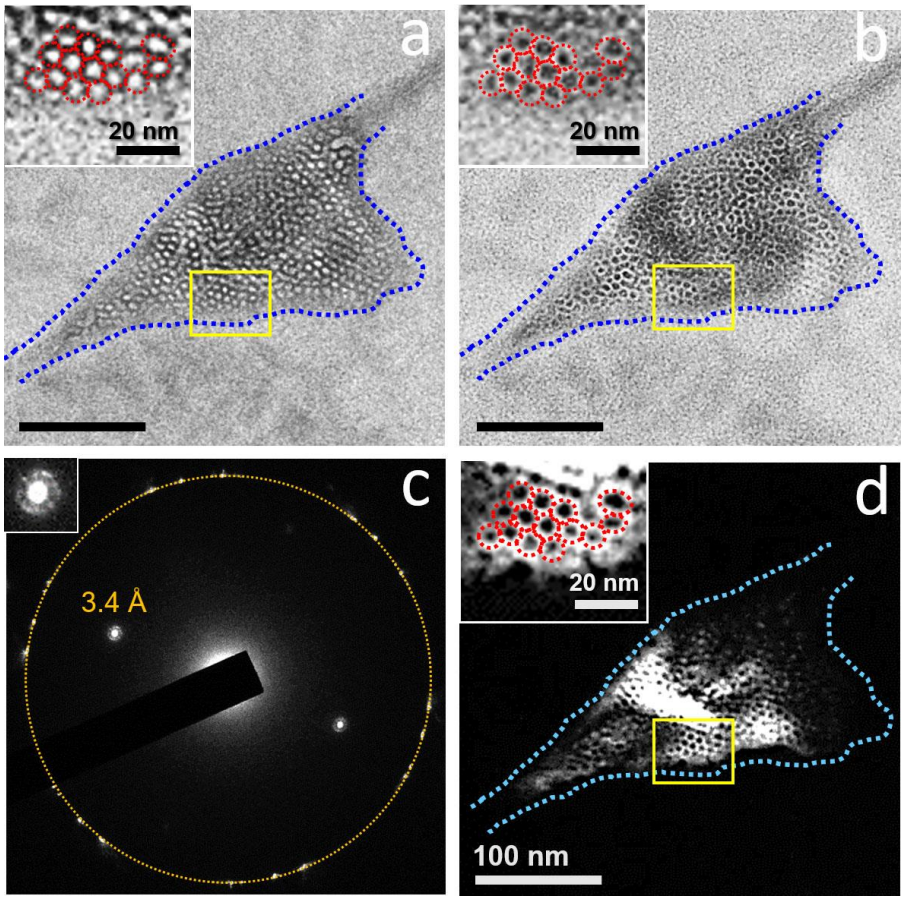

Figure 1. Bright-field TEM images were acquired at (a) underfocus and (b) overfocus. Insets: enlarged views of the regions outlined in yellow. The dashed blue line outlines the pocket containing the clathrate structure. (c) SAED pattern of the regions shown in (a) and (b). The dashed circle indicates the first-order diffraction spots of the multi-layer graphene. Inset: enlarged view of the diffraction beam indicated with d-spacing of 3.4 Å. (d) Dark-field TEM image acquired from the diffracted beam indicated with d-spacing of 3.4 Å in (c).

Acknowledgements
This research was supported by the Ministry of Science and Technology of Taiwan (MOST 106-2112-M-001-025-MY3 and MOST 109-2112-M-001-048-MY3) and Academia Sinica.

References
[1] J. M. Yuk et al., Science **2012**, 336, 61.
[2] W.-H. Hsu, I.-S. Hwang, Chem. Sci. **2021**, 12, 2635–2645.
[3] J. Grdadolnik, F. Merzel, F. Avbelj, Proc. Natl. Acad. Sci. U.S.A. **2017**, 114, 322.
[4] A. J. Jadhav, M. Barigou, Langmuir **2020**, 36, 1699–1708.
[5] M. Alheshibri, V. S. J. Craig, J. Colloid Interface Sci. **2019**, 542, 136–143 (2019).
[6] H. S. Frank, M. W. Evans, J. Chem. Phys. **1945**, 13, 507.

Characterization of Colloidal, Mechanical and Electrochemical Properties of Nanobubbles in Water

Xiaonan Shi, Taha Marhaba, and Wen Zhang*

1 *John A. Reif, Jr. Department of Civil and Environmental Engineering, New Jersey Institute of Technology, Newark, NJ 07102, USA*

E-Mail corresponding/presenting authors: wen.zhang@njit.edu

Abstract

Nanobubbles (NBs) in water exhibit many appealing characteristics, such as a long residence time of bubbles in water due to their low buoyancy and stability against coalesces, collapse or burst. Long retention times in water potentially enhance chemical reactions and mass transfer in processes such as ozonation or aeration. In addition, gaseous NBs may increase the solubility of the gas species (e.g., ozone, oxygen or other gases) that may have low solubility in water or other liquids. Therefore, NBs hold promise in green and sustainable engineering applications in diverse fields (e.g., water/wastewater treatment, food processing, medical applications, and agriculture). In our study, different gaseous NBs (e.g., nitrogen and oxygen) were generated by a hydrophobicized ceramic membrane immersed in deionized water or other electrolyte liquids. The hydrodynamic diameters of NBs (200~400 nm) highly depend on the injection gas pressure and surface hydrophobicity of the ceramic membrane. Moreover, the bubble sizes of both N_2 and O_2 NBs in water suspensions were found to be stable for at least two months under sealed containers (i.e., no light exposure and physical disturbance at room temperature). The colloidal sizes of NBs were in the range from 200 nm to 400 nm measured by dynamic light scattering (DLS), which also determines the zeta potential of NBs to range from -20 mV to -40 mV. We also demonstrated that the bubble size of NBs relatively decreased with increased gas injection pressure and water temperature. The concentrations of O_2 and N_2 NBs in water suspensions measured by nanoparticle tracking analysis (NTA) were $4.16\pm0.438\times10^8$ bubbles ml^{-1} and $6.35\pm1.24\times10^8$ bubbles ml^{-1} respectively at room temperature. As shown in **Fig. 1**, NBs that deposited on the substrate surface of highly oriented pyrolytic graphite (HOPG) or silicon wafer were also imaged by atomic force microscopy (AFM) to measure the mechanical properties of NBs such as elastic modulus and stiffness. O_2 NBs exhibited an elastic modulus and stiffness of 159.46±19.93 MPa and 1.66±0.18 N m^{-1} under the gas injection pressure as 60 psi. Moreover, the average of modulus and stiffness of NBs increased with increased the gas injection pressure, suggesting the increase of the internal pressure of NBs. We further analyzed the electrochemical (EC) activity of different NBs (e.g., oxygen, hydrogen, and nitrogen) using cyclic voltammetry (CV) and scanning electrochemical microscopy coupling with AFM (AFM-SECM), respectively. The CV measurements show that the electrolyte solution (20 mM $K_3Fe(CN)_6$ Cl_3 in 0.5M KCl) containing O_2 NBs showed a higher current peak under the applied potential compared to the same electrolyte solution without NBs, which indicated that O_2 NBs have the potential to facilitate the redox reaction in the solution. This result is further verified by AFM-SECM that shows the surface of single O_2 NBs produced a higher tip current (~4 pA) than the gold substrate (~2 pA) when the conductive tip (electrode) approached the individual NBs or the substrate in a electrolyte solution containing 10 mM $[Ru(NH_3)_6]Cl_3$ solution with 0.1M KCl. Overall, NBs in water exhibit intriguing physical, colloidal and electrochemical properties that deserve systematic studies to better understand their unique aquatic behaviour and potential applications.

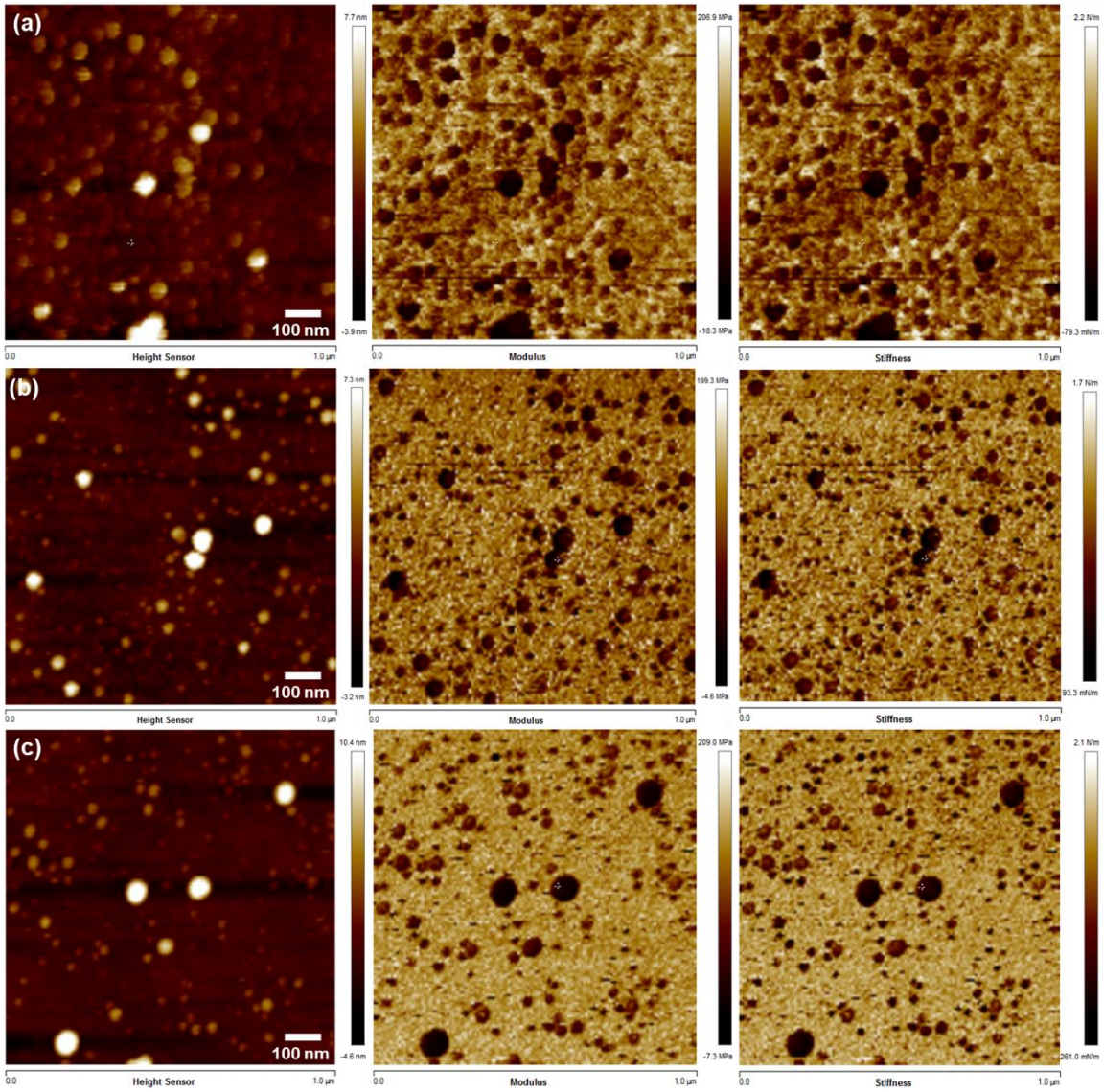

Fig. 1 *AFM height image (left), modulus image (middle) and stiffness image (right) of O_2 NBs with (a) 60psi (b) 70 psi (c) 80 psi gas pressure on silicon surface*

Acknowledgements

This research is partially supported by the United States Department of Agriculture (USDA) National Institute of Food and Agriculture, AFRI project [2018-07549] and the United States Environmental Protection Agency (US EPA) under Assistance Agreement No. 83945101-0. It has not been formally reviewed by USDA or EPA. The views expressed in this document are solely those of authors and do not necessarily reflect those of the Agency. USDA or EPA does not endorse any products or commercial services mentioned in this publication.

References

[1] Xiaonan Shi, Qingquan Ma, Taha Marhaba, and Wen Zhang*. "Probing Surface Electrochemical Activity of Nanomaterials using Hybrid Atomic Force Microscope-Scanning Electrochemical Microscope (AFM-SECM)." ***Journal of Visualized Experiments (JoVE),*** Under revision.

[2] 29. Ahmed Khaled Abdella Ahmed, Cuizhen Suna Likun Hua, Zhibin Zhang, Yanhao Zhang, Wen Zhang*, TahaMarhaba. Generation of nanobubbles by ceramic membrane filters: The dependence of bubble size and zeta potential on surface coating, pore size and injected gas pressure. ***Chemosphere***. 2018. https://doi.org/10.1016/j.chemosphere.2018.03.157.

Gaseous and oily nano-objects: With FLIM and AFM from surface to the bulk

Sergey I. Druzhinin* and Holger Schönherr*

Physical Chemistry I & Research Center of Micro and Nanochemistry and (Bio)Technology (Cμ), Department of Chemistry and Biology, Faculty of Science and Technology, University of Siegen, Adolf-Reichwein-Str. 2, 57076 Siegen

E-Mail corresponding authors: druzhinin@chemie.uni-siegen.de, schoenherr@chemie.uni-siegen.de

Abstract

Gas-filled nano-objects, namely nanobubbles (NBs), irrespective of their location, be it surface-attached or in the bulk liquid, play a crucial role in many natural processes and engineering applications, from mineral processing to drug delivery. The readily observed long term stability of surface NBs observed by atomic force microscopy (AFM), was explained e.g. by pining of the contact line [1, 2] causing an abnormal contact angle. Other nano-objects were shown to be liquid nanodroplets [3] (NDs). As both types of particles are soft, surface NBs can be barely [4] or not reliably distinguished from NDs by AFM imaging. To unequivocally distinguish surface NBs and NDs, and to study their evolution in presence of additives, Fluorescence Lifetime Imaging Microscopy (FLIM) is used here to study NBs and NDs on glass surfaces by the ethanol-water solvent exchange (Figure 1). The fluorescence of the reported dye Rhodamine 6G (Rh6G) is shown to possess substantially different lifetimes (τ) at the interfaces occurring in such a system: 660, 3030, 3260 and 3830 ps at air/water-, water/glass-, water/poly(dimethyl siloxane)-interfaces and in bulk water, respectively. In co-localization experiments, surface NBs labeled with Rh6G are detected by AFM as submersed soft elevated nano-objects with high spatial resolution and by FLIM as brightly fluorescing objects with short-lived fluorescence (Figure 2). NBs are distinguished from AFM-similar poly(dimethyl siloxane) NDs as well as from lubricant oil contamination NDs owing to the characteristic short τ of Rh6G at the air/water interface [5-7]. The successful application of a generalized FLIM approach for the identification of transient electrochemically generated bulk NBs as well as polymer additive stabilized bulk NDs will also be discussed.

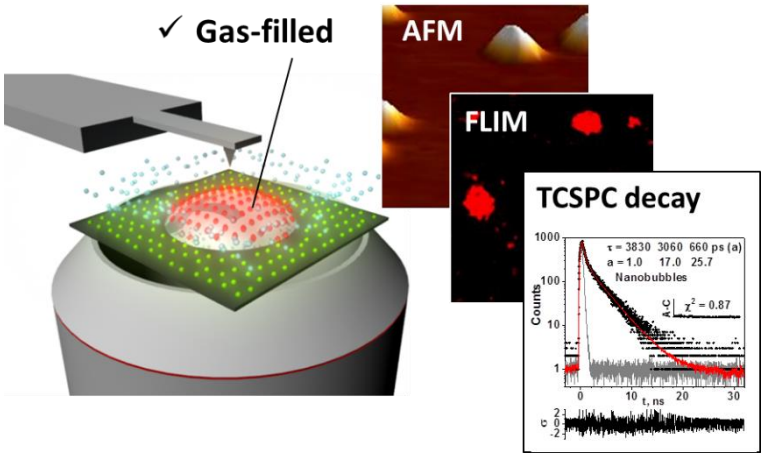

Figure 1. Schematic of the combined AFM-FLIM experiment, in which a dye-labeled NBs on a transparent glass substrate is probed from the top by AFM and from bottom by a confocal fluorescence microscope (left), AFM and FLIM images as well as fluorescence decay determined by time correlated single photon counting (TCSPC). Reproduced from ref [5].

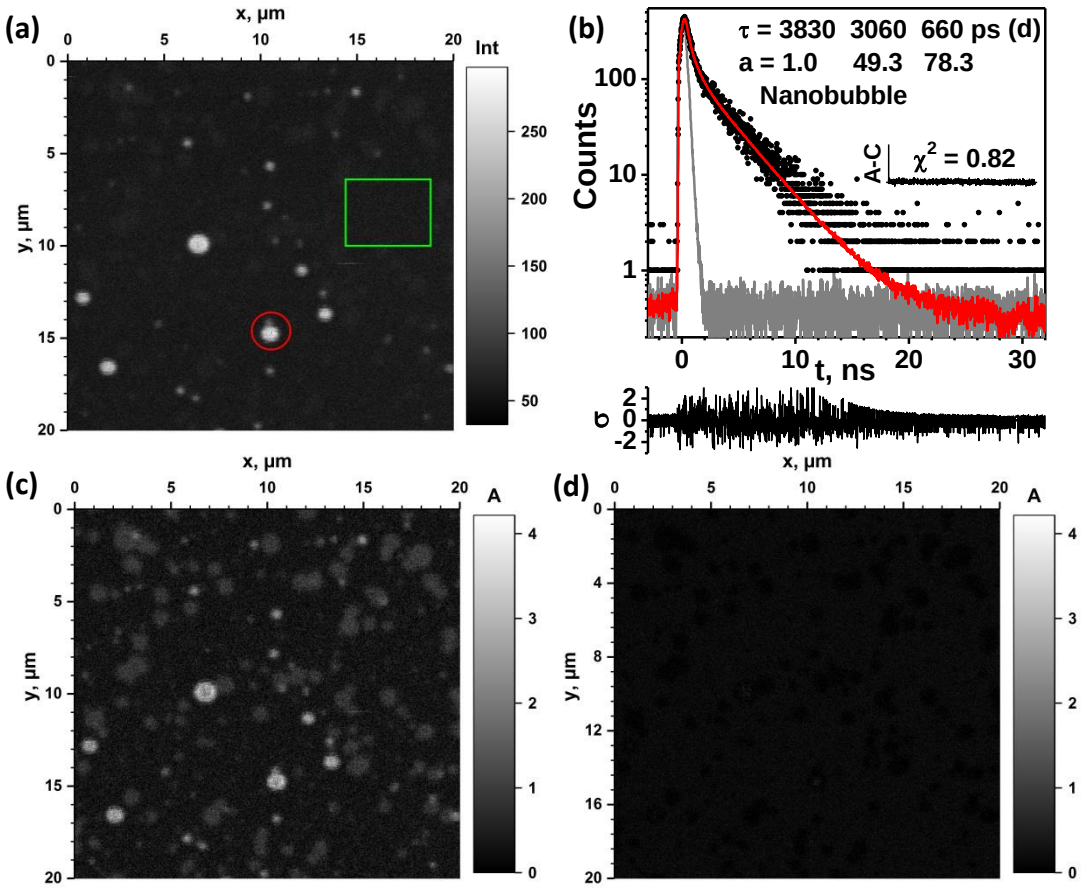

Figure 2. (a) Fluorescence intensity image of NBs nucleated by ethanol-water exchange in the presence of 850 nM Rh6G. (b) Fluorescence decays of the NBs area marked with red circle in image (a). Semi-log plot of the TCSPC fluorescence decays (black dots) of 850 nM Rh6G and together with the corresponding IRF function (gray line) and calculated fits (red line). The weighted residuals deviations σ and the autocorrelation function (A-C) plots are shown, the values of decay times τ and their amplitudes a as well as χ2 are also indicated. The excitation wavelength was 485 nm, the time resolution 16 ps. (c, d) FLIM amplitude images of (a) for: (c) short-lived, 660 ps, and (d) long-lived, 3830 and 3030 ps, fluorescence decay components. Reproduced from ref [5].

References

[1] B.H. Tan, H. An, C.-D. Ohl, Resolving the Pinning Force of Nanobubbles with Optical Microscopy, Phys. Rev. Lett., **2017**, 054501.

[2] C.U. Chan, M. Arora, C.-D. Ohl, Coalescence, Growth, and Stability of Surface-Attached Nanobubbles, Langmuir, **2015**, 7041-7046.

[3] R.P. Berkelaar, E. Dietrich, G.A.M. Kip, E.S. Kooij, H.J.W. Zandvliet, D. Lohse, Exposing nanobubble-like objects to a degassed environment, Soft Matter, **2014**, 4947-4955.

[4] H. An, B.H. Tan, C.-D. Ohl, Distinguishing Nanobubbles from Nanodroplets with AFM: The Influence of Vertical and Lateral Imaging Forces, Langmuir, **2016**, 12710-12715.

[5] N. Hain, S. Handschuh-Wang, D. Wesner, S.I. Druzhinin, H. Schönherr, Multimodal microscopy-based identification of surface nanobubbles, J. Colloid Interface Sci., **2019**, 162-170.

[6] N. Hain, D. Wesner, S.I. Druzhinin, H. Schönherr, Surface Nanobubbles Studied by Time-Resolved Fluorescence Microscopy Methods Combined with AFM: The Impact of Surface Treatment on Nanobubble Nucleation, Langmuir, **2016**, 11155-11163.

[7] H. Schönherr, N. Hain, W. Walczyk, D. Wesner, S.I. Druzhinin, Surface nanobubbles studied by atomic force microscopy techniques: Facts, fiction, and open questions, Jap. J. Appl. Phys., **2016**, 08NA01.

Direct measurement of the internal pressure of the ultrafine bubble using radioactive nuclei

Minoru Tanigaki[1]*, Takuya Yamakura[2], Daiju Hayashi[2], Yoshikatsu Ueda[3], Akihiro Taniguchi[1], Yomei Tokuda[4], and Yoshitaka Ohkubo[1]

1 *Institute for Integrated Radiation and Nuclear Science, Kyoto University, Kumatori, Osaka 590-0494, Japan*
2 *Graduate School of Science, Kyoto University, Sakyo-ku, Kyoto 606-8502, Japan*
3 *Research Institute for Sustainable Humanosphere, Kyoto University, Uji, Kyoto 611-0011, Japan*
4 *Faculty of Education, Shiga University, Otsu, Shiga 520-0864, Japan*

E-Mail corresponding authors: tanigaki@rri.kyoto-u.ac.jp

Abstract

The internal Xe gas pressure of ultrafine bubble has been directly measured for the first time using the γ-γ angular correlation technique, a very common measurement technique in nuclear physics.
A radioactive isotope of ^{125}Xe ($T_{1/2}$ = 16.7 h) was induced inside natural Xe ultrafine bubbles in water at the average diameter of 200 nm by the irradiation of thermal neutrons available from a 5 MW nuclear reactor at Kyoto University.
The asymmetry factor of 55 - 188 keV γ cascade in ^{125}I followed by the β decay of ^{125}Xe was used as the probe of the gas pressure in ultrafine bubbles. Since the emission probability of γ-ray depends on the angle between the nuclear spin and γ-ray, the angular correlation of γ-rays of a γ cascade is affected by the spin alignment of the nuclei at the intermediate state.
Observed asymmetry $A_{22}\overline{G_{22}(\infty)}$ was smaller than the asymmetry factor A_{22}=+0.235 ±0.001 because of the existence of hyperfine interactions at the intermediate state of γ cascade, represented as $\overline{G_{22}(\infty)}$.

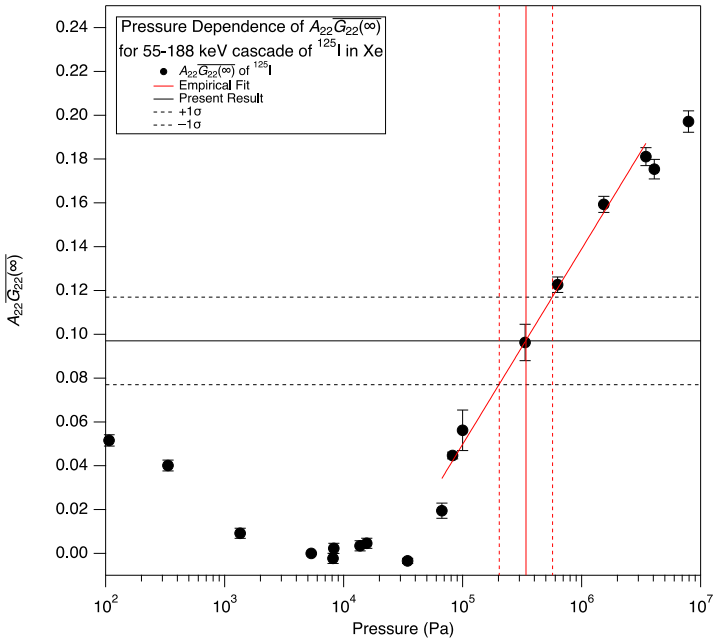

Figure **2** Pressure dependence of $A_{22}\overline{G_{22}(\infty)}$ for the 55-188 keV cascade in ^{125}I.

The internal pressure of the Xe ultrafine bubble is determined to be $3.4^{+2.3}_{-1.3} \times 10^5$ Pa by comparing with the pressure dependence of $A_{22}\overline{G_{22}(\infty)}$ by Berek [1] (Fig. 1). The present result is much lower than the internal pressures reported by Ohgaki [2] for the ultrafine bubbles of N_2, CH_4, and Ar, 6×10^6 Pa, or that from Young-Laplace equation 1.6×10^6 Pa.
A possible explanation for the discrepancy is the existence of Coulomb repulsive force by the electric charge at the surface of an ultrafine bubble.

Acknowledgments
This work was supported by JSPS KAKENHI Grant Number 18K03948, 21K03854.

References

[1]. U. Berek, W. Kreisel, H. Schneider, E. Tierno, and H. Wagner, The limiting values of some perturbed angular correlations in ^{127}I, ^{125}I isotopes, Physics Letters A **1975**, 55, 22.
[2]. K. Ohgaki, N. Q. Khanh, Y. Joden, A. Tsuji, and T. Nakagawa, Physicochemical approach to nanobubble solutions, Chemical Engineering Science **2010**, 65, 1296.

Differentiation of bubbles, particles and droplets by Holographic Particle Tracking.

Fredrik Eklund[1]*, Daniel Midtvedt[3]*, Erik Olsén[2], Benjamin Midtvedt[3], Jan Swenson[2], and Fredrik Höök[2]*

1 *Holtra AB, SE-41467 Göteborg, Sweden*
2 *Division of Nano and Biophysics, Department of Physics, Chalmers University of Technology, SE-41296 Göteborg, Sweden*
3 *Department of Physics, University of Gothenburg, SE-41296 Göteborg, Sweden*

E-Mail corresponding authors: fredrik.eklund@holtra.tech, daniel.midtvedt@physics.gu.se, fredrik.hook@chalmers.se

Abstract

Micro- and nanobubbles are increasingly utilized and explored in many applications, ranging from ultrasound contrast agents and drug delivery systems to mining industry and water purification. Despite increasing industrial use and application related research and development, there is still much uncertainty and controversy surrounding nanobubbles, especially outside the medical field. Light scattering methods such as Dynamic light scattering (DLS) and Nanoparticle Tracking Analysis (NTA) are commonly used to detect freely floating bulk nanobubbles, but light scattering nano-objects that appear in water following vigorous bubble formation and which are commonly interpreted as nanobubbles, may in fact be particle agglomerates [1]. Many methods to detect bubbles and differentiate them from solid particles and oil droplets have been demonstrated, but they are often not entirely unambiguous, and in some cases, expensive and difficult to operate [2].

By applying tracking analysis of submicron particles captured using off-axis digital holographic microscopy imaging, we could determine the size and phase shift of individual particles and bubbles in the diameter size range 0.25-1.5µm [3]. We first demonstrated the method by analyzing a dispersion of three different particle types, close in size and refractive index (RI), and accurately identifying each population (Fig 1 A,B). This would not be possible using regular Nanoparticle Tracking Analysis (NTA), since NTA cannot readily differentiate between particles of different optical properties. We furthermore applied the method on air bubbles stabilized by sorbitan surfactants. Since gas bubbles in water generally give an opposite phase shift compared to solid particles or oil droplets, gas bubbles were readily distinguished from particles of insoluble surfactant in the dispersion. The RI of the bubbles were furthermore determined with the help of size and phase shift. Deviations from the expected refractive index of gas (1.00) surprisingly revealed that most bubbles were in fact clusters of smaller bubbles with a diameter of 0.3 µm or less. The method thus reveals information about individual bubbles and particles which is difficult or impossible to extract by other methods.

We have also used the method to evaluate experiments with nanobubble generation in tap water and natural fresh water. Recent improvements of the method, including a decreased detection limit, has increased the applicability for nanobubbles.

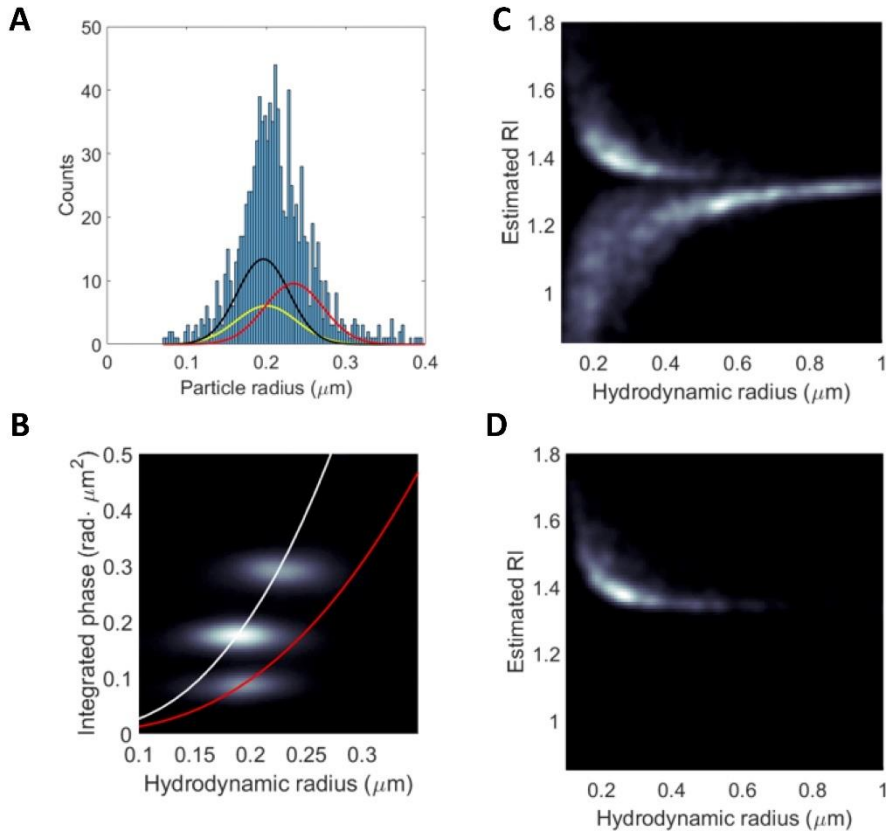

Fig 1. A, B: Holographic particle tracking analysis of a mixture of PSL with radius 0.20 and 0.24µm and Silica with radius 0.22µm. B; White line: RI=1.58, Red line: RI=1.45. C: Sorbitan particles with RI>1.33 and bubbles with RI<1.33 (RI_{H2O}=1.33). D: Same dispersion after exposure to 20 bar pressure, which destroyed the bubbles.

Acknowledgements

This work was supported by the Swedish Research Council, no. 2018-04900, by Excellence Initiative Nano, Chalmers University of Technology, and by Ekwa AB.

References

[1] Alheshibri, M.; Craig, V. S. J., Differentiating between Nanoparticles and Nanobubbles by Evaluation of the Compressibility and Density of Nanoparticles, *The Journal of Physical Chemistry C* **2018**, *122*, 21998-22007

[2] Eklund, F., et al., Differentiating bulk nanobubbles from nanodroplets and nanoparticles, *Current Opinion in Colloid & Interface Science* **2021,** 53, 101427

[3] Midtvedt, D.; Eklund, F.; Olsén, E.; Midtvedt, B.; Swenson, J.; Höök, F., Size and Refractive Index determination of Sub-Wavelength Particles and Air Bubbles by Holographic Nanoparticle Tracking Analysis, Analytical Chemistry **2020**, 92, 1908-1915

Visualization of plus charged nano-bubble surrounded by electrified nanobelt, using Ultra-high voltage electron microscope: Revealed functions of the plus charged nano-bubble

Takeshi Ohdaira and Emi Kitakata

Postal code: 277-0882
Address: 5-1-5, Kashiwanoha, Kashiwa-shi, Chiba-ken, JAPAN
Ohdaira Research and Development Team, Institute for Solid State Physics, Tokyo University
Phone/FAX: +81-4-7136-4944 Mobile phone: +81-80-8559-9799 e-mail:

t.ohdaira@issp.u-tokyo.ac.jp 2nd e-mail: takeshiws.ohdaira@nifty.com **Abstract**

Introduction:

Many investigator are probably thinking that many of both micro-bubble and nano-babble have noncharged or minus charged electrical force. Certainly a lot of generator, which can produce nanobubbles, probably cause either non-charged or minus charged nano-bubbles using cavitation method. In this conference, we will show you that it can be produced large amount, for example 1.5×10^8bubbles/ml, of plus charged nano-bubbles using very simple non-cavitation mechanism in the five seconds. The special feather of plus charged nano-bubble, is the carriage effect of electron.

The carriage effect of electron can cause various function among wound healing effect in medical scene, promote of growth in agriculture, increasing seafood and cleaning level-up in the washing of electronic equipment. At first we have to emphasize that the evidence of surrounding electrical belt of charged nano-bubble can be visualized. We were developed the detector, which consist of the 5nm diameter superparamagnetic charger particle probes (Fig.1).

We had evidences of the electrical belt surrounding the plus charged nanobubble using 5nm diameter superparamagnetic charger particle probes.

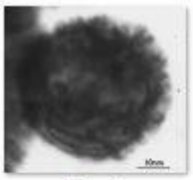

Fig.1

Material and methods:

Recognition of nano-bubbles：

We used the Ultra-high voltage electron microscope, abbreviated UHVEM, for visualization of electrical belt of charged nano-bubble. We used the ultra-low temperature type probe of UHVEM.

Ultra-low temperature type probe of UHVEM can momentary fix the charged nano-bubble of original shape and its location. In this way, investigator can acquire enough time of observation the bubbles. Many type of UHVEM generate high voltage electron beam to the samples.

But high voltage electron beam its-self possibly melt the frozen samples consisted charged nano-bubble. Furthermore the high voltage electron beam can easily attack both the charged nano-bubble and the material consisted charged nano-bubble in the ice. We developed the new UHVEM method of observation for charged nano-babble using ultra-low temperature type probe, which named ‘gradation method’. Transmission type electron microscope has difficulty of making samples. On the

other hand, the combination method of both the ultra-low temperature type probe of UHVEM and gradation method, can recognize the charged nano-bubble 100% at any time.

Charged level recognition:

At first the samples of plus charged nano-bubble water was mixed with newly developed 5nm diameter superparamagnetic probes. Next the mixture coated the tip of ultra-low temperature type probe of UHVEM by using 'gradation method'. We put the ultra-low temperature type probe of UHVEM into the chamber of UHVEM. The focus setting of recognition level of observation of bubbles were easily performed (Fig.2).

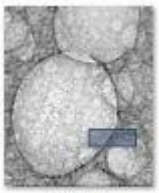

Fig.2

We captured the view of electrical belt made by UHVEM using nano-superparamagnetic probes. For decision making of both charged level and charged polar, the captured movies of boundary of the nano-bubble were calculated by three dimensional level plotting program (Fig.3).

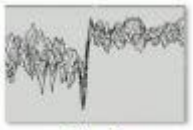

Fig.3

The other elemental detection concerning bubble like functions:
Finally we calculated the concentrations of both little amount of ionized element of plus charged nano-bubble generating material and the other trace elements by Inductively Coupled Plasma method, abbreviated ICP.

Clinical study (Medicine):
Clinical trial was performed. Plus charged nano-bubble water demonstrates its good performance in clinical study for intractable ulcer with diabetes and/or arteriosclerosis obliterans. Field test (Agriculture): Leaf vegetable, edible roots and fruit vegetables were studied in water culture model with plus charged nano-bubble water or minus charged nano-bubble water.

Results:
We can confirmed that the plus charged nano-bubble can be generated by using our newly developed plus charged nano-bubble generator material. We can recognize the polar the electrical belt surrounded the charged nano-bubbles. We can bubbles clearly differ from nano-dusts. Furthermore we recognized the existence of charged nano-bubbles in leaf of plant using combination of both the ultra-low temperature type probe of UHVEM and gradation method. We calculated the concentration of both ionized plus charged nano-bubble generating material and the other trace elements by ICP. But the concentration level of the ionized plus charged nano-bubble generating material was under 0.05ppm level and the other trace elements were less than ppt level.

Clinical study (Medicine):
Plus charged nano-bubble water demonstrates its good performance in clinical study for intractable ulcer with diabetes and/or arteriosclerosis obliterans. 10 patients were studied. All patient completely heal their ulceration.

Field test (Agriculture):
In water culture model, the plants circulated by plus charged nano-bubble water grows up more than them by minus charged nano-bubble water in Leaf vegetable, edible roots and fruit vegetables.

Conclusion:
We can develop the recognizing method of electron-belt surrounded the plus charged nano-bubble. Plus charged nano-bubble might cause the various functions differed from both non-charged nanobubble and minus charged nano-bubble.

Electrochemically Generated Nanobubbles

Valeria Molinero

The University of Utah, Theoretical Chemistry

Gas evolving reactions are ubiquitous in the operation of electrochemical devices, and can result in the formation of bubbles that block the electrode and decrease reaction rates. The deleterious effect of bubbles is amplified by the current trend of miniaturization of electrodes to nanoscopic sizes, as a single nanobubble can grow to cover the whole reactive area. This presentation will discuss our work using molecular simulations and theory to understand the electrochemical formation and stationary states of bubbles on nanoelectrodes, how the size and shape of the electrodes impact the currents that can be obtained when a bubble forms, and how we can use that knowledge to maximize conversion rates on gas producing electrochemical reactions.

Applications in Engineering and Process Techniques I

Surface nanobubbles induce instability of solution-deposited thin films

Pavel Janda[1,*] and Hana Tarábková[1]

1 J. Heyrovsky Institute of Physical Chemistry of the Czech Academy of Sciences, Dolejškova 3, Prague, Czech Republic

E-Mail corresponding authors: pavel.janda@jh-inst.cas.cz

Abstract

Solution-deposited thin films, which serve for various purposes, ranging from surface protection to process mediators, are formed by variety of techniques both on laboratory and industrial scale. Our work indicates, that surface nanobubbles appear to be the most frequent cause of defects forming micro/nano-pores of various shapes in solution-deposited thin films. Presence of nanobubbles during film deposition causes shielding of target surface and degrades properties of deposited film by formation of void spots, which create bypassing channels, decreases film durability and exposes surface, which should be covered.

In case that nanobubble shielding prevents deposition of catalyst film, it limits the deposited amount of catalysts or mediator and thus decreases its overall efficiency. While nanobubble presence is usually indicated by circular hollow pinholes formed in deposited film, nanobubble-induced film instability is manifested upon dewetting, by film slippage causing pinhole deformations.

Correlations of both in-situ AFM images of surface nanobubbles and ex-situ images of identical substrate locations covered by porphyrazine mediator and gelatin as model thin films solution-deposited by various techniques including (specific) adsorption and electrochemical deposition indicate relation between nanobubbles and film defects.

Nanobubbles on different hydrophobic surfaces and their application in low-rank coal flotation

Fanfan Zhang[1,2], Chunyun Zhu[1,2], Yijun Cao[2,3], Holger Schönherr[1,*]

1 *Physical Chemistry I & Research Center of Micro- and Nanochemistry and (Bio)Technology (Cμ), Department of Chemistry and Biology, University of Siegen, Adolf-Reichwein-Str. 2, Siegen 57076, Germany;*
2 *School of Chemical Engineering and Technology, China University of Mining and Technology, Xuzhou 221116, Jiangsu, China;*
3 *School of Chemical Engineering and Technology, Zhengzhou University, Zhengzhou 450066, Henan, China.*

E-Mail corresponding author: schoenherr@chemie.uni-siegen.de

Abstract

In recent decades, nanobubbles (NBs) have attracted widespread scholarly attention and they have been applied in many industrial fields. In the flotation process of particles, NBs are considered to act as "secondary collector", which have the bridging effect between particles and carry bubbles to significantly promote the flotation efficiency of coal and minerals [1]. The morphologies of NBs on different hydrophobic surfaces were investigated by total internal reflection fluorescence (TIRF) microscopy and atomic force microscopy (AFM). The effect of NBs on the interaction of inter-particles was investigated with the colloid cantilever technology. To explore the role of dissolved air concentration and NBs in the flotation of low-rank coal (LRC), de-aerated water (DW), ordinary water (OW), and air-oversaturated water (PW) were prepared. The formation of NBs is closely related to the hydrophobicity of the substrate surfaces, and more and larger NBs form on the strong hydrophobic surface (Figure 1).

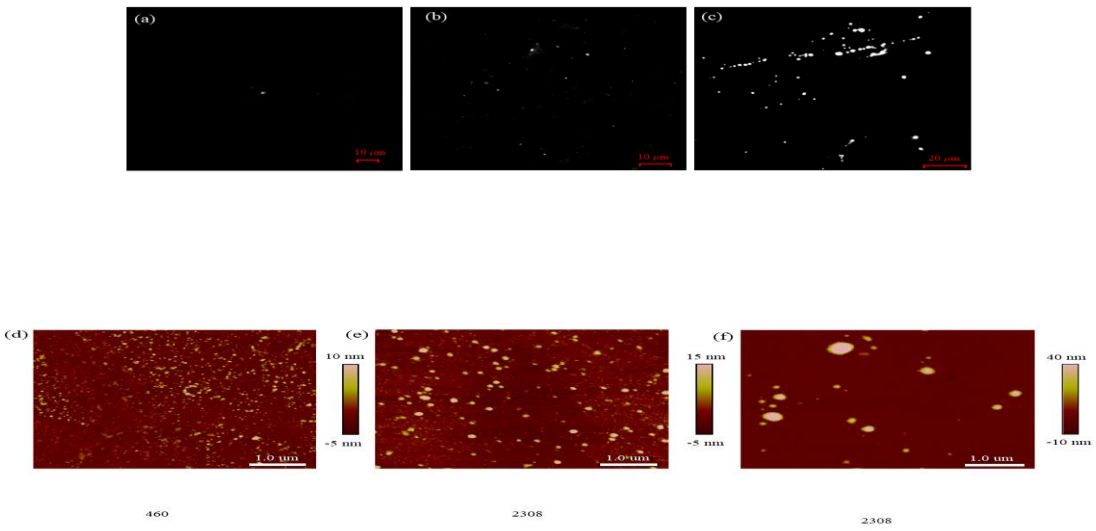

Figure 1. Nanobubbles on different hydrophobic surfaces obtained by total TIRF microscopy (a-c) and AFM (d-f): surfaces (from left to right) were hydrophilic, medium hydrophobic, strongly hydrophobic. Rhodamine 6G was used to label the nanobubbles in the TIRF microscopy experiment.

Furthermore, the magnitude and range of hydrophobic interaction are positively related to the dimension of NBs. With multiple approaches of a hydrophobic colloid to strong hydrophobic surfaces, the hydrophobic interaction is further enhanced due to the merging and cavitation of NBs [2]. As for the flotation performance of LRC, it is positively correlated to the air concentration in aqueous solution, which is confirmed by the induction time measurement. Typical nanobubbles scanned on highly oriented pyrolytic graphite (HOPG) surface in PW are a reasonable explanation of the phenomenon. Besides, the hydrophobic interaction between LRC particle and HOPG in PW is significantly stronger than that in both OW and DW, which is attributed to capillary-bridge effect of NBs on particles surfaces (Figure 2) [3].

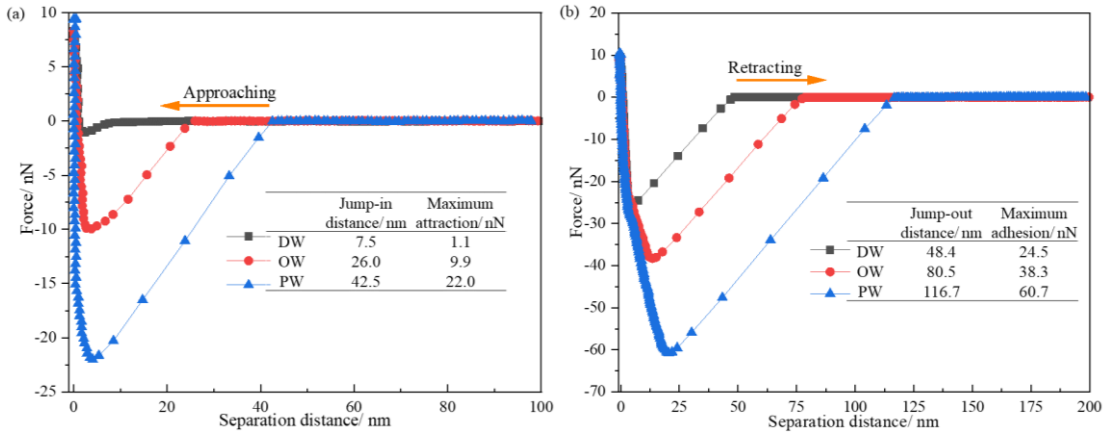

Figure 2. Interaction forces between the low-rank coal particle and HOPG in DW, OW, and PW, respectively: (a) Approaching forces curves; (b) Retracting forces curves.

Acknowledgements

The authors acknowledge funding from the Chinese Scholarship Council (CSC) and the University of Siegen.

References

[1] F. Zhang, L. Sun, H. Yang, et al. Recent advances for understanding the role of nanobubbles in particles flotation, Advances in Colloid and Interface Science 2021, 291, 102403.
[2] F. Zhang, H. Yang, X. Gui, et al. Interfacial nanobubbles on different hydrophobic surfaces and their effect on the interaction of inter-particles, Applied Surface Science 2022, 582, 152184.
[3] F. Zhang, E. Ding, X. Gui, et al. Influence of Air Solubility on the Flotation Performance of Low-Rank Coal, Langmuir 2022, 38, 2467−2477.

Optical evaluation for ultrafine bubble cleaning of contamination in a flow channel

Daniel Niehaus[1], Erika Fujita[2], Michael Schlüter[1], and Koichi Terasaka[3]

1 *Institute of Multiphase Flows, Hamburg University of Technology, Hamburg, Germany*
2 *School of Science for Open and Environmental Systems, Graduate School of Keio University, Yokohama, Japan*
3 *Department of Applied Chemistry, Keio University, Yokohama, Japan*

E-Mail corresponding authors: daniel.niehaus@tuhh.de, ericaf0116@keio.jp, michael.schlueter@tuhh.de, terasaka@applc.keio.ac.jp

Abstract
Regular cleaning of production facilities is very important in pharmaceutical, food processing, and bioplant operations [1]. The possibility of cleaning with ultrafine bubbles (UFBs) has been suggested for cleaning in small systems [2,3]. Adding UFBs to the cleaning solution in Clean-In-Place may reduce the amount of detergent and surfactant required.

However, there is a lack of technology to accurately quantify the cleaning effect of fine bubbles which diameter is less than 1 µm [4] on various pollutants in closed ducts and to provide fundamental data. Therefore, a glass laminar flow channel with optical access was designed as shown in Figure 1 to measure and evaluate the UFB cleaning effect.

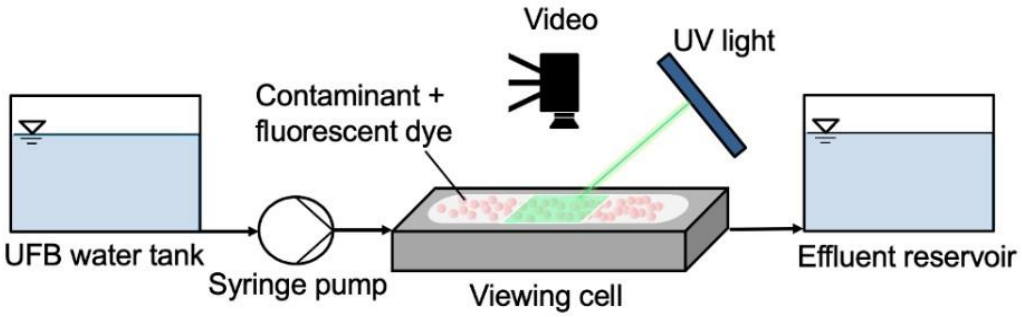

Figure 1. Schematic experimental setup for optical investigation of cleaning by UFBs.

Procedures have been developed to prepare reproducible contaminants and to quantitatively measure the time course of the cleaning process. First, the contaminant suspension was placed on the glass cover panel of the flow channel with fluorescent dye, and then dried as shown in Figure 2. UFB suspending water was laminarly fed into the flow channel attaching the glass cover panel. To compare the cleaning behavior of contaminants adhering to the glass panel with UFB water or UFB-free water, the cleaning process was monitored under UV light and as a function of time recorded by the video camera.

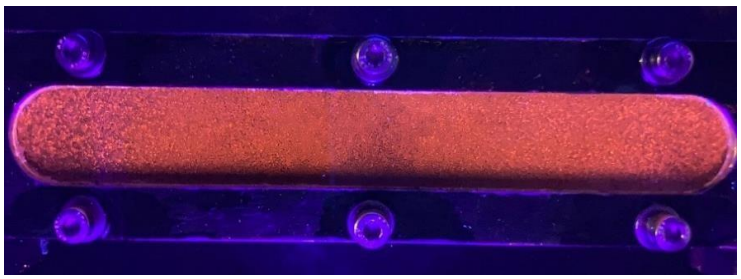

Figure 1. Glass panel coated with silica particles (>0.2 µm) and fluorescent dye.

In addition to the cleaning evaluation by optical measurement, the UFB number concentration at the inlet and outlet of the flow channel was determined by Particle Tracking Analysis (NanoSight NS300, Malvern Instruments, UK).

In this study, we will introduce the experimental setup, details of the measurement method, and the results of the investigation of the cleaning effect of the cleaning solution with and without UFBs on various model contaminants (silica particles, starch, etc.). One of the most important aspects is the effect of flow velocity on the cleaning efficiency of UFBs.

References

[1] Eide, M., Homleid, P., Mattsson, B., Food Sci. Technol., 2003, Vol. 36(3), pp.303–314.
[2] Hata, T., Nishiuchi, Y., Tanaka, K., Okamura, Y., Sakakibara, Y., Terasaka, K., 2018, Int. J. Multiphase Flow, Vol. 32(1), pp. 4–11.
[3] Terasaka, K., Yasui, K., Kanematsu, W., Aya, N. (Eds.), 2021. “Ultrafine Bubbles,” Jenny Stanford Publishing, Singapore.
[4] ISO/TS 80004-1, Nanotechnologies – Vocabulary – Part1: Core terms, 2015.
https://www.iso.org/standard/68058.html

A systematic calibration procedure for bubble dynamics for laser ablation in liquids

Alexander Bußmann[1], Stefan Adami[1], and Nikolaus A. Adams[1]*

1 *Technical University of Munich, Chair of Aerodynamics and Fluid Mechanics, Boltzmannstraße 15, 85748 Garching b. München*

E-Mail corresponding authors: alexander.bussmann@tum.de

Abstract

During laser synthesis and processing colloids (LSPC), nanoparticles emerge from an ablated target surface. Such colloids are used in a wide range of applications, such as optics, or biology [6]. One key part of LSPC is the laser ablation in liquid (LAL), where a laser is focused on the surface of a target surrounded by liquid material.

During the ablation process a vapor bubble is generated as a side effect that affects productivity and purity of the ablated material. Depending on the ablated target material, the evolution of this cavitation bubble differs significantly in time and size. If only the collapse and subsequent cycles of growth and expansion of an isolated bubble are investigated, the analytical Gilmore model gives accurate results for the cavitation dynamics. However, if the full process of initial expansion after optical breakdown is included, the analytical model is not suitable anymore for the lack of defined initial conditions. Furthermore, interactions between multiple bubbles cannot be captured correctly by the analytical model, especially if no a priori information of their interactions is available. Therefore, we seek to investigate the bubble dynamics of a single bubble that has been generated at a wall by a focused laser in a liquid environment by means of numerical simulation. We apply the open-source finite-volume code framework ALPACA that uses a sharp-interface levelset method [3]. A general formulation of the Navier-Stokes equation is applied without any specific adaptation to bubble dynamics. We have demonstrated in earlier works that this model is capable to reproduce accurately the analytical results for single bubble collapse dynamics [5]. Results have been validated extensively for various multi-component simulations [3].

We validate the applied method based on the analytical solution. It has been shown that the Gilmore model gives incorrect results for the subsequent cycles of the cavitation bubble at high initial pressure ratios [2]. This is investigated here in more detail to elucidate the range of validity for the analytical model. Moreover, we investigate the influence of different formulations of equations of state in the bubble interior and exterior that have been proposed by Denner [1].

To simulate the nano-particle generation in LAL, special initial conditions are required for the initially small but highly energetic bubble. We apply the concept of energy-deposit [4] and calibrate the initial conditions with a simple method based on the analytical model. This allows us to correctly capture the dynamics of the first cycle of the cavitation bubble after optical breakdown. To demonstrate the applicability of the method, we compare our numerical simulations with experiments of four different target materials. Furthermore, we investigate the limits of the concept for finite-volume simulations of LAL. As an example, in Figure 1, certain time instances of the evolution of the simulated bubble compared to the experiment are shown for a silver target. The bubble evolution and near wall region agree very well. This motivates further numerical investigations of the process of nano-particle generation in LAL. Especially, the interaction of multiple bubbles and their influence on the productivity are subject of future studies.

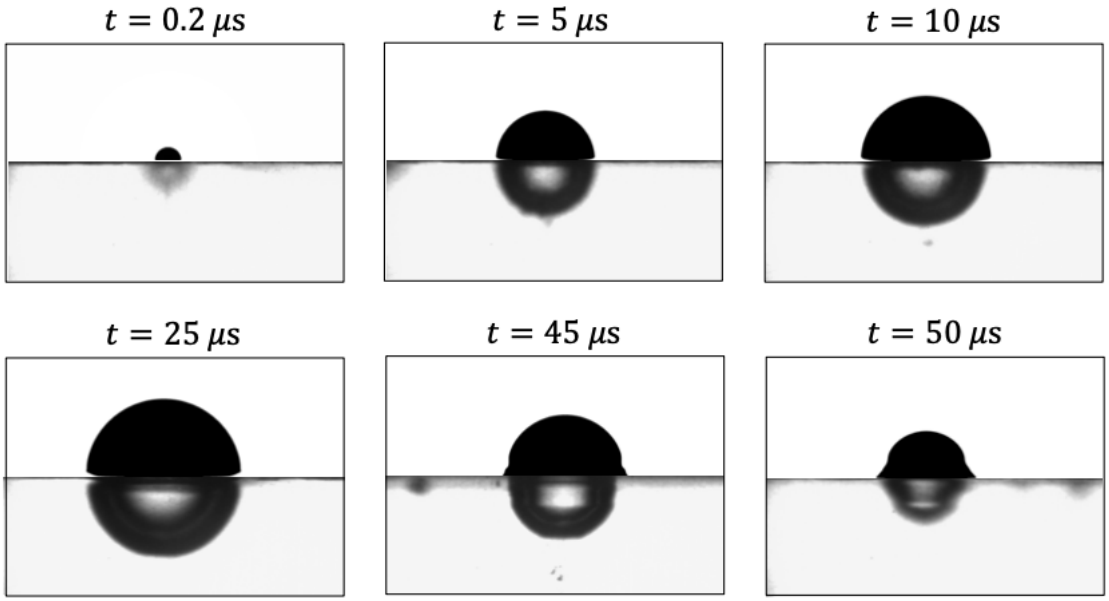

Figure 1. Different time instances of the evolution of a cavitating bubble after optical breakdown of a 12 ps, 2.7 mJ laser at a silver target. For each instance the simulation (top) is compared to the experiment (bottom).

Acknowledgements

The authors want to acknowledge funding by the Deutsche Forschungsgesellschaft (DFG, German Research Foundation) - Project-ID 440395856. The authors gratefully acknowledge the Gauss Centre for Supercomputing e.V. for funding this project by providing computing time at Leibniz Supercomputing Centre.

References

[1] Denner, F. “The Gilmore-NASG model to predict single-bubble cavitation in compressible liquids”. In: *Ultrasonics Sonochemistry* 70 (Jan. 2021), p. 105307. DOI: 10.1016/j.ultsonch.2020.105307.

[2] Fuster, D., Dopazo, C., and Hauke, G. “Liquid compressibility effects during the collapse of a single cavitating bubble”. In: *The Journal of the Acoustical Society of America* 129.1 (Jan. 2011), pp. 122–131. DOI: 10.1121/1.3502464.

[3] Hoppe, N., Winter, J. M., Adami, S., and Adams, N. A. “ALPACA - a level-set based sharp-interface multiresolution solver for conservation laws”. In: *Computer Physics Communications* 272 (Mar. 2022), p. 108246. DOI: 10.1016/j.cpc.2021.108246.

[4] Lauterborn, W., Lechner, C., Koch, M., and Mettin, R. “Bubble models and real bubbles: Rayleigh and energy-deposit cases in a Tait-compressible liquid”. In: *IMA Jour- nal of Applied Mathematics* 83.4 (July 2018), pp. 556–589. DOI: 10.1093/imamat/ hxy015.

[5] Schmidmayer, K., Bryngelson, S. H., and Colonius, T. “An assessment of multicomponent flow models and interface capturing schemes for spherical bubble dynamics”. In: *Journal of Computational Physics* 402 (Feb. 2020), p. 109080. DOI: 10.1016/j.jcp. 2019.109080.

[6] Zhang, D., Gökce, B., and Barcikowski, S. “Laser Synthesis and Processing of Colloids: Fundamentals and Applications”. In: *Chemical Reviews* 117.5 (Feb. 2017), pp. 3990–4103. DOI: 10.1021/acs.chemrev.6b00468.

Experimental investigation into the effect of ultrafine bubbles on interaction between bubble clusters and an acrylic wall under sound field

Shusuke Toriumi[1,*] and Toshihiko Sugiura[1]

1 Keio University, Yokohama, Japan.

E-Mail corresponding authors: sugiura@mech.keio.ac.jp

Abstract

1. Introduction

Volumetric oscillation and translational movement of microbubbles have been applied to various fields including ultrasonic cleaning. It has been studied that this cleaning effect is greatly contributed by friction between translating bubbles and objects to be cleaned [1]. It is also known that the use of water containing ultrafine bubbles can enhance this cleaning effect compared to the use of water without UFBs. This study investigates the effect of UFBs on the interaction between bubble clusters and a wall by experimentally observing the translational motion of bubble clusters along the wall in both water with UFBs and water without UFBs.

2. Theory

2.1. Bjerknes force

Bubbles oscillating in volume near a wall under sound field receive the second Bjreknes force directed toward a nearby wall due to the pressure gradient caused by the reflection of their own radiation pressure from the wall.

2.2. Layer of UFBs

In general, solid walls are negatively charged in water; therefore, an excessive amount of positive charge in the water concentrates near the wall, forming a layer called the electric double layer. According to reference [2], since UFBs in the liquid are negatively charged, they are attracted by the positive charge mentioned above and gather near the wall and adhere to it. In this way, a layer with a high concentration of UFBs can be formed on the wall surface.

3. Experiment

Figures 1 (a) and (b) show the side and top views of the experimental device. Water with UFBs or water without UFBs was kept in an acrylic container, and the pressure was reduced to about 7 kPa. Ultrapure water was used as the water. Bubbles were injected from a syringe. During vertical shaking of the container at 312.5 Hz, the injected bubbles clustered with

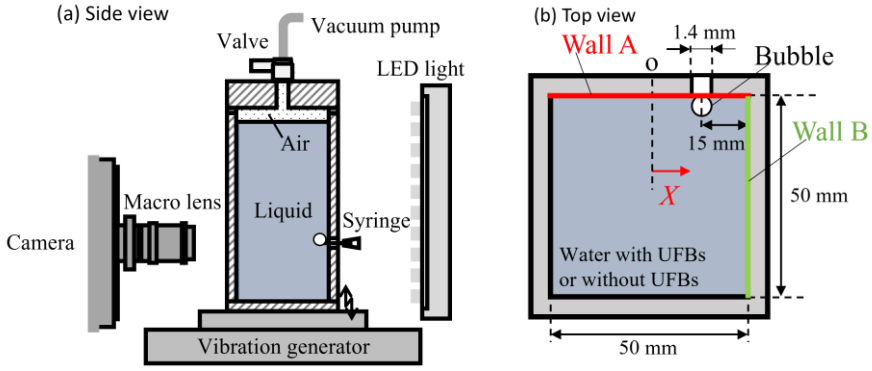

Figure 1. Experimental system.

volume Oscillations an moved along wall A toward wall B by the second Bjerknes force. Motion videos of the bubble clusters were shot with a high-speed camera, and dynamics of the bubble clusters was investigated by image analysis of those video data.

4. Result

Examples of the translational motion obtained by image analysis are shown in Fig. 2 (a) for water with UFBs and Fig. 2(b) for water without UFBs. X denotes the distance of the bubble cluster from the center of the acrylic container. Plots by open circles show observed results of translation, while the solid lines show results obtained by numerically integrating equations of motion, without considering the effect of back wall A, under the Bjerknes force due to the reflection from wall B, which was evaluated by image analysis for four periods of observed volume oscillation of the bubble cluster.

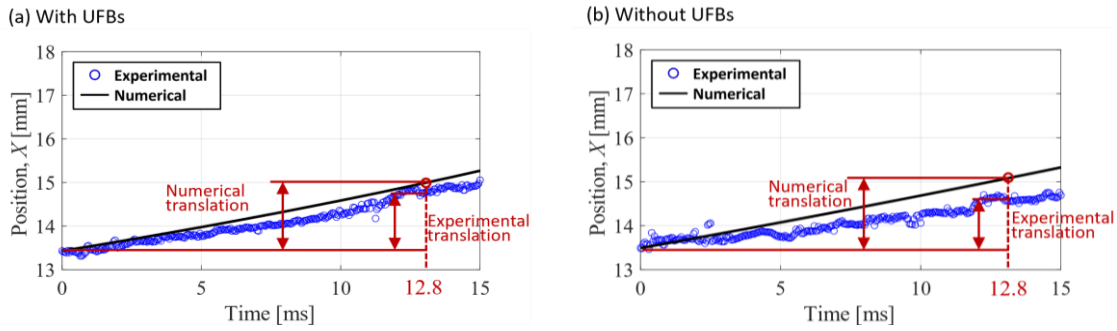

Figure 2. A bubble cluster translation along the wall in water with and without UFBs.

For quantitative evaluation, the difference between the measured translation distance and the numerical value without the back wall at t = 12.8 ms, corresponding to four periods of excitation was normalized by that numerical value, and its average of 20 times was obtained. The average values are 0.16 and 0.29 for water with and without UFBs, respectively. Therefore, since the translation of bubble clusters in water with UFBs is faster, it can be thought that the effect of layered UFBs near the wall reduces the interaction between bubble clusters and the back wall A.

5. Conclusion

By experimentally investigating the translational motion of the bubble cluster along the wall in water with and without UFBs, we found that the effect of layered UFBs near the wall reduces the interaction between bubble clusters and the acrylic wall.

References

[1] R. Azakami, H. Kikuchi, Particle Removal Mechanism in Ultrasonic Cleaning, The Journal of the Surface Finishing Society of Japan 1996, 47, 37-41. (in Japanese)

[2] A. Ushida, T. Hasegawa, et al., Drag Reduction Effect of Nanobubble Mixture Flows through Micro-orifices and Capillaries, Experimental Thermal and Fluid Science 2012, 39, 54-59.

Oxygen nanobubbles for water pollution remediation and ecological restoration

Gang Pan

School of Animal, Rural and Environmental Sciences, Nottingham Trent University, UK

E-Mail corresponding authors: gang.pan@ntu.ac.uk

Abstract

Bulk oxygen nanobubbles have been increasingly used to remediate water pollution in natural waters. However, the need of continuous pumping of oxygen into natural waters represents a great challenge for cost-efficiency and zero carbon due to the large volume and the short retention of oxygen in water. This hurdle may be potentially lifted by loading oxygen micro-nano bubbles into clay porous and manipulating its release/retain properties, which can be purposely delivered into deep waters and the sediment by natural gravity (settling), where the switch of pollutants from sediment to water can be turned off. Here, we will introduce a series of studies of using clay interfacial oxygen nanobubble to: 1) remediate hypoxia/anoxia in sediment and its effect in reducing phosphorus, nitrogen pollution from the internal loads[1-3]; 2) reduction of arsenic toxicity in eutrophic waters and sediments [4]; 3) reduction of greenhouse gas emission from eutrophic waters [5]; 4) reduction of mercury toxicity in eutrophic waters and sediments [6,7]; 5) accelerating aquatic ecological (such as macrophyte) restoration [8-10]. The chemical, physical, and microbial effects and mechanisms of the above-mentioned treatments, including the manipulation of sediment-water cycling of P, N, C, As, Hg, and S, will be analyzed and summarized [11-14].

References

[1] Zhang, H.G., Tao Lyu, Bi, L., Grant Tempero, David P. Hamilton, Pan, G.*, Combating hypoxia/anoxia at sediment-water interfaces: A preliminary study of oxygen nanobubble modified clay materials, Science of The Total Environment, **2018**, 637, 550-560.
[2] H Zhang, T Lyu, L Liu, Z Hu, J Chen, B Su, J Yu, G Pan, Exploring a multifunctional geoengineering material for eutrophication remediation: Simultaneously control internal nutrient load and tackle hypoxia, Chemical Engineering Journal, **2021**, 406, 127206
[3] Gang Pan*, Xiaojun Miao, Lei Bi, Honggang Zhang, Lei Wang, Lijing Wang, Zhibin Wang, Jun Chen, Jafar Ali1, Minmin Pan, Jing Zhang, Bin Yue, and Tao Lyu, Modified local soil (MLS) technology for harmful algal bloom control, sediment remediation, and ecological restoration, Water, **2019**, 11 (6): 1123
[4] Y Tang, M Zhang, J Zhang, T Lyu, M Cooper, G Pan*, Reducing arsenic toxicity using the interfacial oxygen nanobubble technology for sediment remediation, Water Research, **2021**, 205, 117657
[5] Shi, W.Q., Pan, G.*, Chen, Q.W., Song, L.H., Zhu, L., Ji, X.N., Hypoxia Remediation and Methane Emission Manipulation Using Surface Oxygen Nanobubbles, Environ. Sci. Technol., **2018**, 52 (15), 8712–8717
[6] X Ji, C Liu, M Zhang, Y Yin, G Pan*, Mitigation of methylmercury production in eutrophic waters by interfacial oxygen nanobubbles, Water Research, **2020**, 115563
[7] X Ji, C Liu, G Pan*, Interfacial oxygen nanobubbles reduce methylmercury production ability of sediments in eutrophic waters, Ecotoxicology and environmental safety, **2020**, 188, 109888
[8] Shuo Wang, Yunsi Liu, Tao Lyu, Gang Pan, Pan Li, Aquatic macrophytes in morphological and physiological responses to the nanobubble technology application for water restoration, ACS EST Water, **2021**, 1, 2, 376–387
[9] Zhang, H.G., Shang, Y.Y., Tao Lyu, Pan, G.*, Switching Harmful Algal Blooms to Submerged Macrophytes in Shallow Waters Using Geo-engineering Methods: Evidence from a N-15 Tracing Study, Environmental Sciences & Technology, **2018**, 52(20), 11778-11785
[10] Y Wu, T Lyu, B Yue, E Tonoli, EAM Verderio, Y Ma, G Pan*, Enhancement of tomato plant growth and productivity in organic farming by agri-nanotechnology using nanobubble oxygenation, Journal of Agricultural and Food Chemistry, **2019**, 67 (39), 10823-10831
[11] Jun Chen, Honggang Zhang, Lixuan Liu, Jing Zhang, Mick Cooper, Robert JG Mortimer, Gang Pan, Effects of elevated sulfate in eutrophic waters on the internal phosphate release under oxic conditions across the sediment-water interface, Science of the Total Environment, **2021**, 790, 148010
[12] L Wang, J Ali, Z Wang, NA Oladoja, R Cheng, C Zhang, G Mailhot, G Pan*, Oxygen nanobubbles enhanced photodegradation of oxytetracycline under visible light: Synergistic effect and mechanism, Chemical Engineering Journal, **2020**, 124227
[13] LYU, T., Wu, S., MORTIMER, R. and PAN, G*, Nanobubble Technology in Environmental Engineering: Revolutionization Potential and Challenges, Environ Sci Technol., **2019**, 53(13):7175-7176
[14] Bhabananda Biswas, Laurence N. Warr, Emily F. Hilder, Nirmal Goswami, Mohammad M. Rahman, Jock G. Churchman, Krasimir Vasilev, Gang Pan, Ravi Naidub, Biocompatible functionalization of nanoclays for improved environmental remediation, Chemical Society Reviews, **2019**, 48(14):3740-3770

Imaging Single Suface Nanobubbles with Advanced Optical Microscopy

Wei Wang

School of Chemistry and Chemical Engineering, Nanjing University, China

wei.wang@nju.edu.cn https://chem.nju.edu.cn/wanglab

Abstract

The past decade has witnessed the theoretical and experimental debates on the extraordinary long lifetime and low contact angle of surface nanobubbles. While several kinds of imaging techniques have provided promising evidences on the lifetime and gaseous nature of single surface nanobubble, each of them suffered from its own limitations before a consensus can be reached. In the present work, we employed a recently-developed surface plasmon resonance microscopy (SPRM) to visualize single surface nanobubble without labeling for the first time [1]. The quantitative dependence between optical signal and nanobubble volume allowed for resolving the dissolution kinetics, which is a key for understanding the lifetime. A super-localization method was further introduced to monitor the trajectory of its mass center during dissolution, which uncovered the stick-slip behavior in the early stage and the migration behavior in the late stage. The label-free, non-intrusive, quantitative and sensitive features of SPRM and the potential compatibility with atomic force microscopy shed new light on the long-standing puzzle behind surface nanobubbles.

We also summarize the unique features of SPRM that makes it a novel and promising technique in the toolbox for studying surface nanobubbles. First, the non-intrusive and label-free nature of SPRM allows for studying the nanobubbles in its native states under a physiochemical environment that is almost identical to mainstream AFM studies. Second, SPRM signal shows a simple and robust dependence on the volume of nanobubble, facilitating the quantitative kinetics study. Third, enhanced electromagnetic field confined in the SPPs ensures the extraordinary sensitivity for detecting sub-100nm nanobubbles. Fourth, the inverted configuration of SPRM is compatible for integrating an AFM on top of the sample. Similar combination between TIRFM and AFM has been achieved in several groups and has proven powerful. Such combined systems should deliver comprehensive capabilities to characterize surface nanobubbles.

In addition to the dissolution dynamics of surface nanobubbles, we would also like to cover other results regarding hydrogen nanobubbles produced by photocatalysis [2,3] and electro-catalysis [4] of water splitting, nucleation activation energy barrier of single vapor nanobubble [5], and most recent results that we have investigated, including characterizations to the thickness of bubble-liquid interface, surface charge and refractive index of single surface nanobubbles.

References

[1] YJ Wang, J Chen, YY Jiang, X Wang, W Wang, Label-free optical imaging of the dynamic stick-slip and migration of single sub-100nm surface nanobubbles, *Anal. Chem.*, **2019**, 91, 4665.

[2] YM Fang, ZM Li, YY Jiang, X Wang, HY Chen, NJ Tao, W Wang, Intermittent photocatalytic activity of single CdS nanoparticles, *Proc. Natl. Acad. Sci. USA*, **2017**, 114, 10566.

[3] H Su, YM Fang, FY Chen, W Wang, Monitoring the dynamic photocatalytic activity of single CdS nanoparticles by lighting up H2 nanobubbles with fluorescent dyes, *Chem. Sci .*, **2018**, 9, 1448. [4] YJ Wang, TL Yuan, H Su, K Zhou, YL Yin, W Wang, A bubble-STORM approach for super-resolved imaging of nucleation sites in hydrogen evolution reactions, *ACS Sensors*, **2021**, 6, 380.

[5] J Chen, K Zhou, YJ Wang, J Gao, HY Chen, W Wang, Measuring the activation energy barrier for the nucleation of single nanosized vapor bubbles, *Proc. Natl. Acad. Sci. USA*, **2019**, 116, 12678.

Nucleation

Thermally assisted Heterogeneous Cavitation through Gas Supersaturation

Patricia Pfeiffer,[1]* Julian Eisener,[1] Hendrik Reese,[1] Mingbo Li,[2] Xiaotong Ma,[2] Chao Sun,[2] and Claus-Dieter Ohl[1]

1 *Otto-von-Guericke University Magdeburg, Universitätsplatz 2, 39106 Magdeburg*
2 *Center for Combustion Energy, Department of Energy and Power Engineering, Tsinghua University, Beijing 100084, China*

E-Mail corresponding authors: patricia.pfeiffer@ovgu.de

Abstract

So far, the only known mechanism to sustain heterogeneous cavitation is the presence of particles in water that can stably trap gas pockets within hydrophobic crevices. While surface attached nanobubbles and stable nanobubbles are investigated they have not been identified as a cavitation nucleus. In this work, we provide evidence that besides particles, gas supersaturation acts as cavitation nuclei, too.

The most accepted and experimentally tested model for heterogeneous nucleation of cavitation bubbles is the presence of gas and vapor pockets, which are stabilized in hydrophobic crevices [1]. These stabilized gas pockets explosively expand once the pressure is reduced below the Blake threshold. In contrast in pristine water the spinodal limit and thus a much higher tension is needed. In real liquids impurities dominate the cavitation inception process and heterogeneous nucleation occurs at much lower tensions than theoretical predictions indicate [2,3].

In the present work, we test experimentally if locally and temporally modulated gas supersaturation acts as a nucleus for cavitation bubble formation. A rarefaction wave propagating within a liquid sample sandwiched between two glass slides is used for cavitation inception. The wave is a transverse Lamb-type wave, which first reduces the pressure in the liquid, thereby nucleating cavitation bubbles while the trailing pressure wave may collapse the bubbles afterward [4]. The wave is launched from a dielectric breakdown spot created with a focused nanosecond laser pulse (Fig. 1).

Using sufficiently fast imaging modality we can observe if a nucleus was present by detecting a bubble expanding larger than the optical resolution limit. The geometry and technique offer a view on the details of the nucleation events microscopically and at a very high temporal resolution due to the high repeatability of the experiments. Local supersaturation is achieved as follows: nucleating a vapor bubble through heating and letting it dissolve or heating the surface below the boiling temperature. Both methods are probed with a rarefaction wave (Fig. 1).

A simple 2D axisymmetric simulation of the heat introduced by the CW laser is carried out using a finite element solver for the heat equation in Comsol. At 1 ms after stopping the heating, the temperature of the liquid has equilibrated. Heat and gas diffusion are governed by the same diffusion equation, yet the diffusion constant of heat in water is about 100 times higher than that of dissolved gas. This suggests that it is not the higher temperature where the bubble has dissolved but a local gas supersaturation nucleating the cavitation bubble.

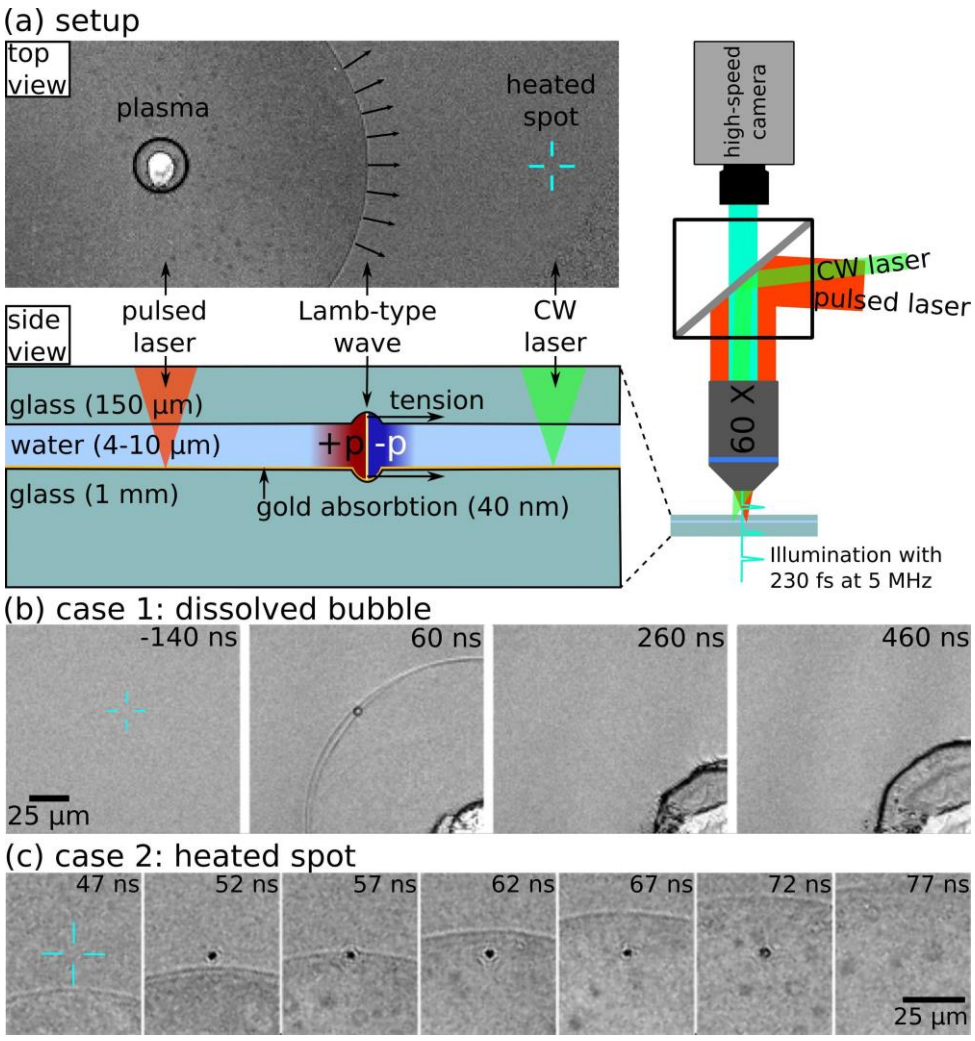

Figure 1. Nucleation of a bubble by a rarefaction wave in a liquid gap. (a) Experimental setup for cavitation inception by a focused pulsed laser. A CW laser is used for local heating. (b) A vapor bubble is created (blue cross) and has dissolved at t=-4 ms. Upon the passage of the rarefaction wave, a single cavitation bubble is nucleated (t=60 ns) at the location where the vapor bubble dissolved. t=0 corresponds to the time when the laser pulse reaches the glass slide. (c) A spot is heated (blue cross) below the boiling temperature. The heated spot acts as a cavitation nucleus once the rarefaction wave passes.

Acknowledgements

We thank A. Eremin for confocal thickness measurements of the liquid gap. We are grateful to A. Dempewolf and O. August for the gold coating.
This work was financially supported by the European Social Fund (No. ZS/2019/10/103050) as part of the initiative "Sachsen-Anhalt WISSENSCHAFT Spitzenforschung/Synergien" and the Deutsche Forschungsgemeinschaft (Programs No. OH 75/3-1, OH 75/4-1 and PF 951/3-1) and the National Natural Science Foundation of China (NSFC, No. 11861131005).

References

[1] Borkent, B. M., Gekle, S., Prosperetti, A., and Lohse, D. Phys. Fluids **21**(10), 102003 (2009).
[2] Holl, J. W. J. Basic Eng. **92**(4), 681–688 (1970).
[3] Crum, L. A. Nature **278**, 148–149 (1979).
[4] Rapet, J., Quinto-Su, P. A., and Ohl, C.-D. Phys. Rev. Applied **14**, 024041 (2020).

A Gibbs Free Energy Approach to Nucleation with Gas Contaminants

Karim Alamé[1] and Krishnan Mahesh[1,*]

1 *University of Minnesota–Twin Cities, 107 Akerman Hall. 110 Union Street S.E., Minneapolis, MN 55455*

E-Mail corresponding authors: kmahesh@umn.edu

Abstract

Cavitation refers to the change of phase from liquid to vapor when pressure drops below vapor pressure. It is an important phenomenon in several engineering applications such as turbomachinery, marine propulsors, lithotripsy and ultrasonic cleaning. At the heart of cavitation lie nuclei whose size varies from the nano to the micron scale. The process begins with a phase change on a molecular level that leads to nucleation. Understanding the nucleation process is essential to obtain insight into the cavitation process, particularly into what is termed `inception'. Nucleation is commonly described as being either homogeneous or heterogeneous and is studied using variants of the Young-Laplace and Rayleigh-Plesset equation. The Gibbs free energy approach provides a generalized description of both homogeneous and heterogeneous nucleation and is the subject of this paper. What makes such treatment feasible is the development in [1] of a numerical methodology that can calculate the equilibrium interface between water and vapor/gas over solid surfaces of arbitrary complexity. The methodology develops a level set algorithm to represent both the solid surface and the water/vapor interface, and an efficient procedure to minimize the Gibbs free energy of the system.

The general expression for Gibbs free energy is given by:

$$G_{tot} = (p_L - p_v - p_G)V + \sigma_{LG}(A_{LG} + A_{SG}\cos\theta_Y) + n_G RT \ln\frac{p_G}{p_G^*} + p^G n_v RT \ln\frac{p_v}{p_v^*} + G_0 p^v(p_L, T, s)$$

where the first term is the bulk energy due to the pressure difference, the second term is the surface energy over the liquid-gas interface and the solid gas interface combined, and the third and fourth terms are the chemical potentials of the gas and vaporous phases. Clearly, the same procedure can be applied regardless of whether the bubble forms inside fluid (homogeneous) or at a solid surface (heterogeneous).

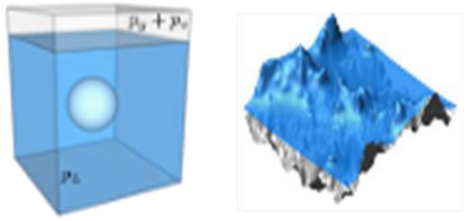

Figure 1: Illustration of a gaseous phase within a liquid for: (left) homogenous nucleation, and (right) heterogenous nucleation.

This paper considers the application of the free energy methodology to a homogeneous system consisting of liquid, vapor and gas. Analytic expressions obtained from the governing equations allow for a straightforward analysis of the stability of the system. Critical radii of bubbles for homogeneous nucleation and the effect of gas content can be derived and studied analytically. By assuming a spherical bubble, the volume and area terms can be written as a function of the bubble radius. The first partial derivative of Gibbs energy with respect to the radius leads to a cubic equation that will be at the heart of the analysis. The cubic equation for the radius of the bubbles is given by the following expression:

$$r^3 + \frac{2\sigma_{LG}}{p_L - p_v} r^2 - \frac{3n_G RT}{4\pi(p_L - p_v)} = 0$$

whose general solution has the following form:

$$r_i = \frac{4\sigma_{LG}}{3|p_L - p_v|}\cos(\alpha_i) - \frac{2\sigma_{LG}}{3(p_L - p_v)} \text{ where}$$

$$\alpha_i = \alpha + \frac{2\pi(i-1)}{3}$$

and

$$\cos(3\alpha) = \frac{|p_L - p_v|}{p_L - p_v}\left\{-1 + 2\left(\frac{9n_G RT}{8\pi\sigma_{LG}}\right)\left[\frac{3(p_L - p_v)}{4\sigma_{LG}}\right]^2\right\}$$

Two representative results are shown in Figure 2. The Gibbs free energy approach provides a continuous description of the nucleation process with varying moles of gas. The results recover the Young-Laplace equations for a pure liquid-vapor system but also generalize to include the effect of contaminant gas. Blake's radius is also obtained as a special case that happens to lie on a saddle point of the Gibbs energy surface. Reversing the signs of the pressure difference leads to a different set of critical radii. This potentially explains the hysteresis observed between the incipience and desinence of cavitation bubbles. It also describes why gas bubbles remain even after a degassing process. Nucleation rates and bubble concentrations can also be derived and will be presented in the talk.

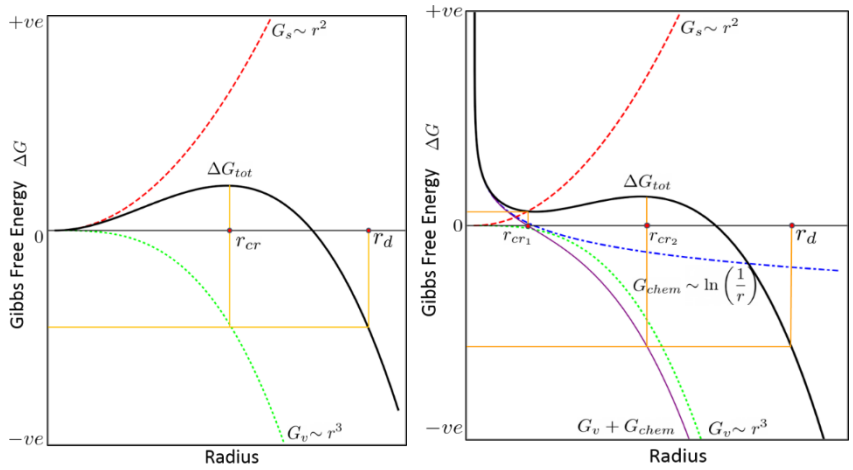

Figure 2. Gibbs free energy of: (left) pure liquid-vapor system, (right) liquid-vapor system gas content.

Acknowledgements

This work is supported by the United States Office of Naval Research under grant ONR N00014-17-12676 with Dr. Ki-Han Kim as the program manager.

References

[1] K. Alamé, S. Anantharamu, K. Mahesh. A variational level set methodology without reinitialization for the prediction of equilibrium interfaces over arbitrary solid surfaces. Journal of Computational Physics, 2020.

Bulk nanobubble generation and characterization in ethanol-water mixtures

Mohit Trivedi[1] and Neelkanth Nirmalkar[1,*]

1 *Department of Chemical Engineering, Indian Institute of Technology Ropar, Rupnagar-140001, Punjab, India*

E-Mail corresponding authors: n.nirmalkar@iitrpr.ac.in

Abstract

The gas-liquid dispersions often encountered in numerous engineering applications, for instance, the development of smart fluids, novel reactor or reaction design for gas-liquid reactions, biomedical applications, cosmetics and foodstuff processing design etc. Therefore, these dispersion systems have shown substantial research potential over last few decades. Recently, nanobuble suspensions have been discovered which possess extralongevity owing to the surface charge. Nanobubble forms when a gas is dispersed in the liquid at an ultra-fine scale (70-200nm). Despite having high Laplace pressure, these suspensions are found be extremely stable (up to months) under standard conditions [1]. Some of their applications include, separation processes (froth flotation), Reactive oxygen species (ROS) generation in biological systems, drug development, treatment of cancer, and waste water treatment. The extraordinary stability of such Nanobubbles is plausibly due to the presence of the surface stresses developed by the electrical charge of the dangling -OH groups at the gas liquid interface, though, this argument still needs further support [1]. Although, most of the nanobuble research is limited to the nanobubble suspension in water by either infusion of gas into water or generation through hydrodynamic cavitation, few studies also reported the nanobubble generation through solventexchange method [2, 3]. Our recent study presented a rich discussion for nanobubble generation via addition of inorganic solutes in water [1]. For organic solvents, despite having scant reported results, there is a significant research gap to accrue detailed information and discussion on the nanobubble generation and to provide strong experimental evidence of their existence based on the refractive index calculation of nanobubbles using Mie theory. Therefore, in this work, we have experimentally investigated the bulk nanobubble generation in ethanol-water mixture. The ethanol and water are taken into a flask ranging from 5% to 50 % ethanol by volume, and stirred for 5 min. The generated bulk nanobubbles are characterized further by using Nanoparticles tracking analysis and Zetasizer DLS (Dynamic light scattering).. The nanobubble size, count vs scattering intensity, zeta potential and refractive index for various ethanol vol% are presented in Fig. 1. The lowest mean Nanobubble diameter/size is observed at 10% ethanol vol% and the size is found to be higher for lower ethanol vol% than the higher vol% except for 50% ethanol vol%. The mean scattering intensity is found to be 3.33 a.u. for 10% ethanol vol%. The maximum zeta potential is observed for 5% ethanol vol% and further found to be decreasing with increasing ethanol vol%. The measured R. I. values are found to be in range of 1-1.07 which is closer to the R.I. of the air (i.e. R.I. = 1), thus identifying and proving the presence of gas filled Nanobubbles.

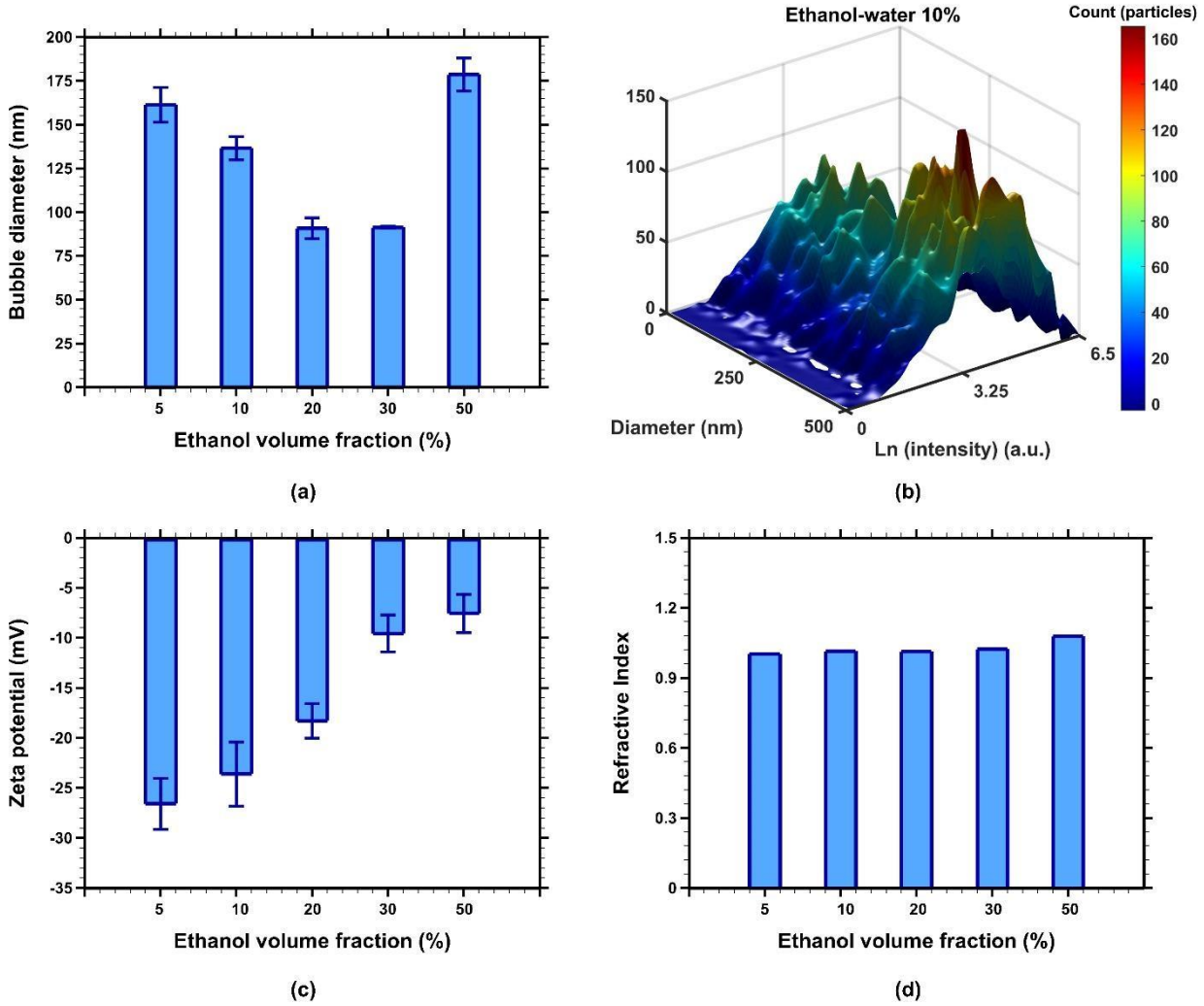

Figure 1. Bulk nanobubbles generated in ethanol-water mixture; (a) Bubble diameter, (b) 3D Histogram of bubble count, size and scattering intensity, (c) Zeta potential values, (d) Refractive Index.

Acknowledgements

This research is funded by TIF-AWaDH (Technology Innovation Hub- Agriculture and Water Technology Development Hub), Department of Science and Technology, India.

References

[1] Agarwal, Kalyani, Mohit Trivedi, and Neelkanth Nirmalkar. "Does salting-out effect nucleate nanobubbles in water: Spontaneous nucleation?." *Ultrasonics sonochemistry* 82 (2022): 105860.

[2] Jadhav, Ananda J., and Mostafa Barigou. “Proving and interpreting the spontaneous formation of bulk nanobubbles in aqueous organic solvent solutions: effects of solvent type and content.” *Soft Matter* 16 (2020): 4502.

[3] Millare, Jeremiah C., and Blessie A. Basilia. “Nanobubbles from Ethanol-Water Mixtures: Generation and Solute Effects via Solvent Replacement Method” *ChemistrySelect* 3 32 (2018): 9268-9275.

Applications: Biology and Medicine II

Mechanisms of Nanobubbles and Soil Interactions in Enhanced Plant Growth

Shan Xue[1], Thu Le[2], Chuanwu Xi[2], Taha Marhaba[1], Wen Zhang[1,*]

[1]John A. Reif, Jr. Department of Civil and Environmental Engineering, New Jersey Institute of Technology, Newark, NJ 07102, USA
[2]Department of Environmental Health Sciences, University of Michigan School of Public Health, Ann Arbor, MI 48109, USA
Corresponding author: E-mail: wen.zhang@njit.edu; Phone: 1-973-596-5520

Abstract
Coordination of water saving, yield and quality increase remains an attractive problem in agricultural production. Dispersion of gaseous nanobubbles (NBs) in water has been recognized an effective way to improve plant growth and seed germination, but potential mechanism of NB on plant growth is unknown yet. In present study, tomato cultivated in greenhouse was subjected to investigate the effects of three mixing ratios of NB water and tap water combined with two different irrigation frequencies on irrigation water use efficiency and plant growth. In addition, the impacts of different gaseous NBs (e.g., oxygen, nitrogen, hydrogen, carbon dioxide and air) on soil chemical properties such as pH, dissolved oxygen (DO) and redox potential and the release kinetics of key elements such as NH_4^+, $NO_3^-$and PO_4^{3-}, K^+ and Mg^{2+} from soil as well as other soil contents such as natural organic matters, and the effects of NBs on the microbiome and enzyme in rhizosphere soil were also evaluated. Moreover, the electrical impedance spectroscopy (EIS) is investigated as a non-destructive method for monitoring root growth of tomato. The results indicated that application of oxygen NB can increase plant growth (height and steam diameter) and irrigation water use efficiency compared to control group (tap water). The results indicated that oxygen NB irrigation, particularly with the high concentration, changed the composition and potential functionality of the soil bacterial community, reduced its diversity. Additionally, oxygen NB application improved soil quality by increasing the rhizosphere soil urease and phosphatase, which promised to stimulate plant root growth and accumulate soil available nutrients. Enzymatic activities in plant leaves including superoxide dismutase, peroxidase, and protein were significantly higher in oxygen nanobubble groups compared with the control. Overall, this study provides stronger support for the nanobubbles to promote the growth of plants.

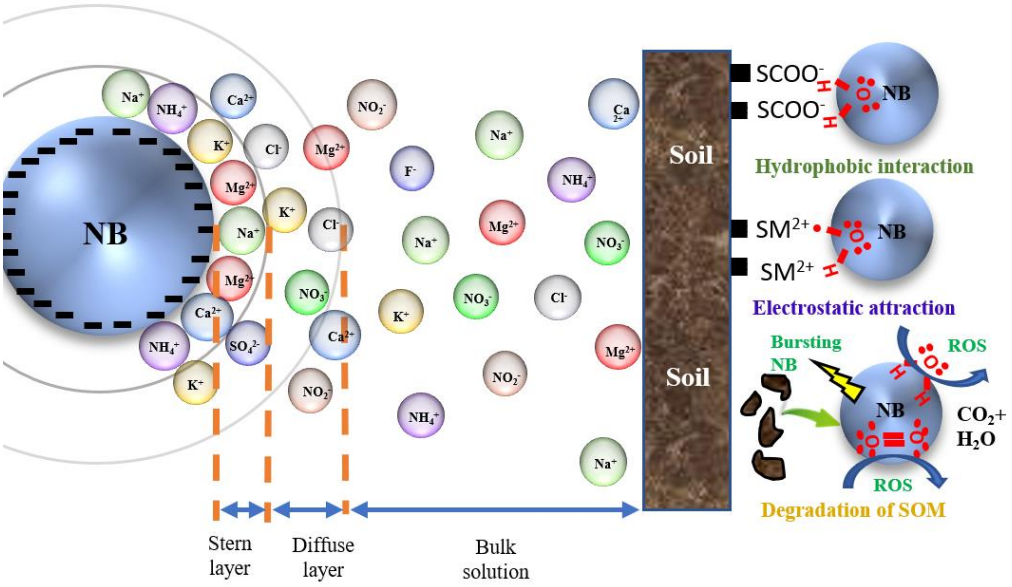

Figure 1 Schematics of the electric double layer of NBs in liquid and interaction mechanisms with soil.

Acknowledgements
This research is partially supported by the United States Department of Agriculture (USDA), the National Institute of Food and Agriculture, AFRI project [2018-07549] and the United States Environmental Protection Agency (US EPA) under Assistance Agreement No. 83945101 and 84001901 (EPA P3 phase I and II). The USDA and the EPA have not formally reviewed this study. The views expressed in this document are solely those of authors and do not necessarily reflect those of the agencies. The USDA and EPA do not endorse any products or commercial services mentioned in this publication.

Investigation of cultures of *Saccharomyces cerevisiae* in presence of oxygen nanobubbles

Paweł Sobieszuk[1,*], Karol Ulatowski[1], and Alicja Strzyżewska[1]

1 *Warsaw University of Technology, Faculty of Chemical and Process Engineering, Warynskiego 1, 00-645 Warsaw, Poland*

E-Mail corresponding authors: pawel.sobieszuk@pw.edu.pl

Abstract

Nanobubble usability is increasing worldwide in environmental processes, cleaning, agriculture and disinfection. Luu et al. (2019) investigated the influence of presence of nanobubbles generated by ultrasonication in culture medium on the growth rate of Gram-negative bacteria [1]. Negative influence on the growth rate and biomass concentration was observed. However, for Gram-positive bacteria the presence of nanobubbles promoted the growth, especially when hydrogen nanobubbles were applied [2]. On the other hand, when the biofilm from seeding suspension was investigated, the presence of air nanobubbles also promoted the growth and activity of microorganisms in biofilm [3]. In this work results of submerged aerobic culture of *Saccaromyces cerevisiae* yeast were presented. The aim of this work was the examination of oxygen nanobubble influence on yeast batch cultures, specifically on the value of specific growth rate and growth phases length. Generation of nanobubbles in water were carried out using cylindric porous-membrane system where the gas was pressurised through the membrane to the flowing liquid which cut off bubbles from the membrane surface. Cultures were carried out in bioreactor (volume 1.5 dm^3) with Rushton stirrer. Culture was aerated using barbotage and additionally oxygen nanobubbles were added to the broth before inoculation. Classic aeration was necessary because the balance of elementary microbial growth showed that the amount of oxygen contained in the nanobubbles is too small to ensure the aerobic growth of the yeast. For this reason, the presented studies concern the influence of the presence of oxygen on the nanobubbles on the growth of cells and the rate of assimilation of the substrate and not the aeration of the culture by the nanobubble method. Two cultures without nanobubbles introduced to the medium were carried out as the reference cultures in addition to two cultures with nanobubbles added to the medium. Concentration of biomass was measured using nephelometry and concentration of carbon source (i.e. glucose) was measured spectrophotometrically using colorimetric method. Profiles of concentration of dry biomass and substrate during batch culture with and without nanobubbles were presented in Figure 1. As one can see, the addition of gas bubbles causes faster cell growth and faster consumption of the substrate. In order to determine the values of growth parameters, a Monod model and a two-parameter growth model were proposed:

$$\mu = \mu_{max} \frac{S}{K_S + S} \qquad \text{Monod model}$$

$$\mu = \mu_{max} \frac{S}{K_S + S} \frac{O}{K_O + O} \qquad \text{Two-parameter model}$$

where: μ – specific grow rate [1/h], μ_{max} – maximal specific grow rate [1/h], K_S – saturation constant in relation to substrate concentration [g/dm^3], K_O – saturation constant in relation to oxygen concentration [mg/dm^3], S – substrate concentration, O – oxygen concentration [mg/dm^3]. The differential balance of biomass and substrate in the batch reactor was formulated.

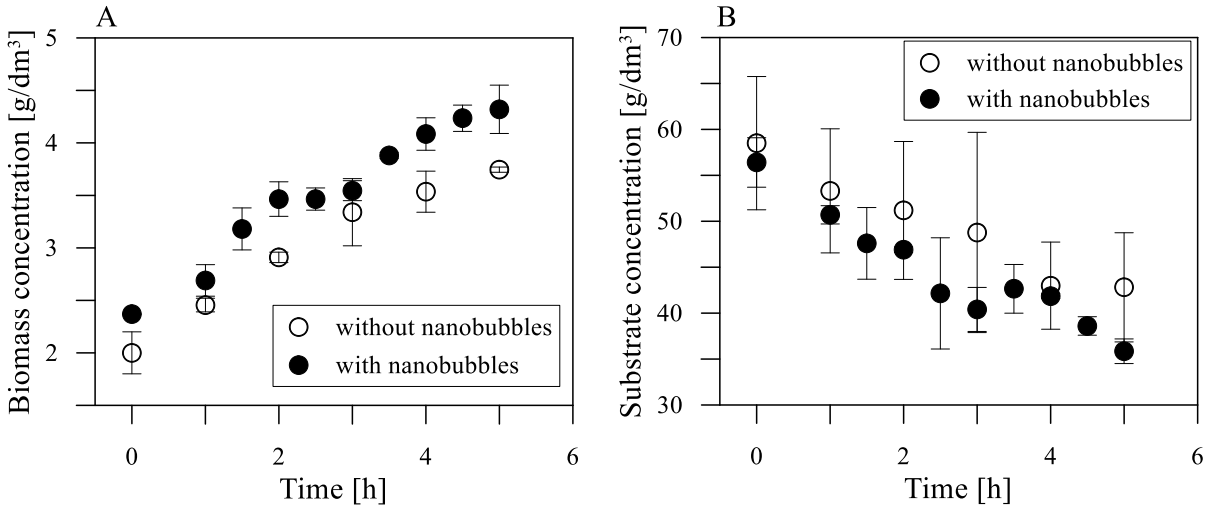

Figure 1. Profile of concentration of dry biomass (A) and substrate (B) during batch cultures

Obtained ordinary differential equations were solved using Matlab software and ode45 method. To determine model parameter values using experimental data presented in Figure 1 the command lsqnonlin for nonlinear least-squares problems was used. Obtained parameters of Monod and two-parameter model are presented in Table 1.

Table 1. Values of growth model parameters. NB - nanobubbles

Parameter	Monod model		Two-parameter model	
	Without NB	With NB	Without NB	With NB
μ_{max} [1/h]	0.519	0.728	0.510	0.646
K_S [g/dm³]	225	226	224	215
K_O [mg/dm³]	N/A	N/A	0.088	0.107

As one can see the maximal specific growth rate for batch cultures is higher in presence of oxygen nanobubbles without the significant change in both saturation constants values. That means that for the same substrate concentration higher growth rate would be achieved. Mechanism of nanobubble-microorganism interaction is not clear, but the obvious conclusion is that the growth is promoted by oxygen nanobubble presence. What is interesting, the similar effect was observed in literature for cultures of Gram-positive bacteria [2] which have similar outer membrane and wall structure.

Presented results were published in Chemical Engineering and Processing – Process Intensification [4].

Acknowledgements

This work was supported by the National Science Centre, Poland (grant number 2018/29/B/ST8/00365).

References

[1] T. Q. Luu, P. N. Hong Truong, K. Zitzmann, K. T. Nguyen, Effects of Ultrafine Bubbles on Gram-Negative Bacteria: Inhibition or Selection?, Langmuir **2019**, 35, 13761–13768.

[2] Z. Guo, X. Wang, H. Wang, B. Hu, Z. Lei, M. Kobayashi, Y. Adachi, K. Shimizu, Z. Zhang, Effects of nanobubble water on the growth of: Lactobacillus acidophilus 1028 and its lactic acid production, RSC Advances **2019**, 9, 30760–30767.

[3] W. Xiao G. Xu, Mass transfer of nanobubble aeration and its effect on biofilm growth: Microbial activity and structural properties, Science of the Total Environment **2020**, 703, 134976.

[4] P. Sobieszuk, A. Strzyżewska, K. Ulatowski, Investigation of the possibility of culturing aerobic yeast with oxygen nanobubble addition and evaluation of the results of batch and semi-batch cultures of Saccharomyces cerevisiae, Chemical Engineering and Processing - Process Intensification **2021**, 159, 108247.

Potential Benefit of oxygen nanobubbles for overcoming hypoxic/anoxic conditions (In vitro)

S. M. Viafara-Garcia[1,2,3,4]* and Juan Pablo Acevedo [1,2,3,4,5]

1 *Center of Interventional Medicine for Precision and Advanced Cellular Therapy (IMPACT), Santiago, Chile*
2 *Centro de Investigación e Innovación Biomédica (CIIB), Universidad de Los Andes, Santiago de Chile*
3 *Laboratory of Tissue Engineering and Biofabrication, School of Medicine, Universidad de Los Andes, Santiago, Chile*
4 *Cell for cells, Santiago, Chile*
5 *Chilean Consortium for Regenerative Medicine, Santiago, Chile*

E-Mail corresponding authors: smviafara@miuandes.cl

Abstract

The Oxygen Micro-Nanobubbles are considered oxygen delivery systems with broad potential benefits to mitigate hypoxic stress. However, nanobubble oxygenation and its effects on UC-MSCs are relevant aspects of cell therapy. This study characterizes bulk oxygen nanobubbles (ONBs) through Dynamic Light Scattering (DLS), Nanoparticle Tracking Analysis (NTA), zeta potential, FT-IR, and fiber-optic oxygen sensor. We produced ONBs in cell culture media and ultrapure water at a concentration of $1.1x10^9$ particles/mL, with a size distribution <200nm and the zeta potential value of -32mv. By another hand, we measured the oxygen delivery by mixing ONBs-enriched solutions with hypoxic or anoxic deoxygenated solutions (1 and 0 mg/L of O_2, respectively). We measured the increase in dissolved oxygen content in the deoxygenated water or DMEM, showing a sustained oxygen release profile of 8.3 mg/L for 70 minutes on ONBs-enriched solutions, which is significatively higher than in mixtures prepared with oxygen saturated solution (4.2 mg/L). Regarding the biological assessment, umbilical cord mesenchymal stem cells (UC-MSCs) were cultured with Dulbecco's modified Eagle's medium containing oxygen ONBs for 24hrs (normoxic/hypoxic conditions). After a colorimetric assay and confocal microscopy, we observed that ONBs do not affect UC-MSCs viability, showing higher metabolic activity within cells exposed to ONBs.

Acknowledgements

Acknowledgement to funding agencies of this Project within the framework of the Regenero Consortium and associated with the execution of the CORFO program "Crea y Valida", code 20CVID-128078,

Micro-scale Hydrodynamic Cavitation-enhanced Doxorubicin (DOX) Treatment

Ilayda Namli,[1,2] Zeynep Karavelioglu,[3] Seyedali Seyedmirzaei Sarraf,[1,2] Sibel Çetinel,[1,2,5], Özlem Kutlu,[1,2,5] Huseyin Uvet,[4] Morteza Ghorbani,[1,2,5] and Ali Kosar[1,2,5]*

1 *Faculty of Engineering and Natural Science, Sabanci University, 34956 Tuzla, Istanbul, Turkey*
2 *Sabanci University Nanotechnology Research and Application Center, 34956 Tuzla, Istanbul, Turkey*
3 *Graduate School of Science and Engineering, Department of Bioengineering, Yildiz Technical University, 34220, Istanbul, Turkey*
4 *Mechatronic Engineering Department, Yildiz Technical University, 34220, Istanbul, Turkey*
5 *Center of Excellence for Functional Surfaces and Interfaces for Nano-Diagnostics (EFSUN), Sabanci University, Orhanli, 34956, Tuzla, Istanbul, Turkey*

E-Mail corresponding author: kosara@sabanciuniv.edu

Abstract

Cavitation is a phase change phenomenon that involves different bubble life cycles including nucleation, expansion, and collapse [1]. Cavitation could be classified into four types: Acoustic cavitation, Optical cavitation, Particle cavitation, and Hydrodynamic cavitation [2]. Micro-scale cavitation applications have gained great significance since they have similar dimensions to biological entities and offer the capability to accelerate processes and to serve as a more controllable approach [3–5]. Acoustic cavitation or/and optical cavitation-enhanced molecular delivery and cell lysis in microscale have been investigated broadly over recent years [3, 5, 6]. For instance, Le Gac et al. [6] demonstrated that sonoporation of human promyelocytic leukemia cells could be achieved by laserinduced cavitation. In the study of Meng et al. [4], a stable microbubble array allowed cell membrane permeabilization utilizing acoustic cavitation. Optimization of such systems requires comprehensive knowledge on the interactions between biological substances and cavitating flows/cavitation bubbles. Although cavitation phenomena have been exploited in biomedical applications, a limited number of studies employed hydrodynamic cavitation in assessment of biological responses [7, 8], and there is a need in the literature to understand its biological and physical impact on biological samples.

This study investigates the biophysical effects of micro-scale hydrodynamic cavitation inside a cascade parallel multi-microchannels on a confluent cell monolayer. The effect of hydrodynamic cavitation on a cancer cell line and a normal cell line as a control group was observed. Doxorubicin (Dox), a chemotherapy drug, was utilized for cancer and normal cell lines. Then, cavitation was applied to both of Dox treated cells and non-treated cells for observing the effects of cavitation on Dox effectiveness for both cell lines. According to the results [Figure 2], the uptake of the Dox decreased the cell viability in both healthy cells (Beas-2B) and cancer cells (A549). In addition, hydrodynamic cavitation-enhanced Dox treatment decreased the cell viability more than only Dox treatment. As an interesting result, hydrodynamic cavitation-enhanced Dox treatment is more effective on the cancer cells compared to the healthy cells. Hence, this study could be a new approach for cancer treatment and has the advantage of minor damage in surrounding healthy cells.

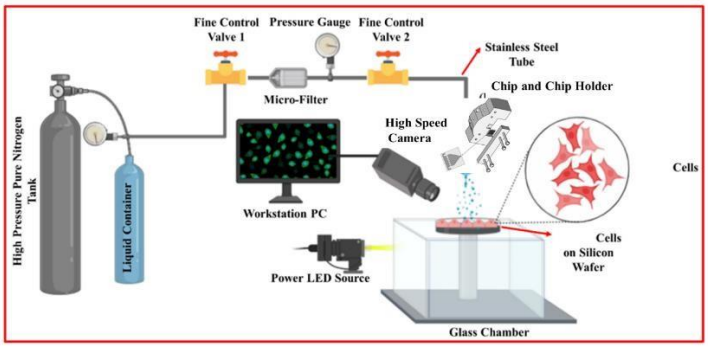

Figure 1. Micro-scale hydrodynamic cavitation experimental setup and application on cell lines. Hydrodynamic cavitation occurs inside the multichannel of microfluidic chip [7].

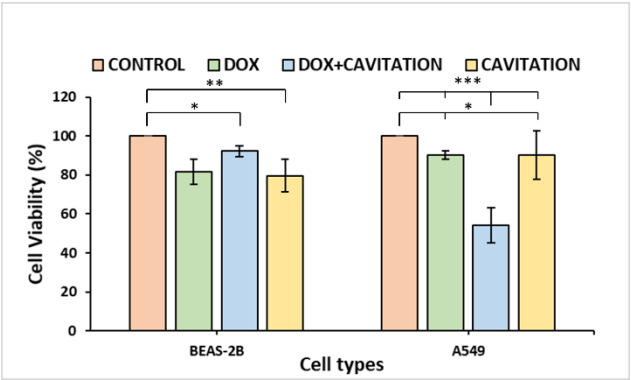

Figure 2. Viability of cells after Doxorubicin treatment, hydrodynamic cavitation application and doxorubicin+ cavitation application. *Error bars indicate standard deviation.[[significant differences were determined using one-way ANOVA [Newman–Keuls multiple comparison test, (* p\0.05, ** p\0.01, *** p\0.001)].*

Acknowledgements

The authors would like to thanks the Sabanci University Nanotechnology Research and Applications Center (SUNUM) for equipment utilization.

References

[1] C. E. Brennen and N. Y. Oxford, “Cavitation and Bubble Dynamics,” 1995.

[2] X. Sun *et al.*, “A review on hydrodynamic cavitation disinfection: The current state of knowledge,” *Sci. Total Environ.*, vol. 737, p. 139606, 2020.

[3] A. N. Hellman, K. R. Rau, H. H. Yoon, and V. Venugopalan, “Biophysical Response to Pulsed Laser Microbeam-Induced Cell Lysis and Molecular Delivery,” *J. Biophotonics*, vol. 1, no. 1, pp. 24–35, 2008.

[4] L. Meng *et al.*, “Sonoporation of cells by a parallel stable cavitation microbubble array,” *Adv. Sci.*, vol. 6, no. 17, p. 1900557, 2019.

[5] Z. G. Li, A. Q. Liu, E. Klaseboer, J. B. Zhang, and C. D. Ohl, “Single cell membrane poration by bubbleinduced microjets in a microfluidic chip,” *Lab Chip*, vol. 13, no. 6, pp. 1144–1150, 2013.

[6] S. Le Gac, E. Zwaan, A. van den Berg, and C.-D. Ohl, “Sonoporation of suspension cells with a single cavitation bubble in a microfluidic confinement,” *Lab Chip*, vol. 7, no. 12, pp. 1666–1672, 2007.

[7] M. T. Gevari *et al.*, “Local Carpet Bombardment of Immobilized Cancer Cells With Hydrodynamic Cavitation,” *IEEE Access*, vol. 9, pp. 14983–14991, 2021.

[8] M. T. Gevari, A. Parlar, M. Torabfam, A. Koşar, M. Yüce, and M. Ghorbani, “Influence of fluid properties on intensity of hydrodynamic cavitation and deactivation of Salmonella typhimurium,” *Processes*, vol. 8, no. 3, p. 326, 2020.

Polysaccharide-shelled nanobubbles: role of polymer/lipid interface on nanostructure and ultrasound-responsive behaviour

Monica Argenziano[1], Anna Scomparin[1], and Roberta Cavalli[1]

1 Department of Drug Science and Technology, via P. Giuria 9, Torino, Italy

E-Mail corresponding author: roberta.cavalli@unito.it

Abstract

Polymer-shelled nanobubbles (NBs) have shown great potential as a nanoplatform for the delivery of drugs, gases and genes [1]. Interestingly, they can be combined with ultrasound (US) to obtain a triggered site-specific delivery of the active molecules. In addition, they can act as US contrast agent. Polysaccharides have been studied as NB shell component due to their biocompatibility, biodegradability and the presence of functional groups suitable for conjugation and derivatization. Moreover, the polymer shell can play an important role affecting the physico-chemical characteristics and the biological properties. Novel hybrid nanobubble systems based on a phospholipid monolayer at the NB interface, coated by a polysaccharide shell were developed [2]. The design of the hybrid lipid/polysaccharide NBs was based on the capability of phospholipid monolayers to adsorb charged polysaccharides, exploiting electrostatic or hydrophobic interactions [3]. The work aims at investigating the impact of a series of polysaccharides either positive or negative charged (i.e. low or medium weight chitosan, methyl chitosan, glycolchitosan, methylglycol chitosan, dextran sulfate and Dextran-DEAE) on the NB nanostructure, stability and ultrasound responsive behaviour. The interaction of polysaccharide with lipid monolayer was investigated by FTIR spectroscopy, Differential Scanning Calorimetry (DSC) and surface tension evaluation. Two different molecules, i.e. doxorubicin and oxygen, were encapsulated in nanobubble formulations having the different polysaccharide shells. The physico-chemical characteristics, loading capacity, stability and *in vitro* release kinetics of the series of NB formulations were evaluated. Moreover, the NB size distribution and *in vitro* release kinetics were determined after US application.

References

[1] M. Argenziano, F. Bessone, C. Dianzani, MA. Cucci, M. Grattarola, S. Pizzimenti, R. Cavalli. Pharmaceutics 2022, 14(2), 341.
[2] M. Argenziano, B. Bressan, A. Luganini, N. Finesso, T. Genova, A. Troia, G. Giribaldi, G. Banche, N. Mandras, A.M. Cuffini, R. Cavalli, M. Prato, Mar Drugs. 2021,19(2),112.
[3] A. Pavinatto, J.A.M. Delezuk, A.L. Souza, F.J. Pavinatto, D. Volpati, P.B. Miranda, S.P. Campana-Filho, O.N. Oliveira, Colloids Surf. B Biointerfaces 2016, 145, 201.

Lipid-Shelled Nanobubbles for Therapeutic Delivery

Damien V. B. Batchelor[1], Radwa H. Abou-Saleh[1,2], Fern J. Armistead[1], Nicola Ingram[3,4], Sally A. Peyman[1], James R. McLaughlan[3,4,] P. Louise Coletta[3], and Stephen D. Evans[1,*]

1 *Molecular and Nanoscale Physics Group, School of Physics and Astronomy, University of Leeds, LS2 9JT, United Kingdom*
2 *Nanoscience and Technology Group, Faculty of Science, Galala University, Galala 43711, Egypt*
3 *Leeds Institute of Medical Research, Wellcome Trust Brenner Building, St James's University Hospital, Leeds, LS9 7TF, United Kingdom*
4 *Faculty of Electronic and Electrical Engineering, University of Leeds, LS2 9JT, United Kingdom*

E-Mail corresponding authors: S.D.Evans@leeds.ac.uk

Abstract

Systemic delivery of therapeutic agents for treating a wide range of diseases can be challenging, where treatment effectiveness is determined by the total dose of drug delivered to the disease site. Thus, new platforms for the non-invasive delivery and triggered release of therapeutics are of significant interest, especially in an aging population where the rate of disease is likely to increase.

Lipid-shelled microbubbles (MBs, 1- 10 µm) are already in widespread clinical use as contrast agents for echocardiography. In combination with ultrasound, MBs can locally increase intra-cellular drug uptake via a process called sonoporation. MBs can be functionalised to act as biomarkers for molecular imaging of disease vasculature and provide localised triggered release of a therapeutic payload. [1] However, they are confined to the vasculature, which can result in poor uptake in the targeted region. Nanobubbles (NBs, < 1 µm) have emerged as promising candidates for ultrasound-triggered drug delivery because of their small size, which allows them to passively extravasate and accumulate within tumour tissue. [2]

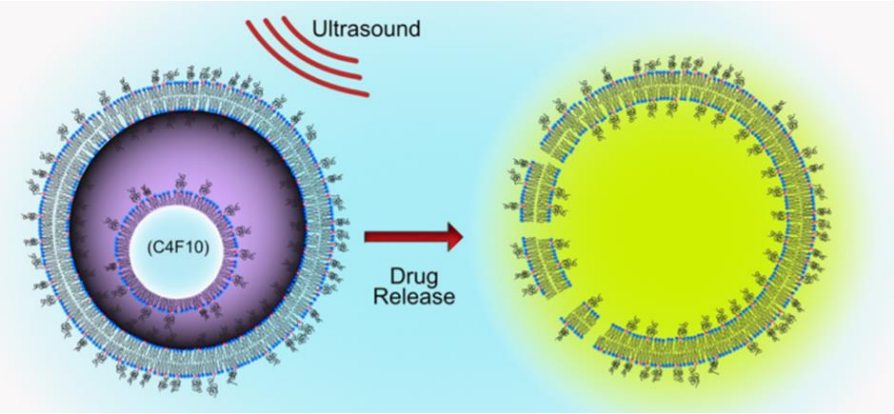

Figure 1 -Schematic of a Nested-Nanobubble, in which a perfluorobutane (C_4F_{10}) is encapsulated within a drug-loaded liposome. The application of high intensity ultrasound leads to liposome rupture and triggered drug release.

Recently, we developed new type of therapeutic NB, Nested-Nanobubbles (Figure 1), by encapsulation of NBs within drug-loaded liposomes in which the encapsulated NB acts as an acoustic trigger for drug release [3]. Although the encapsulated NBs were destroyed by pulsed HIFU, determined by passive cavitation detection, no drug release was observed. Changing modality to continuous wave (CW) HIFU produced release across a range of pressures, likely due to a synergistic effect of mechanical and thermal stimuli. In

combination with theoretical models of droplet vaporisation, we predict that encapsulated NBs contain a mixed population of both gaseous and liquid core particles, which upon CW HIFU undergo rapid phase conversion, triggering liposomal drug release.

One challenge associated with NBs, and potentially limiting their clinical translation, is accurate characterisation of their size and concentration. Their size is typically below the resolution limit of most microscopy systems, and whilst light scattering techniques can be used, the cannot typically distinguish between sub-populations of gas bubble and aqueous cored liposomes present in NB samples. Here, a novel method of using a commercially available Nanoparticle Tracking Analysis (NTA) system was developed, able to distinguish between NBs and liposomes owing to their differing optical properties (Figure 2). This technique was then used to assess the *in vitro* therapeutic performance on-chip of different sized NBs. However, sonoporation efficiency did not depend exclusively on NB size and concentration. It is hypothesized that both the total lipid and liposome concentration, as well as inter-bubble distance plays an important role in NB stability, consistent with previously proposed theories and simulations.

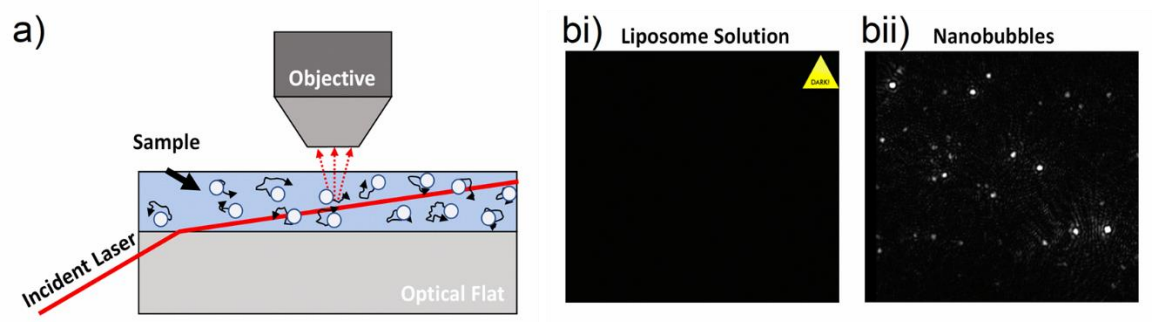

Figure 2 - a) Schematic showing the working principle of NTA, in which the random walk of nanoparticles is tracked by observing light scattered by individual particles. b) Images collected during NTA data acquisition, demonstrating that highly scattering, gas-cored NBs are detected, whereas lower scattering aqueous cored liposomes are not.

Acknowledgements
The authors would like to acknowledge the following funders: Medical Research Council (MR/M009084/1) and Engineering and Physical Sciences Research Council (EP/P023266/1 and EP/S001069/1). S.D.E. is supported by the National Institute for Health Research infrastructure at Leeds. D.V.B.B. thanks K. de Silva for support through the provision of an Alumni PhD scholarship.

References

(1) Ingram, N.; Mcveigh, L. E.; Abou-saleh, R. H.; Batchelor, D. V. B.; Loadman, P. M.; Mclaughlan, J. R.; Markham, A. F.; Evans, S. D.; Coletta, P. L. A Single Short ' Tone Burst ' Results in Optimal Drug Delivery to Tumours Using Ultrasound-Triggered Therapeutic Microbubbles. *Pharmaceutics* **2022**, 1–12.

(2) Batchelor, D. V. B.; Armistead, F. J.; Ingram, N.; Peyman, S. A.; Mclaughlan, J. R.; Coletta, P. L.; Evans, S. D. Nanobubbles for Therapeutic Delivery: Production, Stability and Current Prospects. *Curr. Opin. Colloid Interface Sci.* **2021**, *54*, 101456. https://doi.org/10.1016/j.cocis.2021.101456.

(3) Batchelor, D. V. B.; Abou-Saleh, R. H.; Coletta, P. L.; McLaughlan, J. R.; Peyman, S. A.; Evans, S. D. Nested Nanobubbles for Ultrasound-Triggered Drug Release. *ACS Appl. Mater. Interfaces* **2020**, *12* (26), 29085–29093. https://doi.org/10.1021/acsami.0c07022.

Applications in Engineering and Process Techniques II

Industrial Measurement and Control of Ozone Nanobubble Production

Dirk Thiele[1] and Todd Hay[1]

1 EnSolućion, 12503 Oro Valley Trail, Austin, Texas, 78729

E-Mail corresponding authors: dirk.thiele@ensolucion.com

Abstract

Many factors that impact Nanobubble production are typically unmeasured variables in the control problem of Nanobubble generation. As a result, Nanobubble generation equipment is often underutilized and Nanobubble performance can become unreliable for a specific application when original design parameters such as pH change.

We have deployed a number of machines for novel food safety and wash water treatment solutions using Ozone Nanobubbles. The machines are deployed in several research laboratories at universities and pilot plants in the USA and Canada where graduate students are doing funded research using this technology.

We would like to present our experience around developing new technologies for Ozone Nanobubble Generation, specifically experiences with measurement, inferences and closed loop control of key parameters that impact the performance of Ozone Nanobubbles in sanitization applications. We will discuss the resulting efficacy of Ozone Nanobubbles for application to pathogens on food products, water and surfaces as they were recently found in the research labs.

One of the biggest challenges in developing reliable Ozone Nanobubble generators for research and industry is identifying the root cause of suboptimal performance. Even quantifying the optimal performance in the first place can be a challenge. We developed and refined several methods that allow us to understand machine performance thru inferential measurements and cloud-based dashboards. We will discuss how the ability to store key performance indicators and economic statistics in a cloud based database and remote viewing of emerging data patterns simplified reporting to our customers and funding agencies.

Enhancement of municipal wastewater treatment by use of Micro-Nano-Bubbles

Andrzej Mróz[1] and Jarosław Kupiec[2]

1 *Fine Bubble Technologies Sp. z o.o., 05-500 Piaseczno, Poland*
2 *Fine Bubble Technologies Sp. z o.o., 05-500 Piaseczno, Poland*

andrzej.mroz@finebubble.pl

Abstract

The most energy-consuming elements of the municipal wastewater treatment process are pre-treatment, aeration and dewatering of sludge [1]. The use of Micro-Nano-Bubbles MNB of Air, Oxygen and Ozone technology makes it possible to greatly reduce energy consumption without the need to use expensive and troublesome Fe or Al coagulants.

Nano Ozone Flotation allows the reduction of COD not only by the removal of suspended solids and colloids, but additionally by the decomposition of dissolved pollutants. Overall, it is possible to reduce COD by more than 90%. Solid and colloidal impurities are about 75%, and a further 15% can be reduced as a result of the action of OH *Hydroxyl Radicals generated by exploding MNB. Lower COD, BOD5 and TN, TP, FOG and an increase in the biodegradability of pollutants mean much less excess sludge for separation and dewatering and many times lower Oxygen demand. Oxygenation of wastewater by Micro or Nano-Air bubbles reduces more than four times the energy required for the injection of 1 kg of Oxygen compared to fine-bubble aeration. Activated sludge bacteria are very favorably activated in the presence of MNB and reduce Total Nitrogen much more effectively. Additional advantages of using

MNB are the removal of Micro-pollutants such as Antibiotics, Hormones, Pathogens or Pesticides and Microplastics and the elimination of odors without the need for deodorization [2].

The results of the operation of the modernized sewage treatment plants in which MNB flotation was applied and over a 2 times reduction in operating costs were obtained. The complete "WastewaterTreatment Plant for the Future" built in Poland was presented, where the operating

costs could be reduced approx. 3 times compared to conventional oxygen treatment plants with activated sludge

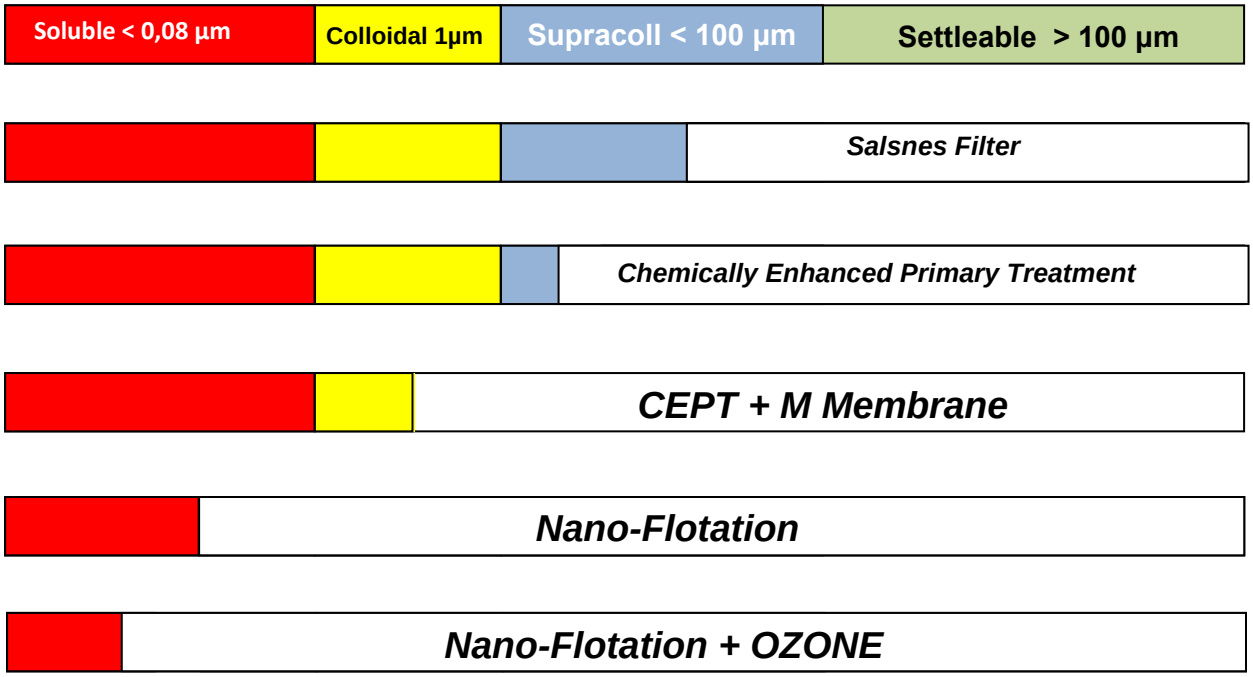

Figure 1. Possible COD reductions using different separation technologies

References

[1] Hallvard Ødegaard, The role of particle separation in energy-neutral wastewater treatment plants for the future, Department of Hydraulic and Environmental Engineering, Norwegian University of Science and Technology (NTNU), N-7491 Trondheim, Norway. hallvard.odegaard@ntnu.no

[2] Petroula Seridou, Nicolas Kalogerakis, Disinfection applications of ozone micro- and nano-bubbles, *Environ. Sci.: Nano*, 2021, **8**, 3493-3510

Comparison efficiency of Ozone and Oxygen Nanobubbles in Degradation of Green Rit Dye.

Priya Koundle[1] and Neelkanth Nirmalkar[1,*]

1 *Department of Chemical Engineering, Indian Institute of Technology, Ropar 140001, India.*

E-Mail corresponding authors: n.nirmalkar@iitrpr.ac.in

Abstract

Ozone gas bubble have been employed for the dye degradation in the literature, however, the scale up of this technology suffers seriously due to the low rate of mass transfer [1-5]. In this work, ozone nanobubbles have been used for the degradation of Green rit dye along with comparison with respect to oxygen nanobubbles. The results depicted that the degradation of green rit dye (200 mg/L) reached to 99% using ozone NBs which was seen to be three times higher than that achieved through oxygen NBs (36%). Nanobubble offers unique characteristics, for instance, long-term stability, high mass transfer coefficient and zeta potential, it is employed to enhance the dye degradation using ozone gas. The objective of the present work was to examine the degradation efficiencies of ozone and oxygen nanobubbles on the dye (green rit) keeping the conditions identical for both cases. One litre of dye solution with a concentration of 200 mg/L was prepared using green rit dye in pure water. Ozone was produced through the principle of corona discharge in an ozone generator by providing high purity oxygen through an oxygen concentrator. The dye solution was placed in an acrylic tank and was recirculated using a diaphragm pump via in-house nanobubble generator. Therefore, the system is operated in a recirculation mode. Ozone nanobubbles are characterized in terms of bubble size distribution, mean diameter and number density of the nanobubble using NanoSight NS30 instrument (Malvern Instrument, UK). A Spectrophotometer (DR3900, HACH) preprogrammed with the calibration curve of the dye was used for the measurement of amount of dye in the treated sample. The color was measured at an absorbance of 526 nm for green rit dye. The experiments were performed for both ozone and oxygen nanobubbles. The mean diameter of the nanobubbles were measured ranging from 118-164 nm with a number density of 3 X 10^8 bubble/mL. A negative charge was also possessed by these nanobubbles ranging from -37 to -39 mV.. Although the collapse of oxygen nanobubbles leads to the formation of free radicals (hydroxyl radicals) a very small amount of degradation of dye (36.8%) was observed for the case of oxygen nanobubbles. On the other hand, ozone nanobubbles exhibit remarkably a good degradation of the dye, 99% of the dye have been degraded in a short span of time.

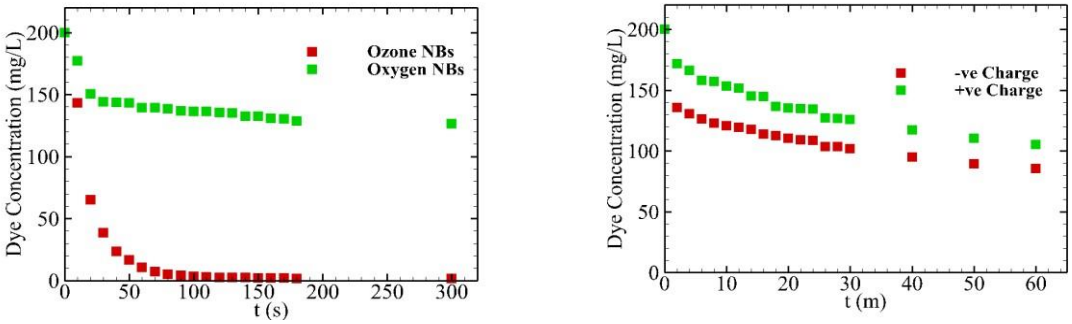

(a) (b)

Figure 1. (a) Comparison of treatment efficiency of ozone and oxygen Nanobubbles (b) Effect of the charge possessed by the Nanobubbles

Acknowledgements

This work was supported by DST (Department of Science and Technology, India).

References

[1] Ma P, Han C, He Q, Miao Z, Gao M, Wan K, Xu E. Oxidation of Congo Red by Fenton coupled with micro and nanobubbles. Environmental Technology. 2022 Feb 1:1-24.

[2] Seridou P, Kalogerakis N. Disinfection applications of ozone micro-and nanobubbles. Environmental Science: Nano. 2021.

[3] Bui TT, Han M. Decolorization of dark green Rit dye using positively charged nanobubbles technologies. Separation and Purification Technology. 2020 Feb 15;233:116034.

[4] Yıldırım AÖ, Gül Ş, Eren O, Kuşvuran E. A comparative study of ozonation, homogeneous catalytic ozonation, and photocatalytic ozonation for CI Reactive Red 194 azo dye degradation. CLEAN–Soil, Air, Water. 2011 Aug;39(8):795-805.

[5] Khuntia S, Majumder SK, Ghosh P. A pilot plant study of the degradation of Brilliant Green dye using ozone microbubbles: mechanism and kinetics of reaction. Environmental technology. 2015 Feb 1;36(3):336-47.

Effect of nanobubbles on particle-bubble-particle interaction and its possible application in froth flotation

Nilanjan Dutta [1] and Neelkanth Nirmalkar[1,*]

1 Department of Chemical Engineering, Indian Institute of Technology, Ropar 140001

E-Mail corresponding authors: n.nirmalkar@iitrpr.ac.in

Abstract

Froth flotation is one of the most significant achievements in the field of mineral processing with applications in processing coal, copper, chalcopyrite, clay, mica to name a few. A traditional froth flotation process takes advantage of the mineral particles' hydrophobic nature to separate them from the gangue that surrounds them. Owing to the high demand for minerals caused by rapid development of new technologies, mineral processing industries are evaluating several options for making use of low-grade ultra-fine mineral particles, which is challenging using conventional flotation methods. The classical collision theory states that collision and attachment probability decrease as particle size decreases [1]. Nanobubbles have been shown to exhibit the capillary bridging effect between particles. Thus, the ultra-fine particles can be aggregated in presence of nanobubbles, and it can be separated by the flotation. . Nanobubbles are gas-filled cavities with sizes ranging from 100 to 200 nm that exhibit incredible stability for long periods even in turbulent environments. Several studies have been carried out over the years to investigate the role of nanobubbles in particle flotation enhancement. The majority of these studies linked this phenomenon to the formation of capillary bridges between particle surfaces and bubble surfaces due to dewetting of the liquid film between them [2]. In this work, we investigated how nanobubbles at different concentrations can improve attachments between coal particles. We measured the wrap angle at various nanobubble concentrations to investigate the effect of nanobubbles on particle-bubble interaction. A greater wrap angle indicates a greater degree of particle attachment to the bubble surface. In Figure 1 it can be seen that nanobubbles exhibit a positive effect on the attachment, as the wrap angle is seen to have increased with the increase in nanobubble concentration. This is not only due to the formation of capillary bridges between particles and bubbles but also to particle aggregation under the influence of nanobubbles, which increases the effective size of the particle flocs exposed to macro bubble for attachment. To address this effect of nanobubbles on particle aggregation, we also conducted particle aggregation test at different nanobubble concentrations. As seen in Figure 2, the coal suspension produced with nanobubble water has resulted in enhancing the degree of aggregation of coal particles. The research carried out under this framework sheds light on the effect of nanobubble concentration on particle-bubble-particle attachment, which is directly related to particle flotation. This opens the door to fine-tuning the froth flotation process's yield simply by varying the nanobubble concentration used during the mineral pre-treatment step.

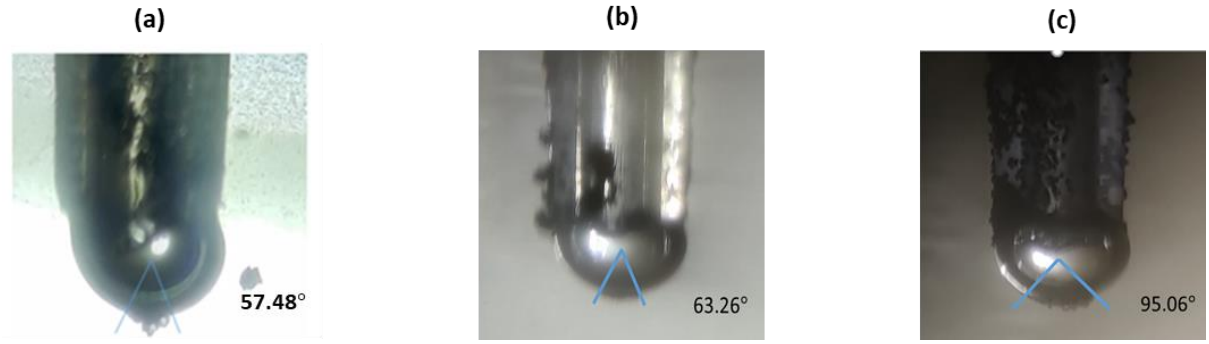

Figure 1. Wrap angle in (a) DI water, (b) Nanobubble concentration: 6.35 X 10^7 nanobubbles/ml, (c) Nanobubble concentration: 1.93 X 10^8 nanobubbles/ml

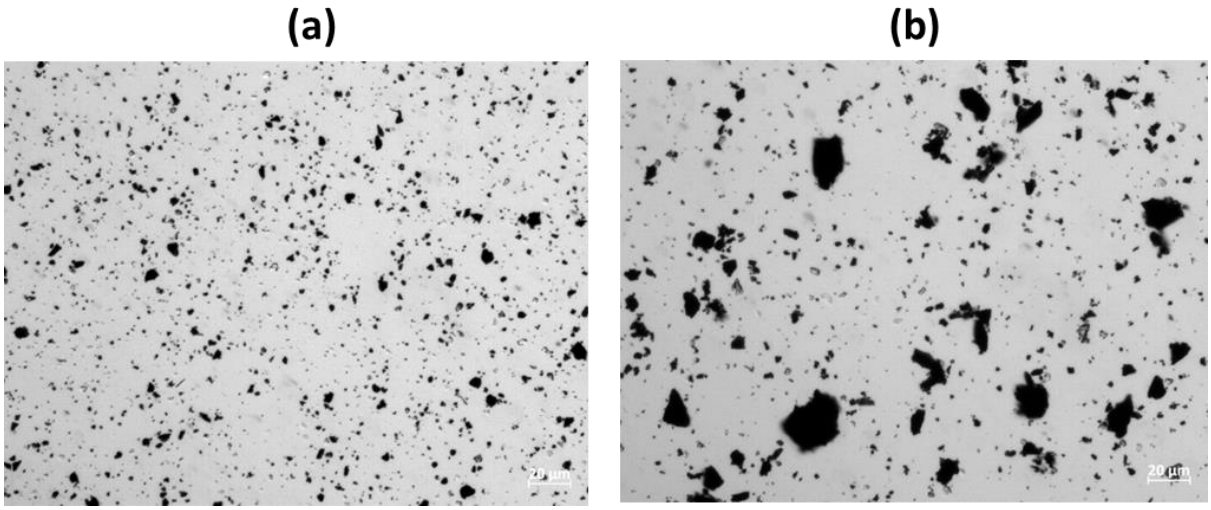

Figure 2. Coal particle aggregation in (a) DI water and (b)Nanobubble water

Acknowledgements

TIF-AWaDH (Technology Innovation Hub- Agriculture and Water Technology Development Hub), Department of Science and Technology, India, provided funding for this research.

References

[1] Yoon, R.H. and Luttrell, G.H., 1989. The effect of bubble size on fine particle flotation. Mineral Procesing and Extractive Metallurgy Review, 5(1-4), pp.101-122.
[2] Stöckelhuber, K.W., Radoev, B., Wenger, A. and Schulze, H.J., 2004. Rupture of wetting films caused by nanobubbles. Langmuir, 20(1), pp.164-168.

An industry example: Prevent embolism in medical devices

Daniel Frese,[1] Andreas Nobis,[2] Olivier Marseille,[2] and Thomas Willers[1,*]

1 KRÜSS GmbH, Borsteler Chausse 85, 22453 Hamburg, Germany
2 Hemovent GmbH, Rottstraße 33, 52068 Aachen, Germany

E-Mail corresponding authors: t.willers@kruss.de

Abstract

Extracorporeal membrane oxygenation is an important technique in the intensive care treatment of critically ill patients. Since blood from the body is passed through a corresponding heart-lung machine, air embolisms caused by the formation of air bubbles are a major risk when using this technique. We explain why stable air bubbles form and what influence the wetting properties of the surface have on this. Using the mobile membrane oxygenator MOBYBOXTM from Hemovent as an example, we show how the choice of a suitable coating can prevent the formation of stable air bubbles. Dynamic contact angle measurements (optical and tensiometric methods) were used to investigate the critical components, namely membrane and housing, with respect to their wetting properties in order to find the optimal coating. A simplified measurement procedure allows Hemovent to check the quality of the coatings as part of in-process quality control.

Nano- and Microdroplets and Microbubbles

Nanodroplet deforms soft substrate: Elasticity vs. capillarity

Binyu Zhao,[1,*] Elmar Bonaccuso,[2] Longquan Chen,[3] and Günter K. Auernhammer[1]

1 *Leibniz Institute of Polymer Research Dresden, Dresden 01069, Germany*
2 *Airbus Central R&T, Materials X, Munich 81663, Germany*
3 *School of Physics, University of Electronic Science and Technology of China, Chengdu 610054, China*

E-Mail corresponding authors: zhao-binyu@ipfdd.de

Abstract

Placing a small liquid droplet on a soft substrate deforms the substrate. The surface tension of the droplet rises a wetting ridge along the three-phase contact line and the Laplace pressure inside the droplet creates a depression (i.e., dimple) underneath the droplet (Figure 1A). The deformation of the substrate is determined by the capillary and elastic energies, which is described by the softness ratio (relating the surface tension and shear modulus of the substrate and the contact radius of the droplet).
Using atomic force microscopy (AFM), we have probed the three-dimensional interfacial configuration of nanodroplets (with different contact radii) and the deformed soft substrates (with different moduli). This allows measuring the ridge height and the dimple depth (Figure 1B) in a range of softness ratios. With increasing the softness ratio, the normalized ridge height increases and then decreases, while the normalized dimple depth increases and approaches to a limiting value. The substrate capillarity overcomes the substrate elasticity in dominating the substrate deformation, illustrating that a substrate becomes relatively soft, when the softness ratio is larger than 1 (Figure 1C). Our results show a direct experimental observation of the elasticity-to-capillarity transition [1].

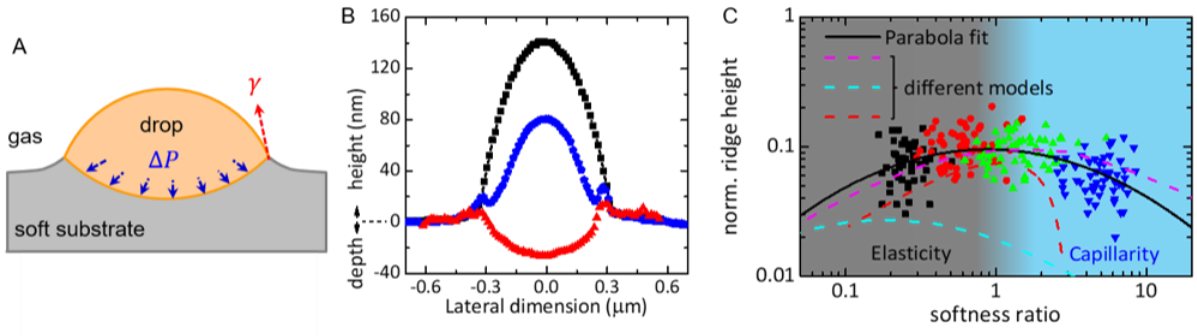

Figure 1. (A) Schematic illustration of the substrate deformation. (B) Profiles of nanodroplet, wetting ridge and dimple probed by AFM. (C) Normalized ridge height versus softness ratio showing the elasticity-tocapillarity transition.

Acknowledgements

The authors acknowledge funding from the National Natural Science Foundation of China (Grant No. 11802055, 11772271) and the German Research Foundation (Project-ID 265191195, SFB 1194).

References

[1] B. Zhao, E. Bonaccurso, G. K. Auernhammer, L. Chen, Elasticity-to-Capillarity Transition in Soft Substrate Deformation, *Nano Letters* **2021**, *21*, 10361-10367.

Towards better understanding of the energy transfer in thermocavitation

J.J. Schoppink[1,*], F.B. Segerink[2], J.A. Alvarez Chavez[2], and D. Fernandez Rivas[1]

1 *Mesoscale Chemical Systems group, Mesa+ Institute and Faculty of Science and Technology, University of Twente, P.O. Box 217, 7500 AE Enschede, the Netherlands*

2 *Optical Sciences group, Mesa+ Institute and Faculty of Science and Technology, University of Twente, P.O. Box 217, 7500 AE Enschede, the Netherlands*

** E-Mail corresponding author: j.j.schoppink@utwente.nl*

Abstract

Over the last decade, there has been increased interest in laser-based jet injections [1]. The principle of this method is shown in Figure 1. A laser is used to create an explosive growing bubble inside a microfluidic channel. This bubble displaces the rest of the liquid, creating a fast microfluidic jet which can penetrate the skin. While initial work on laser-based jet injection relied on pulsed lasers, the use of low-power continuous wave (CW) lasers could result in a more affordable application. These injectors rely on thermocavitation, which is the heating of a highly absorbing liquid by a CW laser, resulting in the formation of a vapor bubble [2].

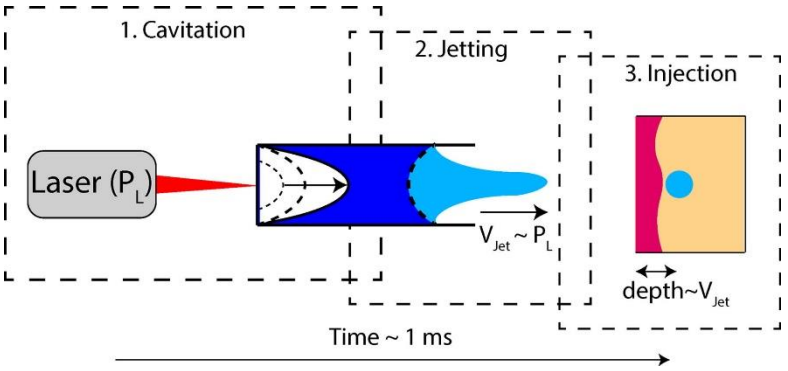

Figure 1: Working principle of laser-based jet injection. Figure taken from [1].

For jet injection, accurate control over these bubble dynamics is essential, but the influence of the laser parameters on the bubble dynamics are not fully understood [1]. It is known that a reduction in laser power results in an increase in nucleation time and maximum bubble size [3]. However, the exact influence of the laser power and especially the beam diameter on the bubble kinetic energy is unknown[1].

We will show recent results on the influence of the laser beam parameters on the moment of nucleation and bubble dynamics. The experimental set-up is shown in Figure 2. We use an IR fiber laser to directly heat the water, in contrast with previous work that relied on highly absorbing dyes. We observe that the nucleation time mainly depends on the laser intensity. Furthermore, the total deposited energy increases with an increasing spot size and/or a decreasing laser power. The bubble size and growth rate depend on this deposited energy. Therefore, the bubble dynamics can be controlled with the laser parameters. This would enable control over the jet velocity as well, which is required for personalized jet injection.

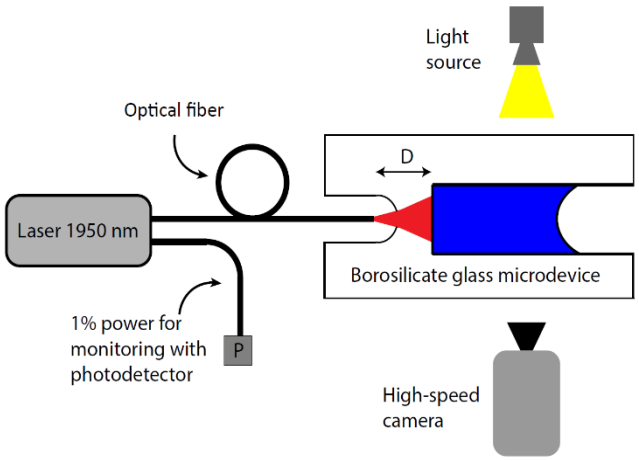

Figure 2: Schematic of the experimental set-up. Distance 'D' controls the laser spot size.

Acknowledgements
The authors acknowledge the funding from the European Research Council (ERC) under the European Union's Horizon 2020 Research and Innovation Programme (Grant Agreement No. 851630), and NWO Take-off phase 1 program funded by the Ministry of Education, Culture and Science of the Government of the Netherlands (No. 18844).

References

[1] J. Schoppink and D. Fernandez Rivas, "Jet injectors: Perspectives for small volume delivery with lasers," *Adv. Drug Deliv. Rev.*, vol. 182, p. 114109, 2022, doi: 10.1016/j.addr.2021.114109.
[2] A. T. Rastopov, S. F. ; Sukhodol'Skii, "Self-organization of the heat cycle due to thermal cavitation during continuous laser heating of a liquid," *Sov. Phys. Dokl.*, vol. 32, p. 671, 1987.
[3] J. P. Padilla-Martinez, C. Berrospe-Rodriguez, G. Aguilar, J. C. Ramirez-San-Juan, and R. Ramos-Garcia, "Optic cavitation with CW lasers: A review," *Phys. Fluids*, 2014, doi: 10.1063/1.4904718.

Electronic structure of ultrafine water cluster deposited on hydrophobic and hydrophilic surfaces explored by soft X-ray emission spectroscopy

Yoshihisa Harada[1,2,*], Ayako Kameda[2], Ralph Ugalino[2], Naoya Kurahashi[1], Hisao Kiuchi [1,2], Subin Song[3], Tomohiro Hayashi[3], Yuki Tabata[4], Akiyoshi Hirano[4], and Shinsuke Inoue[4]

1 *Institute for Solid State Physics, The University of Tokyo, 5-1-5, Kashiwanoha, Kashiwa, Chiba 277-8581, Japan*

2 *Department of Advanced Materials Science, Graduate School of Frontier Sciences, The University of Tokyo, 5-1-5, Kashiwanoha, Kashiwa, Chiba 277-8561, Japan*

3 *Department of Materials Science and Engineering, School of Materials Science and Chemical Technology, Tokyo Institute of Technology, 4259, Nagatsuta-cho, Midori-ku, Yokohama, Kanagawa 226-8503, Japan.*

4 *AISIN CORPORATION, 2-1, Asahi-cho, Kariya, Aichi 448-8650, Japan*

E-Mail corresponding author: harada@issp.u-tokyo.ac.jp

Abstract

In recent years, water clusters called ultrafine water which has several nanometers or less have attracted attention as having a wide range of functions such as humidification, moisture retention, deodorization, air cleaning and sterilization, and static electricity removal. However, little is known about the mechanism of their functions. For example, in moisturizing, penetration into the subcutaneous tissue is considered because the ultrafine water is smaller than the intercellular space on the skin surface. However, this alone cannot account for the long-lasting moisturizing effect [1]. Therefore, it is necessary to clarify the physicochemical properties of ultrafine water to understand those macroscopic functions. In this study, we investigated the electronic structure of ultrafine water deposited on hydrophobic and hydrophilic surfaces using O 1s X-ray emission spectroscopy (XES) to obtain detailed information on the hydrogen-bonded configuration of ultrafine water on those surfaces, and to discuss the relationship between the chemical state and the function of ultrafine water. Figure 1 shows a schematic of the XES process for water. The incident soft X-ray excites a core electron to an unoccupied state (XAS: Fig. 1a), and another soft X-ray emits in the subsequent decay of the core hole (XES: Fig. 1b). When the valence electron decays back to the core hole, XES will represent occupied valence electronic structures of water, which is quite sensitive to various hydrogen-bonded configurations in water [2]. Figure 2 illustrates the experimental setup for

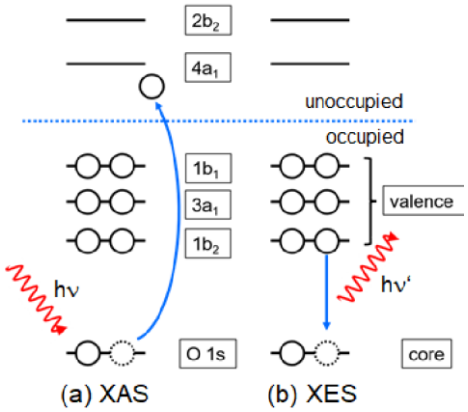

Figure 1 Schematic of the (a) XAS and (b) XES processes for water

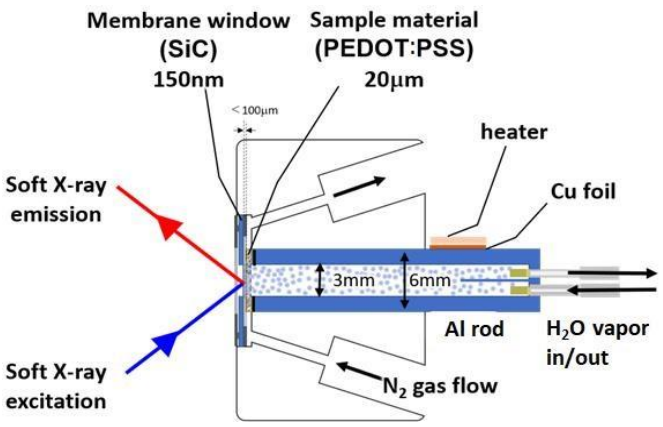

Figure 2 Setup for XES measurement of ultrafine water

the XES measurement. By repeating a heating (by a ceramic heater up to 60 °C) and fully humidifying cycle on a poly(3,4-ethylenedioxythiophene) polystyrene sulfonate (PEDOT:PSS) membrane, ultrafine water of the size of c.a. 1.4 nm is generated. The emitted ultrafine water are deposited on hydrophobic (CF_3: HS-$(CH_2)_{11}$-(O-CH_2-CH_2)-$(CF_2)_5$-CF_3) or hydrophilic (EG_3OH: HS−$(CH_2)_{11}$−(O−CH_2−CH_2)$_3$−OH) self-assembled monolayer (SAM) coated silicon carbide thin membrane which separates vacuum from the atmosphere and effectively transmits incoming and outgoing soft X-rays. The energy dispersion of the emitted soft X-rays is analyzed by the soft X-ray emission spectrometer HORNET at BL07LSU [3] in SPring-8.

The O 1s XES spectrum of ultrafine water on a hydrophobic (CF_3-SAM) surface is shown in Figure 3a. Prior to be installed in a measurement cell, PEDOT:PSS was heat-treated for 15 min. at about 330K for degassing. The CF_3-SAM surface was humidified for approximately 9.5 h with ultrafine water, and the integrated XES spectrum is depicted in blue. In red is a dry spectrum acquired by passing N_2 gas through the measurement cell. The difference between the blue and red spectra generated the black spectrum, which is very similar to that of H_2O gas, apart from a tiny change in the $3a_1$ region.

Figure 3b illustrates the O 1s XES spectra of ultrafine water on the CF_3-SAM exposed to air, where the PEDOT:PSS was not heat-treated prior to the measurement. By exposing the CF_3-SAM to oxygen moieties released from the PEDOT:PSS, the CF_3-SAM should become partly hydrophilic. During the initial 216 min., the XES profile remained unchanged, but subsequently began to grow the $1b_1$' peak around 526eV. The black XES spectrum was derived by subtracting the integrated spectra before 216 min. from those after 216 min. Only the two small peaks indicated by the arrows deviate from the spectrum obtained by using a conventional humidifier which deliver 10µm-order water droplets (not shown).

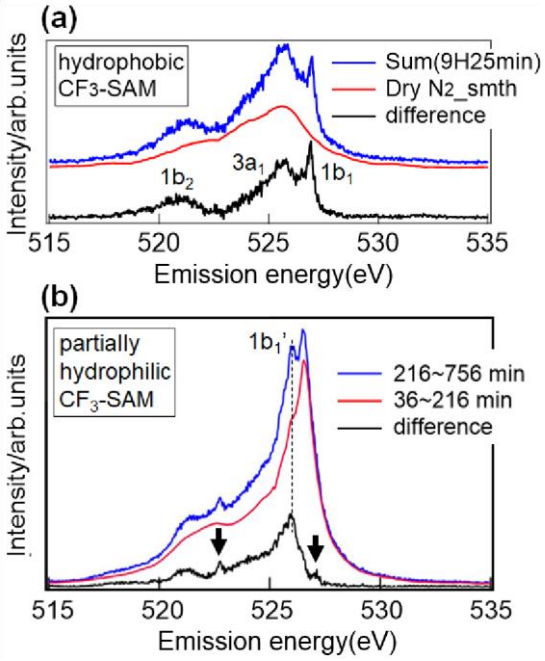

Figure 3 O 1s XES of water on (a) hydrophobic and (b) partially hydrophilic CF_3-SAM. Blue: raw data, Red: background, Black: background subtracted.

We speculate that these two peaks come from specific ionic species, such as OH^- ions [4]; their sharpness indicates that OH^- adsorption occurs at a specific surface site. The fact that ultrafine water forms ions via surface adsorption may explain why it is good for skin moisturization, albeit the method by which OH^- ions are formed is still being debated.

In the presentation we will also present results for the hydrophilic EG3OH-SAM surface and discuss possible difference in interaction of ultrafine water with the hydrophobic and hydrophilic surfaces.

Acknowledgements

This study was supported by JSPS KAKENHI grant number JP19H05717 (Grant-in-Aid for Scientific Research on Innovative Area: Aquatic Functional Materials).

References

[1] N. Nishimura *et al.*, Effect of spraying of fine water particles on facial skin moisture and viscoelasticity in adult women, *Skin Res. Technol.* **2019**, *25*, 294.

[2] T. Tokushima *et al.*, High resolution X-ray emission spectroscopy of liquid water: The observation of two structural motifs, *Chem. Phys. Lett.* **2008**, *460*, 387.

[3] Y. Harada *et al.*, Ultrahigh resolution soft x-ray emission spectrometer at BL07LSU in SPring-8, *Rev. Sci. Instrum.* **2012**, *83*, 013116.

Investigation of adhesion behavior between droplet/bubble and mineral surface

Chunyun Zhu[1,2], Fanfan Zhang[1,2], Xiahui Gui[2], Yaowen Xing[2], Holger Schönherr[1,*]

1 *University of Siegen, Physical Chemistry I & Research Center of Micro- and Nanochemistry and (Bio)Technology (Cμ), Department of Chemistry and Biology, Adolf-Reichwein-Str. 2, Siegen 57076, Germany.*

2 *National Engineering Research Center of Coal Preparation and Purification, China University of Mining and Technology, Xuzhou 221116, China;*

E-Mail corresponding authors: schoenherr@chemie.uni-siegen.de

Abstract

Interaction of bubbles/droplets with solid surfaces play a pivotal role in many industrial applications. In froth flotation, gas bubbles have been used for decades in a selective separation and purification, including coal upgrading, deinking of wastepaper and wastewater treatment [1,2]. It is therefore of great significance to understand the adhesion behavior between bubbles/oil droplets and mineral surfaces. The natural hydrophobicity of coal surfaces with various roughness was characterized by contact angle measurements. The adhesion strength between bubbles/oil droplets and coal surfaces was measured by an adhesion force measurement system and the dynamic extension of three-phase contact line was analyzed by theoretical calculations [3]. As the measurement results show that increasing the surface roughness from 0.23 μm to 2.79 μm, the contact angles decreased and the adhesion forces between bubbles and coal surfaces also decreased from 97.1 μN to 17.9 μN. In addition, the adhesion forces between oil droplets and coal surfaces were decreased with increasing roughness because of the restriction by water. The maximum adhesion forces between oil droplets and mineral surfaces with increasing roughness were 169.5, 145.8, and 121.0 μN, respectively, indicating that decreasing roughness is conducive to improve the modification efficiency of reagents. The distortion of contact line resulted in differences in adhesion force value between the measured and the calculated. The actual length of contact line of water droplets increased with increasing roughness, while the condition of bubbles was opposite. The liquid films, being residual on coal surfaces, impeded the bubble adhesion and reduced the floatability of coal. Reducing the roughness of surface is conducive to enhancing the hydrophobicity of the coal, promoting the expansion of three-phase contact line and thus, improving the flotation efficiency.

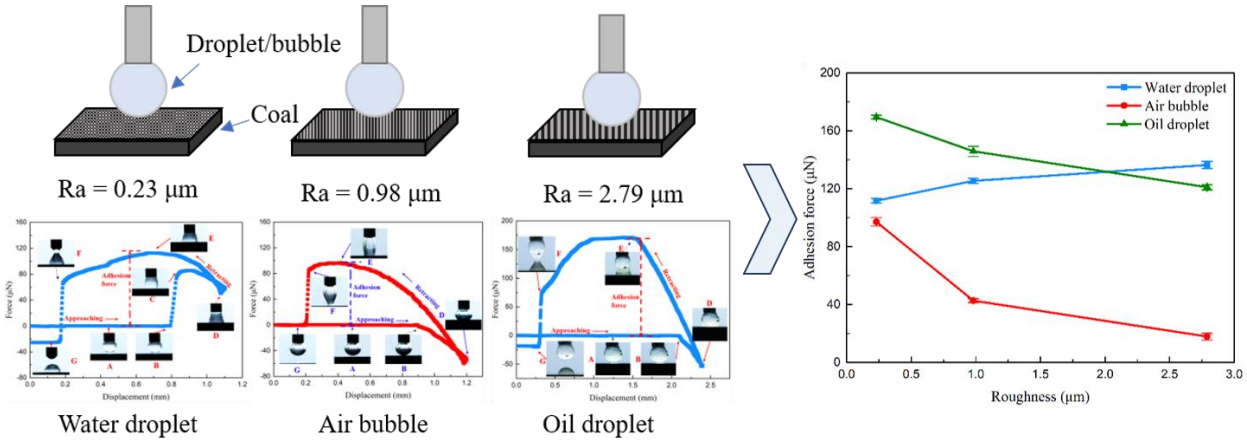

Figure 1. Adhesion forces between bubble/droplet and coal surface with various roughness.

Acknowledgements

The authors acknowledge funding from the Chinese Scholarship Council (CSC) and the University of Siegen.

References

[1] D Wang, Z Zhu, B Yang, et al, Nano-scaled roughness effect on air bubble-hydrophilic surface adhesive strength, Colloid and Surfaces A 2020, 603, 125228.
[2] B Albijanic, O Ozdemir, A.V Nguyen, et al, A review of induction and attachment times of wetting thin films between air bubble and particles and its relevance in the separation of particles by flotation. Adv. Colloid Interface Sci 2010, 159, 1-21.
[3] C Zhu, G Li, Y Xing, et al. Adhesion forces for water/oil droplet and bubble on coking coal surfaces with different roughness, International Journal of Mining Science and Technology 2021, 31, 681-687.

Posters

The fate of bulk nanobubbles under gas dissolution

Hongguang Zhang[1], Shan Chen,[2] Zhenjiang Guo,[2] and Xianren Zhang[3,*]

State Key Laboratory of Organic-Inorganic Composites, Beijing University of Chemical Technology, Beijing 100029, China

E-Mail corresponding authors: zhangxr@mail.buct.edu.cn

Abstract

Artificially added or undesired organic and inorganic contaminants in solution that are interfacial active always tend to be adsorbed on the gas-liquid interface of micro- and nano-bubbles, affecting the stability of the tiny bubbles. In this work, by using molecular dynamics simulations we study how the adsorbed surfactant molecules, with their amphiphilic character, affect the dissolution of the existing bulk nanobubbles under low gas supersaturation environments. We find that depending on the concentration of the dissolved gas and the molecular structure of surfactants, two fates of the bulk nanobubbles whose interfaces are saturated by surfactants are found: either keeping stable or being completely dissolved. With gas dissolution the bubble shrinks, and the insoluble surfactants form a monolayer with an increasing packing density until an extremely low (close to 0) surface tension is reached. In the limit of vanishing surface tension, the surfactant structure crucially affects bubble stability via changing the monolayer elastic energy. Two basic conditions for stable nanobubbles at low gas saturation are identified: vanishing surface tension due to bubble dissolution and positive spontaneous curvature of the surfactant monolayer. Based on this observation, we discuss the similarity between the stability mechanism of bulk nanobubbles and that of microemulsions.

On the Effect of fluid temperature variations in the generation of hydrodynamic cavitating flow patterns on chip

Farzad Rokhsar Talabazar, Araz Sheibani Aghdam,[1,2] Ali Koşar [1,2] and Morteza Ghorbani[1,2,] *

1 *Faculty of Engineering and Natural Science, Sabanci University, Orhanli, Tuzla, Istanbul,34956, Turkey.*
2 *Sabanci University Nanotechnology Research and Application Center, Orhanli, Tuzla, Istanbul,34956, Turkey.*

E-Mail corresponding authors: mghorbani@sabanciuniv.edu

Abstract
Hydrodynamic cavitation is a promising phenomenon in different engineering fields and numerous studies were devoted to its characterization particularly in conventional scale. Although, significant research was carried out in hydrodynamic cavitation, rather less attention has been paid on the effect of working fluid temperature in cavitation inception in micro scale. Therefore, we attempt to investigate the effect of fluid temperature variations on the cavitating flow patterns in microchannels and characterize the inception of cavitating flows. The microfluidic devices capable of generating cavitating flows are fabricated according to the techniques adopted from semiconductor-based microfabrication and based on the theoretical studies. The devices can withstand high pressures which makes it possible to study different flow patterns in broad range of Re numbers with temperature variations. For this purpose, water is chosen as a working fluid and the temperature is varied from 21 to 70 °C. According to the obtained results, it is found that inception occurred in different inlet pressure for various inlet temperatures. In addition, the qualitative results indicate that cavitating flow patterns are changed by fluid temperature variations.

The Hydrodynamic on Chip Concept in Household Appliances

Seyedali Seyedmirzaei Sarraf,[1,2] Mohammadamin Maleki,[1,2] Farzad Rokhsar Talabazar,[1,2] Araz Sheibani Aghdam,[1,2] Kübra Çalışır,[3] Ehsan Tuzcuoğlu,[3], and Morteza Ghorbani[1,2,4]*

1 *Faculty of Engineering and Natural Science, Sabanci University, 34956 Tuzla, Istanbul, Turkey*
2 *Sabanci University Nanotechnology Research and Application Center, 34956 Tuzla, Istanbul, Turkey*
3 *ARÇELİK A.Ş. R&D Center, İstanbul, Turkey*
4 *Center of Excellence for Functional Surfaces and Interfaces for Nano-Diagnostics (EFSUN), Sabanci University, Orhanli, 34956, Tuzla, Istanbul, Turkey*

E-Mail corresponding author: mghorbani@sabanciuniv.edu

Abstract

Cavitation occurs when a liquid at constant temperature reaches to saturated vapor pressure followed by a further drop in pressure to supply the energy required for the rupture of intermolecular bonds of liquid turning it into vapor [1]. Cavitation bubbles experience a cycle of inception, growth, and collapse throughout their evolution. It has been reported that accompanying phenomena occurring with the implosion of cavitation bubbles may include shockwaves, luminescence, high temperatures and pressures, jets and enhanced mixing, as well as radical species production [2][3][4][5]. Hydrodynamic cavitation in which the driving force for the evolution of vapor bubbles is provided by creating low-pressure regions is categorized as one of the tension-based methods [6]. By the advent of microfluidics and the development of microfabrication techniques, the possibility of monitoring and controlling the formation of cavitation bubbles in micro-scale became feasible. Mishra et. al investigated the micro-scale hydrodynamic cavitation on a microfluidic device containing a flow restrictive element for the first time [7]. To reduce the energy required for generation of the hydrodynamic cavitation on chip Ghorbani et. al. proposed microfluidic device containing sidewall roughness at the micro-orifice [8]. Hydrodynamic cavitation on chip concept has been used for several applications including chemical, material production, and cleaning [9][10][11][12], but so far no one has investigated the effect of hydrodynamic cavitation on the detergent particles fragmentation for utilization in household appliances.

This study investigates the effects of hydrodynamic cavitation inside a microfluidic device comprised of a single micro-orifice with sidewall roughness on water samples containing different concentrations of liquid detergent. In addition, effect of the inlet pressure on the bubble generation is considered to find the optimum pressure for household appliances efficacy enhancement. Finally, hydrodynamic cavitation results are compared with samples which are stirred for different time durations in a magnetic stirrer to find a correlation between the effect of cavitation and time. We foresee that cavitation induced mixing would decrease the time required for solving a defined amount of detergent in water paving a way for reducing the energy and time consumption in residential laundry.

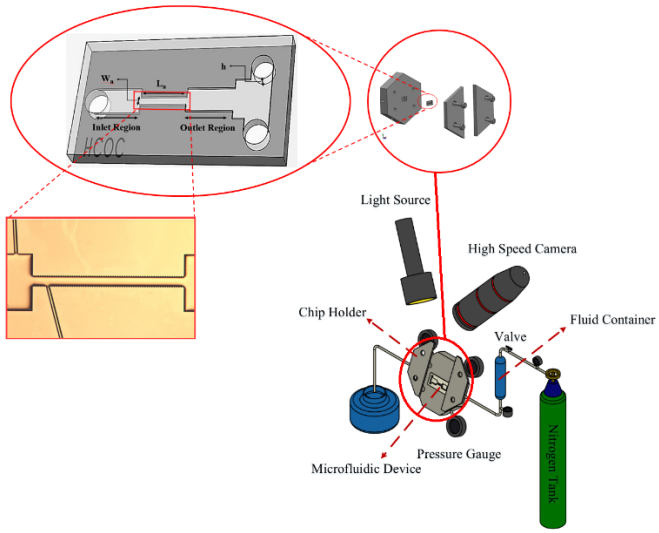

Figure 1. Hydrodynamic cavitation on chip experimental setup for household appliances.

Acknowledgements

This work was supported by Arçelik A.Ş. Equipment utilization support from the Sabanci University Nanotechnology Research and Applications Center (SUNUM) is gratefully appreciated.

References

[1] C. E. Brennen and N. Y. Oxford, "Cavitation and Bubble Dynamics," 1995.

[2] D. J. Flannigan and K. S. Suslick, "Plasma formation and temperature measurement during single-bubble cavitation," *Nature*, vol. 434, no. 7029, pp. 52–55, Mar. 2005, doi: 10.1038/nature03361.

[3] G. Sinibaldi *et al.*, "Laser induced cavitation: Plasma generation and breakdown shockwave," *Phys. Fluids*, vol. 31, no. 10, p. 103302, Oct. 2019, doi: 10.1063/1.5119794.

[4] Tandiono *et al.*, "Sonochemistry and sonoluminescence in microfluidics," *Proc. Natl. Acad. Sci.*, vol. 108, no. 15, pp. 5996–5998, Apr. 2011, doi: 10.1073/pnas.1019623108.

[5] K. Mc Carogher, Z. Dong, D. S. Stephens, M. E. Leblebici, R. Mettin, and S. Kuhn, "Acoustic resonance and atomization for gas-liquid systems in microreactors," *Ultrason. Sonochem.*, vol. 75, p. 105611, Jul. 2021, doi: 10.1016/J.ULTSONCH.2021.105611.

[6] D. Podbevšek, Ž. Lokar, J. Podobnikar, R. Petkovšek, and M. Dular, "Experimental evaluation of methodologies for single transient cavitation bubble generation in liquids," *Exp. Fluids*, vol. 62, no. 8, p. 167, Aug. 2021, doi: 10.1007/s00348-021-03260-1.

[7] C. Mishra and Y. Peles, "Cavitation in flow through a micro-orifice inside a silicon microchannel," *Phys. Fluids*, vol. 17, no. 1, p. 013601, Jan. 2005, doi: 10.1063/1.1827602.

[8] M. Ghorbani, G. Deprem, E. Ozdemir, A. R. Motezakker, L. G. Villanueva, and A. Kosar, "On 'Cavitation on Chip' in Microfluidic Devices with Surface and Sidewall Roughness Elements," *J. Microelectromechanical Syst.*, vol. 28, no. 5, pp. 890–899, 2019, doi: 10.1109/JMEMS.2019.2925541.

[9] Mohammad Jafarpour, A. Sheibani Aghdam, M. Talebian Gevari, Ali Koşar, M. Kemal Bayazıt, and Morteza Ghorbani, "An ecologically friendly process for graphene exfoliation based on the 'hydrodynamic cavitation on a chip' concept," *RSC Adv.*, vol. 11, no. 29, pp. 17965–17975, May 2021, doi: 10.1039/D1RA03352B.

[10] F. Ayela *et al.*, "Hydrodynamic Cavitation through 'Labs on a Chip': From Fundamentals to Applications," *Oil Gas Sci. Technol. – Rev. d'IFP Energies Nouv.*, vol. 72, no. 4, p. 19, Jul. 2017, doi: 10.2516/ogst/2017010.

[11] M. T. Gevari *et al.*, "Deagglomeration of nanoparticle clusters in a 'cavitation on chip' device," *AIP Adv.*, vol. 10, no. 11, p. 115204, Nov. 2020, doi: 10.1063/5.0029070.

[12] B. Verhaagen and D. Fernández Rivas, "Measuring cavitation and its cleaning effect," *Ultrason. Sonochem.*, vol. 29, pp. 619–628, Mar. 2016, doi: 10.1016/J.ULTSONCH.2015.03.009.

Growth and Dynamics of H_2 bubbles at microelectrodes

A. Bashkatov,[1]* S.S. Hossain,[2] X. Yang,[2] G. Mutschke,[2]* and K. Eckert[1,2]

1 *Institute of Process Engineering and Environmental Technology, TU Dresden, 01062 Dresden*
2 *Institute of Fluid Dynamics, Helmholtz-Zentrum Dresden-Rossendorf, Bautzner Landstr. 400, 01328 Dresden*

E-Mail corresponding authors: a.bashkatov@hzdr.de, g.mutschke@hzdr.de

Abstract

The evolution and dynamics of gas bubbles has a strong impact on the efficiency of water electrolysis. Our poster will summarize recent work of our group on the hydrogen evolution at a microelectrode in acidic electrolytes [1-7]. Depending on the applied potential and the electrolyte concentration, three different growth regimes are identified, among them oscillatory growth above a carpet of microbubbles [3, 7]. The discussion of the force balance of the bubbles includes thermocapillary effects [1,2] and an electric force caused by charge adsorption at the interface [6,7].

Acknowledgements

This work was supported by the German Aerospace Center (DLR) with funds provided by the Federal Ministry for Economic Affairs and Energy (BMWi) due to an enactment of the German Bundestag under grant no. DLR 50WM2058 (MADAGAS II project).

References

[1] X. Yang, D. Baczyzmalski, C. Cierpka, G. Mutschke, K. Eckert; Marangoni convection at electrogenerated hydrogen bubbles; Phys. Chem. Chem. Phys. 20 (2018) 11542-11548.
[2] J. Massing, G. Mutschke, D. Baczyzmalski, S. Hossain, X. Yang, K. Eckert, C. Cierpka; Thermocapillary during hydrogen evolution at microelectrodes; Electrochimica Acta 297 (2019) 929-940.
[3] A. Bashkatov, S.S. Hossain, X. Xang, G. Mutschke, K. Eckert; Oscillating Hydrogen Bubbles at Pt Microelectrodes; Phys Rev. Lett. 123 (2019) 214503.
[4] S.S. Hossain, G. Mutschke, A. Bashkatov, K. Eckert; The thermocapillary effect on gas bubbles growing on electrodes of different sizes; Electrochimica Acta 363 (2020) 136461.
[5] A. Bashkatov, X. Yang, G. Mutschke, B. Fritzsche, S. Hossain, K. Eckert; Dynamics of single hydrogen bubbles at Pt microelectrodes in microgravity; Phys. Chem. Chem. Phys. 23 (2021) 11818-11830.
[6] S. S. Hossain, A. Bashkatov, X. Yang, G.Mutschke, and K. Eckert. The force balance of hydrogen bubbles growing and oscillating on a microelectrode. Submitted to Phys. Rev. E, 2022.
[7] A. Bashkatov, S. S. Hossain, G. Mutschke, X. Yang, H. Rox, I. M. Weidinger, and K. Eckert. On the growth regimes of hydrogen bubbles at microelectrodes. Submitted to Phys. Chem. Chem. Phys. , 2022.

A new hydrodynamic generator for bulk nanobubbles production; characterization and evaluation of properties and applications

E.P. Favvas[1]*, A.A. Sapalidis[1], D.S. Karousos[1], E. Patounas[2], G.Z. Kyzas[3], V. Koutsos[2], and A. Ch. Mitropoulos[3]

1 *Institute of Nanoscience and Nanotechnology, NCSR Demokritos, Aghia Paraskevi, 11361, Attica, Greece*
2 *School of Engineering, Institute for Materials and Processes, The University of Edinburgh, King's Buildings, Robert Stevenson Road, EH9 3FB, UK*
3 *Department of Chemistry, International Hellenic University, St. Lucas 65404, Kavala, Greece*

**e.favvas@inn.demokritos.gr (email of presenting author)*

Abstract

A "low" pressure generator, operating at approx. 3 bar, produces bulk nanobubbles (BNBs) through hydrodynamic cavitation process (Fig. 1).

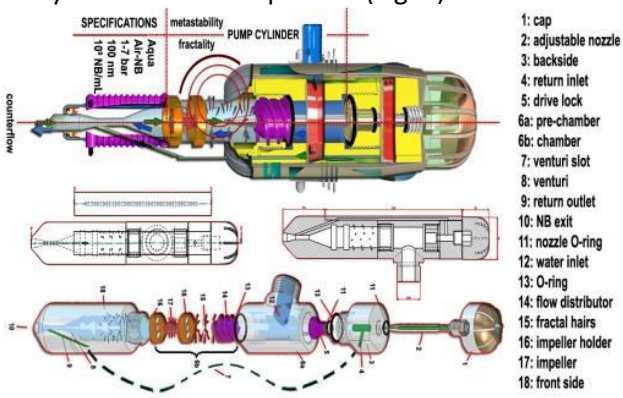

Figure 1. Design of the low pressure NBs' generator.

An innovative feature of the apparatus is the formation of a metastable fluid cylinder of length L and radius R, between 4.5R < L < 2πR, combined with the counter-flow of the mixed fluid and the surface roughness. The nanobubbles' generator takes advantage of a Venturi tube, which is the most widely used hydrodynamic cavitation device. When the gas-liquid mixture passes through a Venturi tube, bubbles are formed due to the decrease and subsequent increase in the local pressure. In this generator, in addition to the hydrodynamic cavitation, due to the Venturi tube, rough/fractal surface characteristics are also exploited to affect the fluid flow, transmuting the system from a liquid/gas mixture to a colloidal phase. The produced water solutions, enhanced with gaseous bulk nanobubbles, were investigated in applications/projects, such as: 1) Nanobubbles' effect on heavy metal ions adsorption by activated carbon, 2) Effect of agitation on batch adsorption process facilitated by using nanobubbles, and 3) Nanobubbles' effect on desalination via direct contact membrane distillation (DCMD).

The effect of mixing time, pH and salinity on the size distribution of both air-NBs and O_2-NBs (*in both cases: bulk nanobubbles*) was evaluated by dynamic light scattering (DLS). Since bulk NBs is considered a colloidal system, their stability is indicated also by the ζ-potential value. Both vapor pressure and water contact angle properties were investigated. Cryogenic scanning electron microscopy (cryo-SEM) images were taken after rapid freezing with liquid nitrogen at both high-pressure of 2000 bar and ambient pressure (Fig. 2). Mixing time, during the NBs' generation process, is a key parameter regarding the size control and stability on NBs. The salt concentration also affects the size of the NBs; the effect of pH was also examined and it is shown that pH is not linearly correlated to NB size.

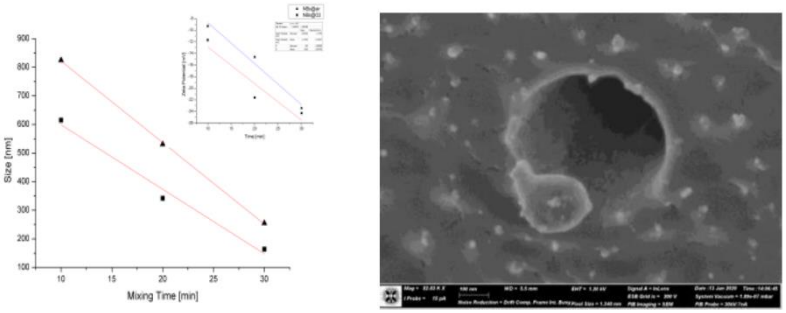

Figure 2. Left: NBs' size vs. mixing time (inset: ζ-potential vs time); Right: Cryo-SEM of a single NB into water phase.

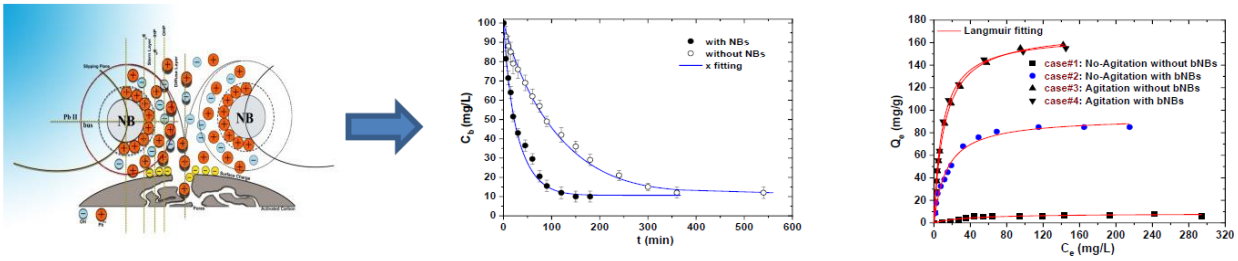

Figure 3. Left: Proposed model of Pb^{2+} adsorption onto activated carbon in presence of gaseous NBs, Center: kinetic experimental data for the adsorption of Pb^{2+} onto activated carbon with and without NBs in water, and, Right: the effect of agitation process on Pb^{2+} onto activated carbon with and without NBs in water.

Pb^{2+} adsorption: NBs cannot drastically influence the adsorption capacity of material. However, the primary and most impressive effect of NBs was to accelerate the adsorption process by 366% and the secondary effect was to modify the shape of the kinetic curve. The ability for achieving high Pb^{2+} adsorption in batch process without shaking/agitation is a new high attention-getting method for industry since the required energy requirement decreases, because of the action of air-NBs (Fig. 3).

Membrane Distillation: In addition, for the DCMD experiments, using a flat sheet PTFE on PP support membrane (*having 0.2 μm pore size diameter*), performance evaluation was conducted by using a feed solution containing 0.5M NaCl, with feed and distillate side temperatures 60 and 17°C respectively. The best performance was achieved by using O_2-NBs increasing the water flux by 85% while retaining 99.95% salt rejection efficiency (Fig. 4).

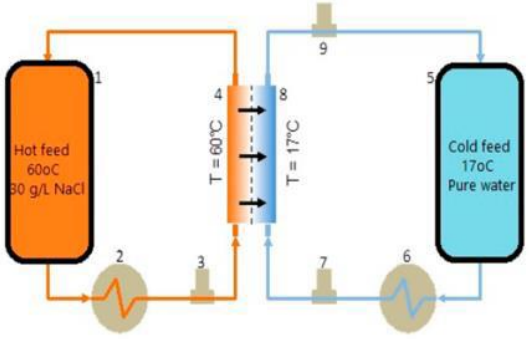

Figure 4. Experimental membrane distillation (MD) set-up.

Future activities include further investigation of operation parameters and an extended characterization of NBs in order to be used as green surfactants for the decontamination of surfaces, including membranes, from organic pollutants.

Acknowledgements

Authors E.P.F, A.A.S. and D.S.K. would like to thank the project "*Intelligent Water Treatment for water preservation combined with simultaneous energy production and material recovery in energy intensive industries (intelWATT)*"**,** E**U** Horizon 2020 Research & Innovation Programme**,** Grant Agreement No 958454**.**

References

[1] M. Alheshibri, J. Qian, M. Jehannin and V.S. Craig, A History of Nanobubbles, *Langmuir* **2016**, 32, 11086 – 11100.

[2] E.D. Michailidi, G. Bomis, A. Varoutoglou, E.K. Efthimiadou, A.Ch. Mitropoulos, E.P. Favvas, book chapter "Principles and Applications of Nanobubbles", in book "Advanced low-cost separation techniques in interface science: Opportunities and new challenges", Elsevier Publisher, *Interf. Sci. and Technol.*, **2019**, 30, 69–99.

[3] Z. Che and P.E. Theodorakis, Formation, dissolution and properties of surface nanobubbles, *J. Colloid Interf. Sci.* **2017**, 487, 123–129.

[4] G.Z. Kyzas, G. Bomis, R. Kosheleva, E.K. Efthimiadou, M. Kostoglou, E.P. Favvas, A.C. Mitropoulos, Nanobubbles effect on heavy metal ions adsorption by activated carbon, *Chem. Engin. J.* **2019**, 356, 91–97.

[5] E.D. Michailidi, G. Bomis, A. Varoutoglou, G.Z. Kyzas, G. Mitrikas, E.K. Efthimiadou, A.Ch. Mitropoulos, E.P. Favvas, Bulk nanobubbles: Production and investigation of their formation/stability mechanism, *J. Coll. Interf. Sci.* **2020**, 564, 371–380.

[6] G.Z. Kyzas, E.P. Favvas, M. Kostoglou, A.C. Mitropoulos, Batch adsorption process without agitation by using bulk nanobubbles, *Colloid Surface A* **2020**, 607, 125440.

[7] E.P. Favvas, G.Z. Kyzas, E.K. Efthimiadou, A.Ch. Mitropoulos, Production methods of Bulk NBs, stability mechanisms and applications, *Curr. Opin. Colloid Interface Sci.* **2021**, 54, 101455.

Nanobubbles influence on membrane separation processes

Jarosław Kupiec[1] and Andrzej Mróz[2]

1 *Fine Bubble Technologies, Sp. z o.o., 05-500 Piaseczno, Poland; jaroslaw.kupiec@fine-bubble.pl*
2 *Fine Bubble Technologies, Sp. z o.o., 05-500 Piaseczno, Poland; andrzej.mroz@finebubble.pl*

Abstract

Membrane filtration is one of the most popular method for water treatment. However, membrane fouling is still a major challenging issue because it results in decreased permeate flux and increased transmembrane pressure.

Three processes of cross-flow membrane filtration, with and without nanobubbles, were performed during the lab-scale research work to evaluate the impact of air nanobubbles on permeate flux. The microfiltration process consisted of removing fine kaolin from the water. In the case of nanofiltration and reverse osmosis, tap water was purified. The method used to generate the nanobubbles was the flow of the feed stream through a special pump. This resulted in the formation of gas bubbles, including nanobubbles that were stable. The gas used in the study was air. Then the feed with or without nanobubbles flowed through the membrane module. The permeate flow was measured during the study.

The results for microfiltration, nanofiltration and reverse osmosis were compared. Data has been shown clearly that air nanobubbles can increase the efficiency of membrane filtration. These results indicated that nanobubbles could be successfully used for cleaning membrane surfaces. The method did not require the use of chemicals and advanced equipment.

Nanostructure-dependent nanobubble drag reduction on NiTi self-adaption surface

Yan Lu[1,*] and Chao Wang[1]

1 *Key Laboratory of Metallurgical Equipment and Control Technology, Wuhan University of Science and Technology; Wuhan 430081, China*

E-Mail corresponding authors: yanlu@wust.edu.cn

Abstract

The investigations of natural superhydrophobic surfaces of plants and animals showed that the wettability property is governed by the nanostructure characteristics of the surface [1-2]. As a result of the improved surface hydrophobic by morphology, the trapping of gas is promoted the on surface cavities to induce friction drag reduction [3,4], but gas cushion cannot stably exist [5-8]. Nanoscapic gas bubbles which exhibit along lifetime and considerable stability [9], may help Improve the situation. In this study, molecular-dynamics simulations are performed to analyze the formation behavior of nanobubble and the effect of nanobubble flow on the nanochannel with various surfaces morphologies. Results show that the existence of gaseous nanobubbles can be trapped by the surface cavities, which replace the dense and orderly absorbed liquid layer in nonbubble flow. Nanochannels with smooth surface and nanostructure surface are compared. For the smooth surface, nanobubbles are attracted by the solid surface with a relatively small contact angle, and density fluctuations near the surface increased. Conversely, the nanostructure surface exhibited strongly attractive toward nanobubbles, which may help decrease the drag coefficient. Moreover, introducing the surface morphology can further improve the effect on drag reduction.

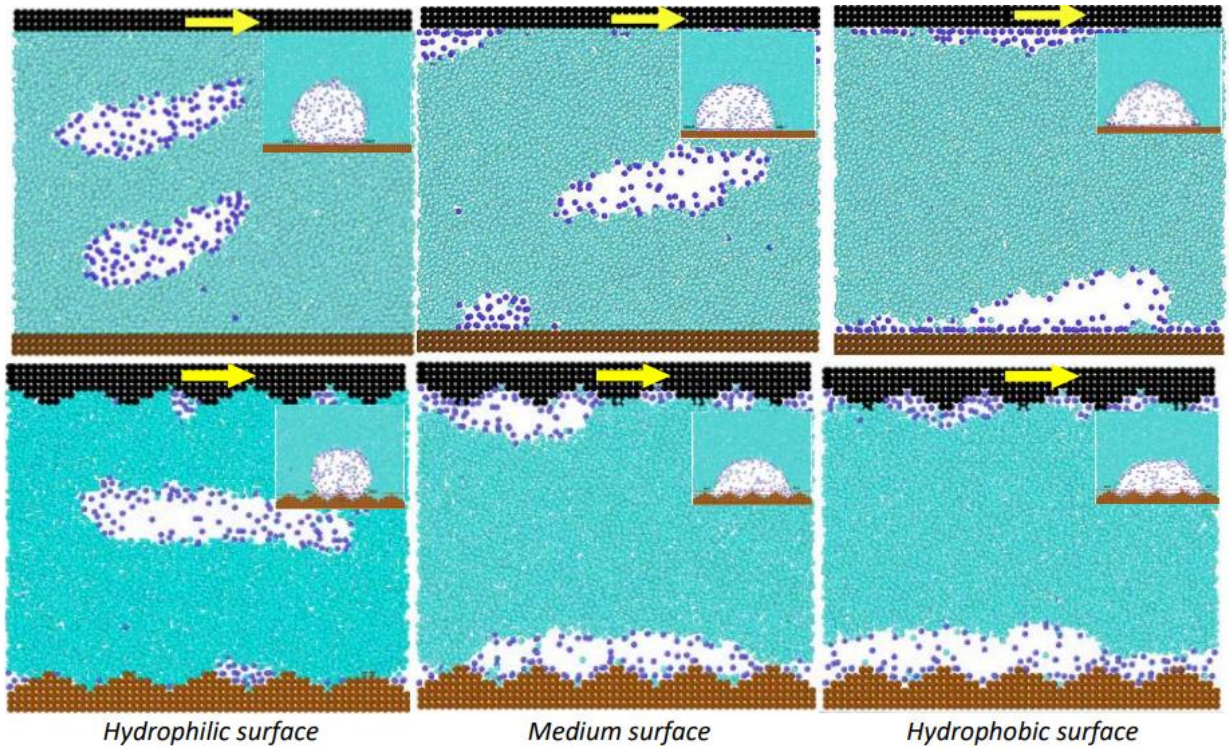

Figure 1. Snapshot of nanobubble behavior as liquid flowed through the nanochannel flow with various wettability surfaces with smooth and cone-shaped morphologies

Acknowledgements

The author would like to thank the National Natural Science Foundation of P.R.China for financial support(ID 51875417 and 51975425). This research was conducted using computational resources at the Center for Computation and Visualization, Brown University. Professor Huajian Gao of the Brown University is also acknowledged for his fruitful discussions during this study.

References

[1] Bhushan B, Jung YC. Natural and biomimetic artificial surfaces for superhydrophobicity, selfcleaning, low adhesion, and drag reduction. Prog Mat. Sci 2011;56:1.
[2] Su Y, Ji B, Zhang K, Gao H, Huang Y, Hwang K. Nano to micro structural hierarchyis crucial for stable superhydrophobic and water-repellent surfaces. Langmuir 2010;26(7):4984–9.
[3] Lu Y. Superior lubrication properties of biomimetic surfaces with hierarchical structure. Tribol Int 2018;119:131–42.
[4] Bhushan B, Jung YC. Natural and biomimetic artificial surfaces for superhydrophobicity, selfcleaning, low adhesion, and drag reduction. Prog Mater Sci 2011;56:1.
[5] Zhang XH, Maeda N, Craig VSJ. Physical properties of nanobubbles on hydrophobic surfaces in water and aqueous solutions. Langmuir 2006;22(11):5025–35.
[6] Ishida N, Inoue T, Miyahara M. Nano bubbles on a hydrophobic surface in water observed by tapping-mode atomic force microscopy. Langmuir 2000;16(16):6377–80.
[7] Yang JW, Duan J, Fornasiero D, Ralston J. Very small bubble formation at the solidwater interface/contact angle and stability of interfacial nanobubbles. J Phys Chem B 2003;107:6139–47.
[8] Zhang XH, Quinn A, Ducker WA. Nanobubbles at the interface between water and a hydrophobic solid. Langmuir 2008;24(9):4756–64.
[9] Lu YH, Yang CW, Fang CK, Ko HC, Hwang IS. Interface-induced ordering of gas molecules confined in a small space. Sci Rep 2014;4:7189.

Dr.Lu is currently a professor at Wuhan University of Science and Technology. She received her PhD degree in mechanical engineering from Wuhan University of Technology in 2013. Her major is tribology and surface engineering. She has more than forty peer-reviewed journal articles(in Int. J. Heat Mass Tran., Tribol. Int.etc). Dr. Lu received number of awards and grants from many organizations and funding agencies, including the National Science Foundation, China Postdoctoral Science Foundation of PRChina, etc..